National Library of Canada
Acquisitions and Bibliographic Services Branch
395 Wellington Street
Ottawa, Ontario
K1A 0N4

Bibliothèque nationale du Canada
Direction des acquisitions et des services bibliographiques
395, rue Wellington
Ottawa (Ontario)
K1A 0N4

Your file Votre référence

Our file Notre référence

NOTICE

The quality of this microform is heavily dependent upon the quality of the original thesis submitted for microfilming. Every effort has been made to ensure the highest quality of reproduction possible.

If pages are missing, contact the university which granted the degree.

Some pages may have indistinct print especially if the original pages were typed with a poor typewriter ribbon or if the university sent us an inferior photocopy.

Reproduction in full or in part of this microform is governed by the Canadian Copyright Act, R.S.C. 1970, c. C-30, and subsequent amendments.

AVIS

La qualité de cette microforme dépend grandement de la qualité de la thèse soumise au microfilmage. Nous avons tout fait pour assurer une qualité supérieure de reproduction.

S'il manque des pages, veuillez communiquer avec l'université qui a conféré le grade.

La qualité d'impression de certaines pages peut laisser à désirer, surtout si les pages originales ont été dactylographiées à l'aide d'un ruban usé ou si l'université nous a fait parvenir une photocopie de qualité inférieure.

La reproduction, même partielle, de cette microforme est soumise à la Loi canadienne sur le droit d'auteur, SRC 1970, c. C-30, et ses amendements subséquents.

Canada

UNIVERSITY OF ALBERTA

ANOMALOUS KINETICS AND THE QUANTITATIVE RELATIONSHIP BETWEEN Ca^{2+} AND Na^{+} SORPTION ON CONTROLLED PORE-GLASS OXINE

BY

DAVID MARC VERMEULEN

A THESIS

SUBMITTED TO THE FACULTY OF GRADUATE STUDIES AND RESEARCH

IN PARTIAL FULFILLMENT OF THE REQUIREMENTS FOR THE DEGREE OF MASTER OF SCIENCE

DEPARTMENT OF CHEMISTRY

EDMONTON, ALBERTA

SPRING 1994

National Library
of Canada

Acquisitions and
Bibliographic Services Branch

395 Wellington Street
Ottawa, Ontario
K1A 0N4

Bibliothèque nationale
du Canada

Direction des acquisitions et
des services bibliographiques

395, rue Wellington
Ottawa (Ontario)
K1A 0N4

Your file Votre référence

Our file Notre référence

The author has granted an irrevocable non-exclusive licence allowing the National Library of Canada to reproduce, loan, distribute or sell copies of his/her thesis by any means and in any form or format, making this thesis available to interested persons.

L'auteur a accordé une licence irrévocable et non exclusive permettant à la Bibliothèque nationale du Canada de reproduire, prêter, distribuer ou vendre des copies de sa thèse de quelque manière et sous quelque forme que ce soit pour mettre des exemplaires de cette thèse à la disposition des personnes intéressées.

The author retains ownership of the copyright in his/her thesis. Neither the thesis nor substantial extracts from it may be printed or otherwise reproduced without his/her permission.

L'auteur conserve la propriété du droit d'auteur qui protège sa thèse. Ni la thèse ni des extraits substantiels de celle-ci ne doivent être imprimés ou autrement reproduits sans son autorisation.

ISBN 0-612-11401-5

Canada

UNIVERSITY OF ALBERTA

RELEASE FORM

NAME OF AUTHOR	DAVID MARC VERMEULEN
TITLE OF THESIS	ANOMALOUS KINETICS AND THE QUANTITATIVE RELATIONSHIP BETWEEN Ca^{2+} AND Na^{+} SORPTION ON CONTROLLED PORE-GLASS OXINE
DEGREE	MASTER OF SCIENCE
YEAR THIS THESIS GRANTED	1994

Permission is hereby granted to THE UNIVERSITY OF ALBERTA LIBRARY to reproduce single copies of this thesis and to lend of sell such copies for private, scholarly or scientific research purposes only.

The author reserves all other publication rights and other rights in association with the copyright in the thesis, and except as hereinbefore provided neither the thesis nor any substantial portion thereof may be printed or otherwise reproduced in any material form whatever without the author's prior written permission.

D. Marc Vermeulen

(Student's signature)

3277-142 nd Avenue

Edmonton, Alberta

Canada T5Y 1H9

DATE April 22, 1994

UNIVERSITY OF ALBERTA

FACULTY OF GRADUATE STUDIES AND RESEARCH

The undersigned certify that they have read, and recommend to the Faculty of Graduate Studies and Research for acceptance, a thesis entitled ANOMALOUS KINETICS AND THE QUANTITTATIVE RELATIONSHIP BETWEEN Ca^{2+} AND Na^{+} SORPTION ON CONTROLLED PORE GLASS OXINE submitted by DAVID MARC VERMEULEN in partial fulfillment for the requirements for the degree of MASTER OF SCIENCE.

F. F. CANTWELL, Supervisor

J. A. PLAMBECK

M. J. DUDAS

DATE April 22, 1994

ACKNOWLEDGEMENTS

I would like to thank the following people who without them I could not have completed this project.

My supervisor, and my friend Dr. F.F. Cantwell who moulded me into the analytical chemist I am today.

Oreola Donini who performed the capacity studies on the CPG-Oxine.

My parents who gave me the freedom and the support early in my life to enable me to tackle any and every obstacle that came my way.

And especially, my best friend and my strongest supporter, my wife Stacey, who without her help over the past 4 years I would not have accomplished what I have.

ABSTRACT

A small column packed with a sorbent composed of a derivative of the ligand 8-hydroxyquinoline covalently bound to Controlled Pore Glass (CPG-OXINE) has previously been used to measure free (hydrated) Ca^{2+} ion concentration by the "column equilibration method". The loading curve, which is a plot of moles of Ca^{2+} sorbed versus time, exhibits a maximum in the range of 1 to 4 min followed by a decrease to an equilibrium plateau value in about 2 hours. It is observed that this "overshoot" of equilibrium in the loading curve can be eliminated by preconditioning the column with a solution containing the same buffer and electrolyte concentration as the sample solution but containing no Ca^{2+}. In addition a slow sorption of Na^{+} by CPG-OXINE is observed. The absolute rate of Na^{+} uptake is about forty times faster than the rate of decrease in moles of Ca^{2+} sorbed but the first-order rate constants for the two processes are nearly identical. Sorption of Ca^{2+} is due both to complexation by immobilized oxine, which depends on the electrical potential of the glass surface, and to another process (es) such as cation exchange in the diffuse part of the electrical double layer. When the pH of the solution in contact with the CPG-Oxine is raised (*e.g.* to pH = 7.00), there is a relatively rapid ionization of SiOH groups to SiO^{-} at the surface of CPG and in its hydrated glass (gel) layer. About one-third of the SiO^{-} groups are in the hydrated glass layer and two-thirds are at the CPG surface. The presence of all these SiO^{-} groups generates a negative electric potential at the CPG surface (Ψ_0) and also in the solution adjacent to the surface (Ψ_x) where the immobilized oxine is to be found. The potential Ψ_x influences the extent of complexation of Ca^{2+} by oxine. Slowly (*i.e.* hours), some Na^{+} from solution diffuses into the hydrated glass layer reducing the negative charge and the negative potential Ψ_x and, consequently, reducing the extent of complexation of Ca^{2+} by oxine. An electrical double layer model is developed to describe all of these effects quantitatively. It is found that for bulk solution

pH = 7.00 and ionic strength of 0.02 mol/L the oxine is located 6 ± 1 A away from the glass surface. A linear relationship is predicted and found between logarithm of the sorbed concentration of Ca^{2+} (mmol/g) and the potential Ψ_x (volt). The derived model should also be relevant to the slow drift of electroosmotic flow rate that is observed during the "conditioning" period in fused silica capillaries.

TABLE OF CONTENTS

CHAPTER		PAGE
ONE	INTRODUCTION	1
	I.1 BACKGROUND ON CONTROLLED PORE GLASS-OXINE	1
	I.2 THEORY OF COLUMN EQUILIBRATION	3
	I.3 DOUBLE LAYER SORPTION MODEL FOR CALCIUM ON CPG-OXINE	7
	I.4 RESEARCH OBJECTIVES	14
TWO	ANOMALOUS KINETICS OF Ca^{2+} SORPTION ON CONTROLLED PORE GLASS-OXINE	17
	II.1 INTRODUCTION	17
	II.2 EXPERIMENTAL	19
	II.2.1 REAGENTS AND CHEMICALS	19
	II.2.2 APPARATUS	20
	II.2.3 COLUMN PREPARATION	22
	II.2.4 PREPARATION OF TEST SOLUTIONS	30
	II.2.5 EXPERIMENTAL PROCEDURE	30
	II.2.6 CAPACITY MEASUREMENT	32
	II.2.7 Ca^{2+} LOADING STUDY	33
	II.2.8 PRECONDITIONING STUDIES	38
	II.2.9 Na^{+} SORPTION STUDIES WITH WATER WASH	38
	II.2.10 Na^{+} SORPTION STUDIES WITH BUFFER WASH	39
	II.3 RESULTS AND DISCUSSION	40
	II.3.1 CAPACITY	40

II.3.2 Ca^{2+} LOADING STUDY 40
II.3.3 PRECONDITIONING STUDIES 41
II.3.3.1 PRECONDITIONING WITH BUFFER AND ELECTROLYTE SOLUTIONS 41
II.3.3.2 ADDITIONAL PRECONDITIONING STUDIES 44
II.3.3.3 SORPTION PROCESSES 52
II.3.4 Na^{+} SORPTION STUDIES WITH WATER WASH 58
II.3.5 Na^{+} SORPTION STUDIES WITH BUFFER WASH 60
II.4 CONCLUSIONS 65

THREE QUANTITATIVE EXPLANATION OF THE RELATIONSHIP BETWEEN THE SORPTION OF Ca^{2+} AND Na^{+} ON CONTROLLED PORE GLASS OXINE IN TERMS OF AN ELECTRICAL DOUBLE LAYER MODEL 68
III.1 INTRODUCTION 68
III.2 EXPERIMENTAL 70
III.2.1 REAGENTS AND CHEMICALS 70
III.2.2 Ca^{2+} SORPTION RATE 70
III.2.3 Na^{+} SORPTION RATE 71
III.2.4 Na^{+} EQUILIBRIUM STUDY 71
III.3 RESULTS AND DISCUSSION 72
III.3.1 EQUILIBRIUM SORPTION OF Na^{+} 72
III.3.2 MODIFIED DOUBLE LAYER SORPTION MODEL FOR CALCIUM 79
III.3.3 DESORPTION RATE OF Ca^{2+} 80
III.4 CONCLUSIONS 87

FOUR FUTURE STUDIES 90

IV.1 FUTURE STUDIES 90

IV.1 SODIUM SORPTION PHENOMENON ON OTHER GLASS SURFACES AND SILICA 90

IV.2 NEW AND IMPROVED PACKINGS AND SUPPORTS 90

REFERENCES 92

APPENDIX DATA FOR THESIS FIGURES 97

LIST OF TABLES

TABLE PAGE

2.1 Instrument conditions for monitoring Ca^{2+} and Na^{+} with the Perkin Elmer Model 4000 Spectrophotometer 25

2.2 Instrument conditions for monitoring Ca^{2+} and Na^{+} with the Varian SpectraAA-10 Spectrophotometer 26

2.3 Instrument conditions for monitoring Cu^{2+} with the Perkin Elmer Model 290 B Spectrophotometer 27

3.1 Parameters relating to the sorption of Na^{+} on CPG-Oxine at pH = 7.00 at various bulk solution concentrations of Na^{+} 74

3.2 Parameters relating to the sorption of Ca2+ and Na+ from a solution containing 2.0×10^{-5} M Ca^{2+}, 0.0200 M $NaClO_4$ and 0.0100 M HEPES at pH = 7.00. Ionic strength is 0.0224 M; $x = 5.7 \times 10^{-8}$ cm and $\gamma_{Ca} = 0.549$ 83

A.1 Cu^{2+} washing study data. Used to determine appropriate wash time to rid the column of interstitial Cu^{2+} solution 98

A.2 Cu^{2+} loading study data. Used to determine appropriate load time for Cu^{2+} on the CPG-Oxine to achieve equilibrium 99

A.3 Cu^{2+} capacity study data. Used to determine the capacity of the CPG-Oxine 100

A.4 Ca^{2+} loading study data on CPG-Oxine. 2.00×10^{-5} M Ca^{2+} in 0.0200 M $NaClO_4$ and 0.0100 M HEPES buffer solution at pH = 7.00. Load times up to 4 minutes 101

A.5 Ca^{2+} loading study data on CPG-Oxine. 2.00×10^{-5} M Ca^{2+} in 0.0200 M

$NaClO_4$ and 0.0100 M HEPES buffer solution at pH = 7.00. Load times upto 240 minutes 102

A.6 Ca^{2+} loading study data on CPG alone. 2.00 x 10^{-5} M Ca^{2+} in 0.0200 M $NaClO_4$ and 0.0100 M HEPES buffer solution at pH = 7.00. Load times up to 240 minutes 103

A.7 Ca^{2+} loading study data on CPG-Oxine. 2.00 x 10^{-5} M Ca^{2+} in 0.0200 M $NaClO_4$ and 0.0100 M HEPES buffer solution at pH = 7.00 (Solid Circles). Buffer preconditioning study data on CPG-Oxine. Preconditioning solution made up of 0.0200 M $NaClO_4$ and 0.0100 M HEPES at pH = 7.00 (Open Squares). Load times up to 240 minutes..... 104

A.8 Ca^{2+} loading study data on CPG-Oxine. 2.00 x 10^{-5} M Ca^{2+} in 0.0200 M $NaClO_4$ and 0.0100 M HEPES buffer solution at pH = 7.00 (Solid Circles). Buffer preconditioning study data on CPG-Oxine. Preconditioning solution made up of 0.0100 M HEPES only at pH = 7.00 (Open Squares). Load times up to 240 minutes..... 105

A.9 Ca^{2+} loading study data on CPG-Oxine. 2.00 x 10^{-5} M Ca^{2+} in 0.0200 M $NaClO_4$ and 0.0100 M HEPES buffer solution at pH = 7.00 (Solid Circles). Buffer preconditioning study data on CPG-Oxine. Preconditioning solution made up of 0.0200 M $NaClO_4$ only at pH = 7.00 (Open Squares). Load times up to 240 minutes..... 106

A.10 Ca^{2+} loading study data on CPG-Oxine. 2.00 x 10^{-5} M Ca^{2+} in 0.0200 M $NaClO_4$ and 0.0100 M HEPES buffer solution at pH = 7.00 (Solid Circles). Buffer preconditioning study data on CPG-Oxine. Preconditioning solution made up of 0.0200 M $NaClO_4$ and 0.100 M HEPES at pH = 7.00 (Open Squares). Load times up to 240 minutes..... 107

A.11 Ca^{2+} loading study data on CPG-Oxine. 2.00×10^{-5} M Ca^{2+} in 0.0200 M $NaClO_4$ and 0.0100 M HEPES buffer solution at pH = 7.00 (Solid Circles). Buffer preconditioning study data on CPG-Oxine. Preconditioning solution made up of 0.200 M $NaClO_4$ and 0.0100 M HEPES at pH = 7.00 (Open Squares). Load times up to 240 minutes..... 108

A.12 Ca^{2+} loading study data on CPG-Oxine. 2.00×10^{-5} M Ca^{2+} in 0.0200 M $NaClO_4$ and 0.0100 M HEPES buffer solution at pH = 7.00 (Solid Circles). Buffer preconditioning study data on CPG-Oxine. Preconditioning solution made up without any sodium content; The solution made up of 0.0200 M NH_4ClO_4 and 0.0100 M HEPES at pH = 7.00 (Open Squares). Load times up to 318 minutes..... 109

A.13 Sodium wash study of CPG-Oxine. CPG-Oxine loaded with a 0.0200 M $NaClO_4$ Solution at pH = 7.00. Column then washed for various lengths of time with N_2 sparged DI water. Wash times up to 18 minutes..... 110

A.14 Sodium wash study data. Data collected by loading the CPG-Oxine column for 2 minutes with 0.0200 M $NaClO_4$ (pH = 7.00) and washing for various lengths of time with 0.0100 M HEPES solution (pH = 7.00)..... 111

A.15 Sodium sorption study data. Data collected by loading the CPG-Oxine column for various lengths of time with 0.0200 M $NaClO_4$ (pH = 7.00) and washing for 30 seconds with the 0.0100 m HEPES solution..... 112

A.16 Desorption curve data for Ca^{2+}. The two minute loading curve point from Figure 2.9A is considered to be zero (that is all data points are minus two minutes from the experimental data). The rest of the data is then generated as $\Delta\overline{N}_{Ca} = \overline{N}_{Ca,\ 2\ minutes} - \overline{N}_{Ca,\ load\ time\ (t \geq 2\ mins)}$ 113

A.17 Sodium sorption study data. Data collected by loading the CPG-Oxine column, until equilibrium has been reached (2 hour load time verified by 4 hour load time) with 0.0200 M $NaClO_4$ (pH = 7.00) and washing for 30 seconds with the 0.0100 m HEPES solution. 114

A.18 Data for Na^+ sorption isotherm of Na^+ within the hydrated glass layer. Data from Figure 3.1 plotted according to equation 3.4. Points are experimental data; solid line is least squares fit 115

LIST OF FIGURES

FIGURE		PAGE
1.1	Structure of the immobilized derivative of 5-phenylazo-8-hydroxyquinoline	2
1.2	Concept of column equilibration technique. (a) After complete breakthrough, the CPG-Oxine is at equilibrium with sample stream. (b) A breakthrough curve	4
1.3	Diagrammatic representation of a breakthrough curve with shallow bed conditions within the column	6
1.4	Diagrammatic representation of an overshoot phenomenon (not to scale) (a) Expected loading curve slowly approaching equilibrium (b) Anomalous overshoot phenomenon studied in this thesis	16
2.1	Diagram of operating system	21
2.2	Diagram of slider from valve V1 in Figure 2.1	23
2.3	Diagram of an enlargement of centre hole (column) from Figure 2.2	24
2.4	Diagram of the 7 cm x 1.5 mm (alternate) CPG-Oxine column used for Na^+ sorption experiments	29
2.5	Plot of capacity washing study data. A 1.26×10^{-3} M Cu^{2+} in 0.0900 M HOAC/NaOAc (pH = 5.00) loaded for 10 minutes and washed for increasing lengths of time with N_2 sparged DI water	34
2.6	Plot of loading study data for the capacity study. A 3.15×10^{-4} M Cu^{2+} solution in 0.0900 M HOAC/NaOAc (pH = 5.00) was loaded for increasing lengths of time and washed for 10 minutes with N_2 sparged DI water	35
2.7	Loading curve for Cu^{2+} in 0.0900 M HOAC/NaOAc (pH = 5.00) on CPG-Oxine. The capacity is 1.0×10^{-5} mol Cu^{2+} per gram of CPG-Oxine	36

2.8 Loading curve for Ca^{2+} on CPG-Oxine normalized by the 2 minute sorption value of Ca^{2+} on CPG-Oxine. Value for $\overline{N}_{Ca}$ for the 2 minute load is 5.94×10^{-4} mmol/gram 42

2.9 Loading curves for Ca^{2+} on CPG-Oxine (curve A) and CPG (curve B), all normalized by the 2 minute sorption value of Ca^{2+} on CPG-Oxine. The solid line in (A) is first-order fit using k_{Ca} obtained from Figure 2.18. The solid line for (B) is an empirical fit..... 43

2.10 Preconditioning curve (open squares) and loading curve (solid circles) for Ca^{2+} on CPG-Oxine, normalized by the 2 minute sorption value of Ca^{2+} on CPG-Oxine from the loading curve. Value of $\overline{N}_{Ca}$ for the 2 minute load is 5.94×10^{-4} mmol/gram. Solid line is first-order fit as in Figure 2.9A 45

2.11 Preconditioning curve (open squares) and loading curve (solid circles) for Ca^{2+} on CPG-Oxine normalized by the 2 minute sorption value of Ca^{2+} on CPG-Oxine from the loading curve. Value of $\overline{N}_{Ca}$ for the 2 minute load is 5.94×10^{-4} mmol/gram. Preconditioning is done with a solution containing only 0.0100 M HEPES buffer at pH = 7.00..... 46

2.12 Preconditioning curve (open squares) and loading curve (solid circles) for Ca^{2+} on CPG-Oxine normalized by the 2 minute sorption value of Ca^{2+} on CPG-Oxine from the loading curve. Value of $\overline{N}_{Ca}$ for the 2 minute load is 5.94×10^{-4} mmol/gram. Preconditioning is done with a solution containing only 0.0200 M $NaClO_4$ at pH = 7.00..... 47

2.13 Preconditioning curve (open squares) and loading curve (solid circles) for Ca^{2+} on CPG-Oxine normalized by the 2 minute sorption value of Ca^{2+} on CPG-Oxine from the loading curve. Value of $\overline{N}_{Ca}$ for the 2 minute load is 5.94×10^{-4} mmol/gram. Preconditioning is done with a solution containing 0.0100 M HEPES and 0.0200 M $NaClO_4$ at a pH = 7.00 49

2.14 Loading curves for Ca^{2+} on CPG-Oxine normalized by the 2 minute sorption value of Ca^{2+} on CPG-Oxine from the loading curve. Value of $\overline{N}_{Ca}$ for the 2 minute load is 5.94×10^{-4} mmol/gram. Solid circles represent normal sample conditions (2.00×10^{-5} M Ca^{2+} in 0.0200 M $NaClO_4$). Open squares represent a 10 fold increase in electrolyte concentration (2.00×10^{-5} M Ca^{2+} in 0.200 M $NaClO_4$) 50

2.15 Loading curves for Ca^{2+} on CPG-Oxine normalized by the 2 minute sorption value of Ca^{2+} on CPG-Oxine from the loading curve. Value of $\overline{N}_{Ca}$ for the 2 minute load is 5.94×10^{-4} mmol/gram. Solid circles represent normal sample conditions (2.00×10^{-5} M Ca^{2+} in 0.0200 M $NaClO_4$ and 0.0100 M HEPES). Open squares represent a loading solution void of sodium; loading solution contains 2.00×10^{-5} M Ca^{2+} in 0.0200 M NH_4ClO_4 and 0.0100 M HEPES 51

2.16 Plot of moles of Na^+ per gram that remains sorbed on CPG-Oxine after a 2 minute load followed by a wash of varying lengths of time with N_2 sparged, DI water 59

2.17 Plot of moles of Na^+ per gram that remains sorbed on CPG-Oxine after a 2 minute load followed by a wash, for varying lengths of time, with 0.0200 M HEPES solution (pH = 7.00) 61

2.18 Plot of strongly held Na^+ versus load time. Residual Na^+ washed with 0.0200 M HEPES (pH = 7.00) for 30 seconds. Solid line is a first-order fit as per equation 2.5 63

2.19 Desorption curve for Ca^{2+}. Two minute loading point from Figure 2.9A considered to be zero. All points are then determined as such: $\Delta\overline{N}_{Ca} = \overline{N}_{Ca,\ 2\ minutes} - \overline{N}_{Ca,\ load\ time\ (t \geq 2\ mins)}$ 64

3.1 Sorption isotherm of Na^+ on CPG-Oxine from pH = 7.00 bulk solution. The points are experimental data; solid line is predicted from equation 3.4 using values of $K_H^{Na} = 76$ and $(\overline{SiO^-}) = 9.6 \times 10^{-3}$, obtained from Figure 3.2 76

3.2 Diagrammatic representation of the region near the glass-solution interface lining the pores in CPG-Oxine. Average pore diameter is 500 Å, so the pore liquid, to the right of the glass surface, contains both the diffuse part of the electrical "double layer" and bulk solution. The hydrated glass layer, to the left of the glass surface, is probably more than one O-Si-O interatomic distance in depth. For ease of representation, bond lengths are inconsistent with one another and not to scale 77

3.3 Plot of $\ln(\overline{N}_{Ca}/\gamma_{Ca})$ vs Ψ_x to test the linear dependence predicted by equation 3.6. Points are data from columns 9 and 10 from Table 3.2. Oxinate is located at x = 5.7 x 10-8 cm. The line is a linear least-squares fit having a slope of -38.9 86

LIST OF SYMBOLS

SYMBOL	DESCRIPTION
A_{sp}	specific surface area for CPG-Oxine (cm^2/g)
AAS	atomic absorption spectrophotometry
AES	atomic emission spectrophotometry
Ca^{2+}	free calcium ion
$[Ca^{2+}]$	Ca^{2+} concentration (moles/L)
$\overline{Ca}^{2+}$	free calcium ion near the charge surface
$\overline{CaOX}^{+}$	1:1 complex between Ca^{2+} and $\overline{OX}^{-}$
CPG-Oxine	5-P-Oxine bound on Controlled Pore Glass
Cu^{2+}	free copper ion
$\overline{D}_{Na}$	diffusion coefficient of Na^+ in the hydrated gel layer (cm^2/s)
F	faraday constant (c/mole)
$\overline{H}^{+}$	hydrogen ion near the charge-surface
$\overline{HOX}$	neutral bound 5-P-Oxine species
$\overline{H_2OX}^{+}$	protonated bound 5-P-Oxine species
$\overline{K}_{a1}$	first acid dissociation constant for bound 5-P-Oxine
$\overline{K}_{a2}$	second acid dissociation constant for bound 5-P-Oxine

SYMBOL	DESCRIPTION
$\overline{K}_{a2}'$	acidity quotient in terms of the bulk solution a_H
$K_{Ca, IEX}$	ion exchange distribution coefficient for Ca^{2+}
$K'_{Ca, IEX}$	conditional ion exchange distribution coefficient for Ca^{2+}
K_{Na}	distribution coefficient for Na^+
Na^+	free sodium ion
$[Na^+]$	Na^+ concentration
$\overline{N}_{Ca}(CPG)$	total number of millimoles of sorbed calcium per gram of CPG only
$\overline{N}_{Ca}(CPG\text{-}Ox)$	total number of millimoles of sorbed calcium per gram of CPG-Oxine
$\overline{N}_{Ca}$	number of millimoles of calcium complexed per gram of CPG-Oxine; that is $\overline{N}_{Ca} = [\ \overline{N}_{Ca}(CPG\text{-}Ox) - \overline{N}_{Ca}(CPG)\ ]$
$\overline{N}_{Ca, IEX}$	millimoles of sorbed calcium, not complexed by bound 5-P-Oxine, in the diffuse part of the electrical double layer as a result of cation exchange for Na^+
$\overline{N}_{Na, t}$	concentration of Na^+ sorbed at time t on CPG-Oxine (mmol/g)

SYMBOL	DESCRIPTION
$\overline{N}_{Na,\ equil}$	concentration of Na^+ sorbed at equilibriumon CPG-Oxine (mmol/g)
$\overline{OX^-}$	anionic bound 5-P-Oxinate species
$\overline{pH}$	pH of the solution at a distance x cm away from (but close to) the charge-surface
$\overline{pK_a}$	negative of the value log $\overline{K}_a$
Q	surface concentration of ionized silanol groups (mmol/gram)
R	ideal gas constant (J mol^{-1} K^{-1})
T	absolute temperature (K)
V_x	volume per gram of CPG-Oxine in a thin layer of solution located at a distance x cm from the charge-surface
Z	charge on the ionized surface group without sign
Z.	charge on the ionized surface group with sign
a_{Ca}	activity of Ca^{2+} in the bulk solution
$\bar{a}_{Ca}$	activity of Ca^{2+} at a distance x cm away from (but close to) the charge-surface
a_H	activity of hydrogen ion in the bulk solution

SYMBOL	DESCRIPTION
$\bar{a}_{H,x}$	activity of hydrogen ion at a distance x cm away from the charge-surface
c	ionic strength of the bulk solution (mol/L)
c_e	concentration of the effluent discharging from the column
c_i	concentration of the influent sample solution
$\bar{\alpha}_{Ox}$	fraction of bound 5-P-Oxine ionized
$\bar{\beta}_1$	stability constant for $\overline{CaOX^+}$
γ_{Ca}	activity coefficient for Ca^{2+} in bulk solution
$\gamma_{DL,i}$	ionic activity coefficient of species i in the diffuse layer
γ_{GC}	constant
γ_i	ionic activity coefficient of species i in the bulk solution
ψ_o	electrical potential of the charge-surface in volts
ψ_x	electrical potential at distance x cm away from the charge-surface in volts
ε_o	permitivity of a vacuum. Has a value of $(1.12 \times 10^{-12}$ coul/V·cm)
λ_o	distribution coefficient for Ca^{2+} on CPG-Oxine (L/g)

SYMBOL	DESCRIPTION
σ_o	surface charge density of CPG-Oxine (coul/cm$^{2)}$
ζ	Zeta potential
$\Gamma_{DL,Ca^{2+}}$, $\Gamma_{DL,Na^{+}}$	surface excess of the calcium or sodium ions in the diffuse layer (mol/cm$^{2)}$
$\bar{v}_{Oxine}$	moles of bound 5-P-Oxine per gram of CPG-Oxine
$1/\kappa$	"thickness" of the diffuse part of the electrical double layer (cm)

CHAPTER ONE

INTRODUCTION

I.1 BACKGROUND ON CONTROLLED PORE GLASS-OXINE

Oxine (or 8-Hydroxyquinoline) has been characterized extensively by researchers and has been shown to complex with over 20 metal ions (1,2). Once the oxine has been immobilized on some support such as the nonpolar styrene-divinylbenzene copolymer Amberlite XAD-2 or glass it can be used in a number of ways such as:

1. Pre-concentrating trace metal ions prior to their quantitative measurement (3-11),
2. Removing trace concentrations of metal ions from an electrolyte solution (12), and
3. A column packing material for chromatographic separations (13-17).

The packing used in the present work was supplied by the Pierce Chemical Company. The packings' trade name is "Controlled Pore Glass-Oxine" which is referred to in the following pages as CPG-Oxine. The preparation of the CPG-Oxine has been previously described (18). A number of workers have immobilized oxine on controlled pore glass via covalent bonding. In this case the oxine is azo-linked to an arylamine which is coupled to the CPG via γ-aminopropyltriethoxyquinoline. The structure of the CPG-Oxine derivative 5-phenyl-8-hydroxyquinoline (5-P-Oxine) which is immobilized on the controlled pore glass is shown in Figure 1.1.

The advantages of using CPG versus something like the nonpolar styrene-divinylbenzene copolymer Amberlite XAD-2 are its high mechanical strength (19,20) good swelling stability (required for use in high pressure and continuously changing solvent composition often encountered in chromatographic systems), and the fast metal sorption/desorption kinetics observed. There are two main disadvantages of using CPG-

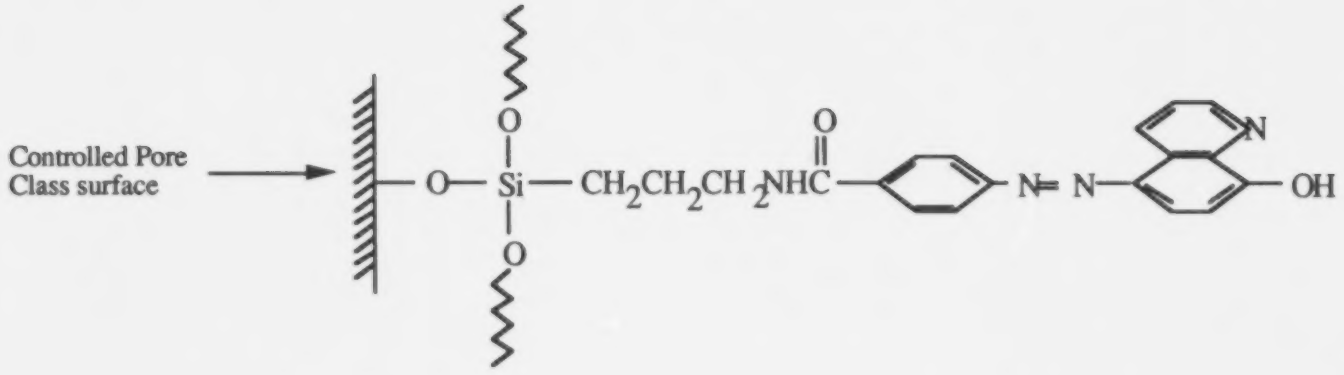

Figure 1.1 : Structure of the immobilized derivative of 5-phenylazo-8-hydroxyquinoline.

Oxine. Extended operation at high pH results in hydrolysis of the glass substrate and cleavage of the bonded phase (5,15,18). Also because of its relatively low capacity, CPG-Oxine can only be used for samples containing either trace or low level metal concentrations (3,9,18,20,21).

I.2 THEORY OF THE COLUMN EQUILIBRATION TECHNIQUE

Equilibrium distribution methods are used for metal speciation in two ways. The batch method has been a popular, commonly used technique in the past, with mixed results (22-27). More recently, the column equilibration technique has been used with better, more reproducible analytical results (28-30). The column equilibration technique which is the basis for the present study is described below.

Consider a solution containing the metal of interest, M^{2+}, and a relatively high concentration of electrolyte (eg., $NaClO_4$). If this solution is passed through and equilibrated with a known weight of sorbent, such as CPG-Oxine (Figure 1.2a, taken directly from reference 47), the following equilibria will occur:

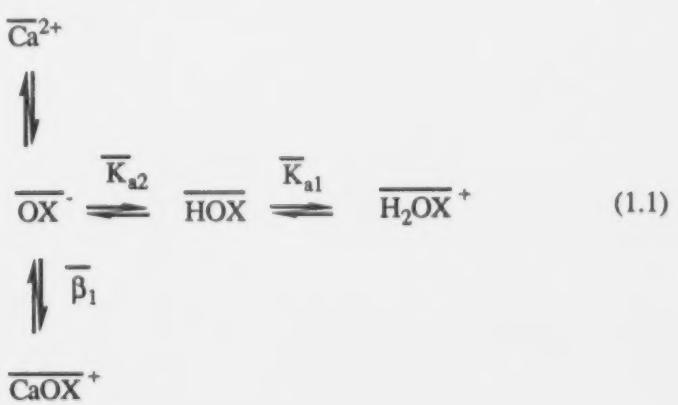

(1.1)

where $\overline{Ox}^{-}$ represents the ligand sites on the glass and $\overline{K}_{a1}$ and $\overline{K}_{a2}$ are the acid dissociation constant for protonated bound oxine and for neutral bound oxine respectively.

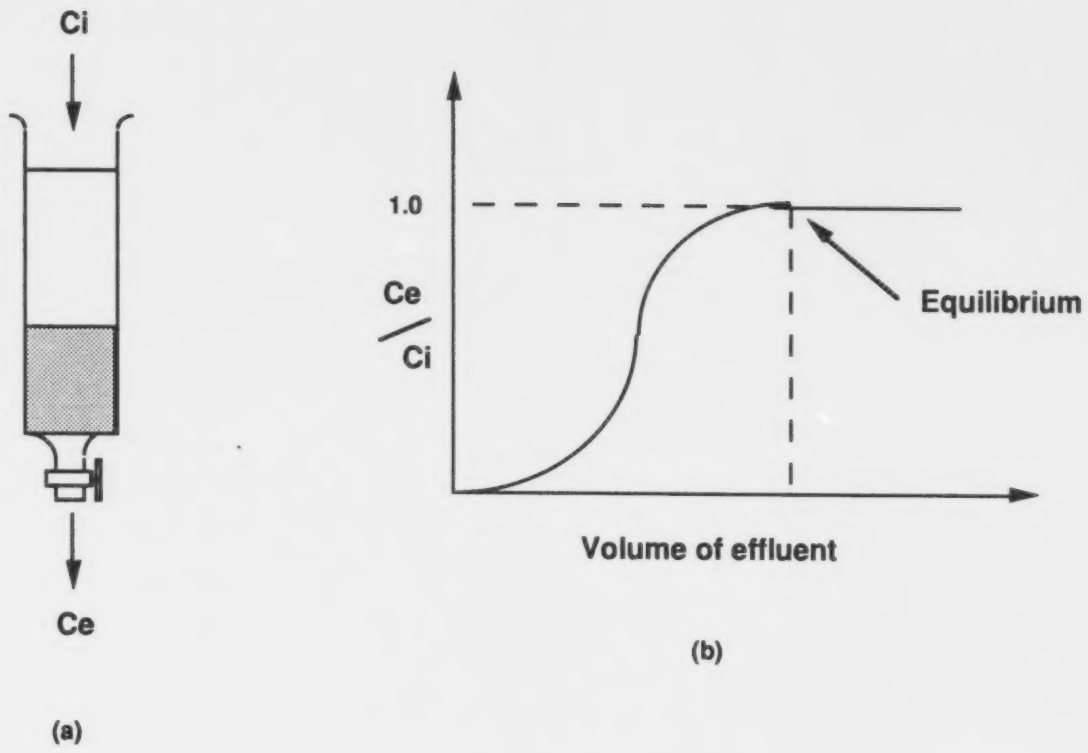

Figure 1.2: Concept of column equilibration technique (a) CPG-Oxine is at equilibrium with sample stream. (b) A breakthrough curve.

$\bar{\beta}_1$ is the stability constant for $\overline{CaOX^+}$ complex, assuming a 1:1 complexation. If one monitors the effluent while the sorbent approaches equilibrium with the sample solution, one will see a plot similar to Figure 1.2b. This is a **breakthrough curve**, which is a plot of C_e/C_i versus volume of effluent passed through the column. Initially, $C_e/C_i < 1$ and thus the sorbent within the column is still sorbing metal ion from the sample solution. As the volume of the sample solution through the column increases, the ratio C_e/C_i approaches 1. Finally, over time $C_e = C_i$, and complete breakthrough has occurred; That is, the CPG-Oxine is in equilibrium with the sample solution so that no more metal ions are sorbed as the sample solution flows through the column.

During the experiments carried out in the present work, **shallow bed** conditions were maintained. In a shallow bed system the length of the column is sufficiently short and the flow rate (really the linear velocity) of the solution is sufficiently high that all of the packing within the length of the column is immersed at all times (even well before the packing has come to equilibrium with the solution) in a unchanging sample solution (where concentration is very close to that of the influent sample solution). That is, $c_e \cong c_i$ within detectable limits. If one had a sensitive enough instrument one could detect the difference between c_e and c_i. This concept is shown diagrammatically in Figure 1.3.

During column equilibration experiments it is desirable to maintain **trace loading** conditions. If the affinity of the metal ion for the sorbent is such that the metal ion sorbs only on a very small fraction (<1%) of the exchange sites, *i.e.*

$$[\overline{CaOX^+}] << [\overline{HOX}] + [Ox^-] + [\overline{CaOX^+}] \qquad (1.2)$$

this is known as trace loading conditions. The distribution coefficient for Ca^{2+} between the solution and the CPG-Oxine, λ_0, is defined as:

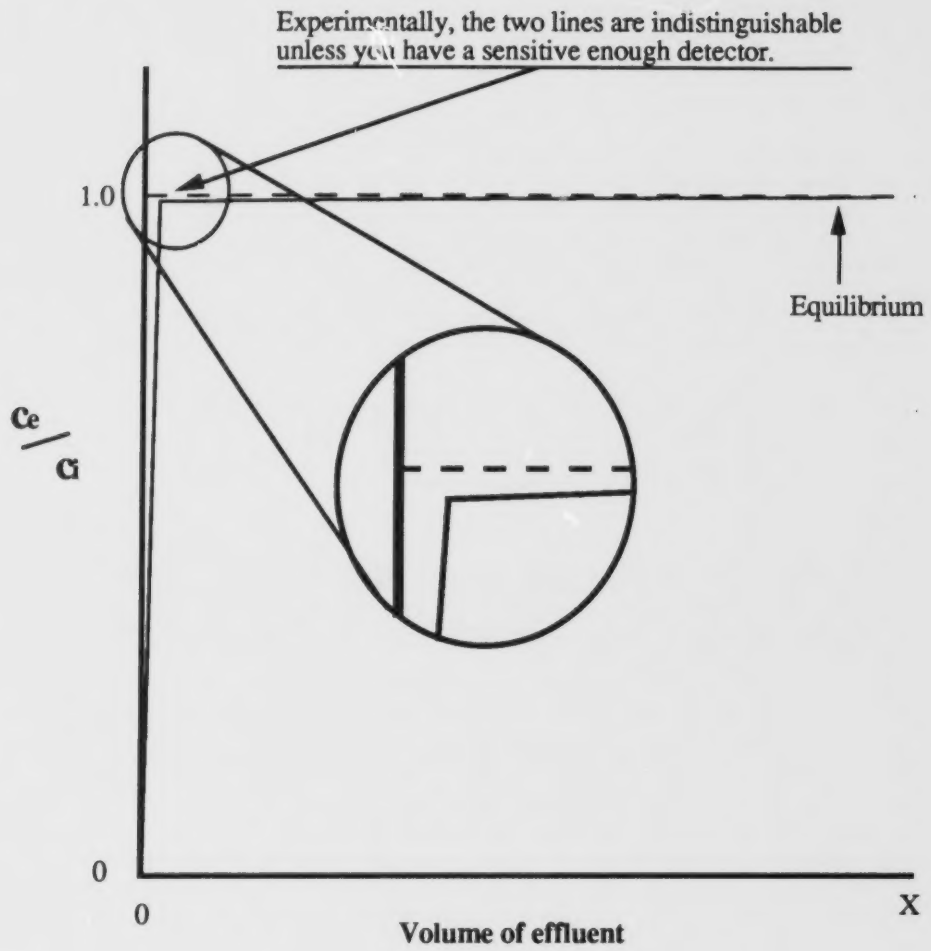

Figure 1.3: Diagrammatic representation of a breakthrough curve with shallow bed conditions within the column.

$$\lambda_O = \frac{\text{Moles of Sorbed Calcium per gram of CPG-Oxine}}{[Ca^{2+}]} \qquad (1.3)$$

Under trace loading conditions, λ_o is a constant. Knowing that, one can thus determine the $[Ca^{2+}]$ in unknown calcium containing solutions. To do this, one would run a series of experiments where one loaded increasing $[Ca^{2+}]$ sample solutions on the column, eluting the sorbed calcium and thus determining λ_o. When λ_o is determined, one would load the unknown Ca^{2+} containing solution, elute and use equation 1.3 to determine $[Ca^{2+}]$.

I.3 DOUBLE LAYER SORPTION MODEL FOR CALCIUM ON CPG-OXINE

Because 5-P-Oxine is an ampholyte containing both a weakly basic heterocyclic nitrogen as well as a weakly acidic phenol group, the degree of ionization of the compound depends on the pH of the solution. But, not only is the bulk solution pH important, the pH immediately adjacent to the surface ($\overline{pH}$) is important in that this determines the degree of ionization of the 5-P-Oxine bound to the surface. The $\overline{pH}$ in most cases is not the same as the pH of the bulk solution due to the nature of the charged surface(42,81,82).

In a previous study (34) $\overline{pH}$ for small-pore diameter (3.2 nm) CPG was related to pH via the polyelectrolyte gel model. (35-37). However, in the present study the pore size of the CPG-Oxine is considerably larger (nominally 50 μm, (19)). With the ionic strength of the sample solution used for the studies in this thesis at 0.02240 M, the "thickness", $(1 / \kappa)$, of the electrical double layer near the charged surface lining the pores is ≈15-20 nm (38,39). The relatively thin electrical double layer means that the bulk solution in the middle of the pores is not influenced by the surface potential. Therefore for this particular

CPG the ionization of the bound 5-P-Oxine can be explained in terms of the "ionizable surface group model".

The basis of this model lies in the relationship between the surface charge density (σ_0, coul/cm^2) and electrical potential of the charge-surface (ψ_0, volt). This relationship is given by the Guoy-Chapman equation (39-41) which, at 25°C, has the form:

$$\sinh\left(\frac{Z \cdot F \cdot \psi_O}{2 \cdot R \cdot T}\right) = (8.53 \times 10^4) \cdot c^{-1/2} \cdot \sigma_O \qquad (1.4)$$

where Z has the value one (with no sign), and is the charge for the silanolate groups, R is the ideal gas constant (8.3144 J/mol·K), F is the Faraday constant (96,485 coul/equiv), T is the absolute temperature (298 K) and c is the ionic strength of the bulk solution (mol/L). Surface charge density (σ_0) can be determined from the surface concentration of the silanolate groups (Q, mmol/gram) as follows:

$$\sigma_o = \frac{Z \cdot F \cdot Q}{1000 \cdot A_{sp}} \qquad (1.5)$$

Here A_{sp} is the specific surface area of the CPG-Oxine which is 7.0 x 10^5 cm^2/gram (19).

The electrical potential at distance x away from the charge surface (ψ_x) can be calculated using the following series of expressions (38,39):

$$\psi_x = \frac{2 \cdot R \cdot T}{Z \cdot F} \cdot \ln\left(\frac{1 + \gamma_{GC} \cdot \exp(-\kappa \cdot x)}{1 - \gamma_{GC} \cdot \exp(-\kappa \cdot x)}\right) \qquad (1.6)$$

where

$$\gamma_{GC} = \frac{\exp\left(\frac{Z \cdot F \cdot \psi_o}{2 \cdot R \cdot T}\right) - 1}{\exp\left(\frac{Z \cdot F \cdot \psi_o}{2 \cdot R \cdot T}\right) + 1} \qquad (1.7)$$

and,

$$\kappa = \left(\frac{2000 \cdot Z^2 \cdot F^2}{\varepsilon_o \cdot D \cdot R \cdot T}\right)^{1/2} \cdot c^{1/2} \qquad (1.8)$$

In these expressions Z has the value one (with no sign), ε_o is the permitivity of a vacuum (1.12×10^{-12} coul/V·cm), D is the dimensionless dielectric constant of water divided by 4π (*i.e.* $78.3/4\pi$) and c is the ionic strength of the bulk solution (mol/L).

The Boltzmann equation shown below (39,40,42) is used to give the relationship between the activity of the hydrogen ion in the bulk solution (a_H) and at a distance x cm away from the charge surface ($\bar{a}_{H,x}$).

$$\bar{a}_{H,x} = a_H \cdot \exp\left(-\frac{F \cdot \psi_x}{R \cdot T}\right) \qquad (1.9)$$

ψ_x can be calculated from Equation 1.6, where the surface charge density can be calculated using Equation 1.5.

In a homogeneous aqueous solution the 5-phenylazo-8-hydroxyquinolinium cation has a pK_{a1} of 3.2 (for cation to neutral species) and a pK_{a2} of 8.6 (for neutral to anionic species) (43). Even if substituents are added at the o-, m-, and p-positions of the 5-phenylazo group of the 5-phenylazo-8-hydroxyquinolinium cation, the pK values do not change by more than ± 0.7 units unless they are very strong electron-withdrawing or donating groups (43). Thus, deprotonation of the cationic group on bound 5-P-Oxine is complete at pH > 6 so that 5-P-Oxine can be treated as a monoprotic acid at pH > 6:

$$\overline{HOX} + \overline{H_2O} \Leftrightarrow \overline{OX^-} + \overline{H_3O^+} \qquad (1.10)$$

The species $\overline{HOX}$ is neutral and is shown in Figure 1.1 (the bar indicates a species in the vicinity of the glass surface). The second dissociation constant, corresponding to the deprotonation from the phenolic hydroxyl group on the 8-hydroxyquinoline ligand in the bound 5-P-Oxine and is given by (39,40):

$$\overline{K}_{a2} = \frac{\overline{[OX^-]}_x \cdot \bar{a}_{H,x}}{\overline{[HOX]}_x} \qquad (1.11)$$

Substituting for $\bar{a}_{H,x}$ in Equation 1.11 from Equation 1.9 gives the following equation where the acidity quotient, $\overline{K}_{a2}'$, is related to the acidity constant ($\overline{K}_{a2}$, with no prime), given in terms of the activity of H^+ at location x by the expression:

$$\overline{K}_{a2}' = \overline{K}_{a2} / \exp\left(-\frac{F \cdot \psi_x}{R \cdot T}\right) = \frac{\overline{[OX^-]}_x \cdot a_{H,x}}{\overline{[HOX]}_x} \qquad (1.12)$$

or,

$$\overline{K}_{a2}' = \overline{K}_{a2} \cdot \exp\left(+\frac{F \cdot \psi_x}{R \cdot T}\right) = \frac{\overline{[OX^-]}_x \cdot a_{H,x}}{\overline{[HOX]}_x} \qquad (1.13)$$

Examining the above equations it is clear that $\overline{K}_{a2}$ is independent of ψ_x, while $\overline{K}_{a2}'$ varies with ψ_x.

The complexation of Ca^{2+} with $\overline{OX^-}$ shown previously in Equation 1.1 can also be included in the "ionizable surface-group model". The stability constant for the complex is:

$$\bar{\beta}_1 = \frac{\overline{[CaOX^+]}_x}{\overline{[OX^-]}_x \cdot \bar{a}_{Ca}} \qquad (1.14)$$

Once again the Boltzmann equation can be used to relate the activity of Ca^{2+} at a distance x cm away from, but close to, the charge-surface ($\bar{a}_{Ca}$) to its activity in the bulk solution (a_{Ca}) (40,44):

$$\bar{a}_{Ca} = a_{Ca} \cdot \exp\left(-\frac{2 \cdot F \cdot \psi_x}{R \cdot T}\right) \qquad (1.15)$$

In the column equilibration experiments CPG-Oxine is first equilibrated with a bulk solution containing Ca^{2+} with an activity a_{Ca} and then the equilibrated CPG-Oxine is eluted with a 0.15 M HNO_3 solution. Therefore, the total number of moles of sorbed calcium per gram of CPG-Oxine ($\bar{N}_{Ca}$(CPG-Ox)) can be expressed as:

$$\bar{N}_{Ca}(\text{CPG-Ox}) = \overline{[CaOX^+]}_x \cdot V_x + \bar{N}_{Ca,\,IEX} \qquad (1.16)$$

where V_x is the volume per gram of CPG-Oxine in the thin layer of solution located at a distance x cm from the charge-surface; $\overline{[CaOX^+]}_x$ is the concentration of complexed calcium in this thin layer of solution. $\overline{[CaOX^+]}_x$ can be expressed by Equation 1.14, as:

$$\overline{[CaOX^+]}_x = \bar{\beta}_1 \cdot \overline{[OX^-]}_x \cdot \bar{a}_{Ca} \qquad (1.17)$$

where $\bar{a}_{Ca}$ is given by Equation 1.15, and

$$\overline{[OX^-]}_x = \frac{\bar{\alpha}_{OX} \cdot \bar{\nu}_{Oxine}}{V_x} \qquad (1.18)$$

$\bar{\nu}_{Oxine}$ is the moles of bound 5-P-Oxine per gram of CPG-Oxine. Substituting for $\bar{a}_{Ca}$ and $\overline{[OX^-]}_x$ in Equation 1.17 from Equations 1.15 and 1.18 gives

$$\overline{[CaOX^+]}_x = \overline{\beta}_1 \cdot \frac{\overline{\alpha}_{OX} \cdot \overline{\nu}_{Oxine}}{V_x} \cdot a_{Ca} \cdot \exp\left(-\frac{2 \cdot F \cdot \psi_x}{R \cdot T}\right) \qquad (1.19)$$

where, $\overline{\alpha}_{OX}$ is defined in terms of both the activity of H^+ in the bulk solution, $a_H = 1.0 \times 10^{-7}$ mol/L, and the acid dissociation quotient for the phenolic hydroxyl group on the immobilized oxine, $\overline{K}_{a2}'$ (45,46):

$$\overline{\alpha}_{OX} = \frac{\overline{K}_{a2}'}{\overline{K}_{a2}' + a_H} \qquad (1.20)$$

Combining equations 1.13 and 1.20 and taking into account that at pH = 7.00, $a_H >> \overline{K}_{a2}'$ gives the following expression:

$$\overline{\alpha}_{OX} = \overline{K}_{a2} \cdot a_H^{-1} \cdot \exp\left(+\frac{F \cdot \psi_x}{R \cdot T}\right) \qquad (1.21)$$

which is the fraction of bound 5-P-Oxine ionized. The quantity $\overline{N}_{Ca,\,IEX}$ in Equation 1.16 is the moles of sorbed Ca^{2+} not complexed by bound 5-P-Oxine. This Ca^{2+} would be present in solution in the diffuse part of the electrical double layer as a result of cation exchange for Na^+. The SiO^- fixed charge sites on the glass surface create the cation exchangers. The ion-exchange equation can be stated as:

$$Ca^{2+} + 2\,\overline{R^-Na^+} \Leftrightarrow \overline{R_2Ca} + 2\,Na^+ \qquad (1.22)$$

The conditional ion-exchange constant K_{IEX}' is:

$$K_{IEX}' = \frac{(\Gamma_{DL,Ca} \cdot \gamma_{DL,Ca}) \cdot [Na^+]^2 \cdot \gamma_{Na}^2}{([Ca^{2+}] \cdot \gamma_{Ca}) \cdot \Gamma_{DL,Na}^2 \cdot \gamma_{DL,Na}^2} \qquad (1.23)$$

where $\Gamma_{DL,Ca^{2+}}$ and $\Gamma_{DL,Na^{+}}$ are the surface excesses of all the Ca^{2+} and Na^{+} in the diffuse layer (mol/cm^2); $\gamma_{DL,i}$ is the ionic activity coefficient of species i in the diffuse layer; γ_i is the ionic activity coefficient of species i in the bulk solution. The ion-exchange distribution coefficient for Ca^{2+} is:

$$K'_{Ca,\,IEX} = \frac{\Gamma_{DL,Ca}}{[Ca^{2+}]} = \frac{\overline{N}_{Ca,\,IEX}}{[Ca^{2+}]} = K'_{IEX} \cdot \frac{\Gamma^2_{DL,Na} \cdot \gamma^2_{DL,Na} \cdot \gamma_{Ca}}{[Na^{+}]^2 \cdot \gamma^2_{Na} \cdot \gamma_{DL,Ca}} \qquad (1.24)$$

At trace conditions of ion exchange the surface excess of sodium ($\Gamma_{DL,Na}$) can be expressed as:

$$\Gamma_{DL,Na} \cong \frac{Q}{1000 \cdot A_{sp}} = \frac{\sigma_o}{Z \cdot F} \qquad (1.25)$$

where Q is the surface concentration of ionized surface groups (mmol/g). Equation 1.24 can be combined with Equation 1.25 to give the expression:

$$K'_{Ca,\,IEX} \approx K'_{IEX} \cdot \frac{\left(\frac{Q}{1000 \cdot A_{SP}}\right)^2}{[Na^{+}]^2} \cdot \frac{\gamma^2_{DL,\,Na} \cdot \gamma_{Ca}}{\gamma^2_{Na} \cdot \gamma_{DL,\,Ca}} \qquad (1.26)$$

further rearranging gives:

$$K_{Ca,\,IEX} = K'_{IEX} \cdot \frac{\left(\frac{Q}{1000 \cdot A_{SP}}\right)^2}{[Na^{+}]^2} \cdot \frac{\gamma^2_{DL,\,Na} \cdot \gamma_{Ca}}{\gamma^2_{Na} \cdot \gamma_{DL,\,Ca}} \cdot 1000 \cdot A_{SP}$$

$$= \frac{\overline{N}_{Ca,\,IEX}}{[Ca^{2+}]} \qquad (1.27)$$

Rearranging Equation 1.27 one can get the ion-exchange term for Ca^{2+} on CPG-Oxine ($\overline{N}_{Ca,\,IEX}$, from Equation 1.16) which can be expressed as the number of moles of sorbed calcium per gram of CPG-Oxine:

$$\overline{N}_{Ca,\,IEX} = [Ca^{2+}] \cdot K_{IEX} \cdot 10^{-6} \cdot \frac{\bar{\gamma}^2_{DL,Na} \cdot \bar{\gamma}_{Ca}}{\bar{\gamma}^2_{Na} \cdot \gamma_{DL,Ca}} \cdot \frac{Q^2}{[Na^+]^2} \qquad (1.28)$$

Finally, combining Equations 1.16, 1.19, 1.21 and 1.28 gives an equation which quantitatively expresses the moles of Ca^{2+} sorbed per gram of CPG-Oxine, $\overline{N}_{Ca}$(CPG-Ox), when Ca^{2+} is present at trace conditions:

$$\overline{N}_{Ca}(CPG\text{-}Ox) = [Ca^{2+}] \cdot \gamma_{Ca} \cdot \bar{v}_{Oxine} \cdot \bar{\beta}_1 \cdot \bar{K}_{a2} \cdot a_H^{-1} \cdot \exp\left(-\frac{F \cdot \psi_x}{R \cdot T}\right) +$$

$$[Ca^{2+}] \cdot 10^{-6} \cdot K_{IEX} \cdot \frac{\bar{\gamma}^2_{Na} \cdot \gamma_{Ca}}{\gamma^2_{Na} \cdot \bar{\gamma}_{Ca}} \cdot \frac{Q^2}{[Na^+]^2} \qquad (1.29)$$

1.4 RESEARCH OBJECTIVES

Previous studies of CPG-Oxine have explored its acid-base character (45) and its ability to complex Ca^{2+} (46). During these studies an unexpected phenomenon was observed while performing a simple Ca^{2+} equilibration study. In this equilibration study a loading curve was generated. A loading curve is a plot of the **number of moles of Ca^{2+} sorbed** versus the **loading time**. The loading curve, instead of slowly approaching an equilibrium value over time, as in Figure 1.4a, passes through a local maximum and then slowly approaching a sustained equilibrium.. Shown diagrammatically (not to scale) in Figure 1.4b, is this overshoot phenomnon.

In previous studies this phenomenon was studied at a rudimentary level in that only four basic studies were done: 1. the effect of particle size within the column, 2. the effect

of column size itself (10 mg versus 40 mg of CPG-Oxine packing), 3. the effect of preconditioning the column with 0.0100 M HEPES before sample loading, and 4. sodium sorption on the CPG-Oxine. A basic investigation of the kinetic phenomena involved was not undertaken at that time. Therefore, the objective of this thesis is to provide a basic understanding of the kinetics involved in the Ca^{2+} sample loading.

An improved column equilibration technique, which ensured shallow bed conditions with-out a buffer wash, was developed to undertake these studies. The double-layer sorption model is combined with a porous-gel model in explaining the link between the Ca^{2+} sorption/desorption and the Na^{+} sorption.

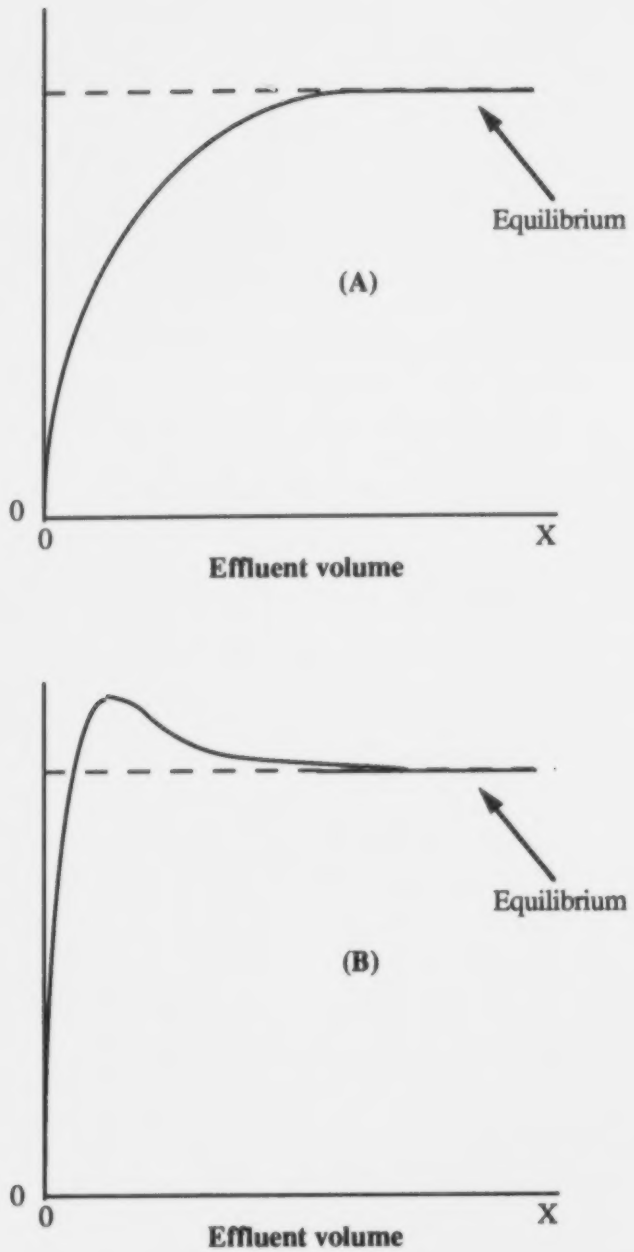

Figure 1.4 (A) Expected loading curve slowly approaching equilibrium. (B) A diagrammatic representation of the overshoot phenomenon (not to scale) shown slowly approaching the equilibrium value from above, not below as expected.

CHAPTER TWO

Anomalous Kinetics of Ca^{2+} Sorption on Controlled Pore Glass-Oxine

In this chapter the principles underlying the column equilibration technique and the shallow bed kinetic technique are presented. The apparatus used to measure the amount of sorbed Ca^{2+} and Na^{+} is described. The conditions to be used for loading, washing (in the case of sodium only), and eluting the CPG- Oxine column are discussed.

II.1 INTRODUCTION

With a "column equilibration method" the Ca^{2+}-containing sample solution is pumped through a small column of CPG-Oxine for a sufficiently long period of time that the entire column comes to equilibrium with the solution. This is the *loading step*. The Ca^{2+}-containing sample solution is typically buffered at pH = 6 to 8 and contains a relatively large concentration of inert electrolyte (*e.g.* $NaClO_4$) in order to operate in the linear region of the Ca^{2+} sorption isotherm. A brief water wash of the column may be performed after the loading step. The column is next eluted with dilute nitric acid into the flame of an atomic absorption spectrophotometer in order to measure the amount of Ca^{2+} that has been sorbed. The column is then ready to be loaded with the next Ca^{2+}-containing sample solution. It is a key point of interest for the presently reported study that the Ca^{2+} loading step is performed on a column that has previously been eluted with acid.

Verification that the column has reached equilibrium with the Ca^{2+}-containing sample solution during the loading step is obtained by measuring a *loading curve* (28,46,47). This is a plot of moles of Ca^{2+} sorbed versus time during which the solution

has been pumped through it. An unexpected feature of the loading curve for Ca^{2+} on CPG-Oxine is the fact that it passes through a maximum at about 1 to 4 min, followed by a decrease to the equilibrium plateau value after about 2 hours (46,47). Since the loading curve represents an approach of the system to equilibrium, this maximum would appear to be an "overshoot" of equilibrium.

Although equilibrium "overshoot" is rare in heterogeneous kinetics, it is not unknown. It has been reported for ion exchange in ternary counterion systems where, for example, two different counterions are exchanging for a third counterion and the diffusion rate of one of the two exchanging ions is greater than that of the second exchanging ion (48-50). The loading curve for the faster-diffusing ion may exhibit a maximum. For example, in the simultaneous exchange of anionic cyano-complexes of silver and of zinc for the anion CN^-, the silver-cyano species diffuse into the anion exchange resin faster than the zinc-cyano species so that the loading curve for the silver-cyano species exhibits a distinct maximum (50).

It would seem, at first thought, that the sorption of Ca^{2+} by CPG-Oxine is not analogous to a ternary ion exchange system, so that the reason for the "overshoot" in the Ca^{2+} loading curve is not obvious. Furthermore, this kind of "overshoot" phenomenon was not observed in the loading curve of Mg^{2+} on a sorbent prepared by binding 8-hydroxyquinoline onto the nonpolar styrene-divinylbenzene copolymer Amberlite XAD-2 (51,52). This suggests that it may arise from the properties of Controlled Pore Glass.

Since Controlled Pore Glass has many uses in separation science and technology, such as that of a column packing in size-exclusion chromatography (53) and that of a support for immobilizing both ligands and reagents for affinity chromatography (54), it is important to elucidate the processes giving rise to the anomalous kinetics of Ca^{2+} sorption on CPG-Oxine. An understanding of surface-charge effects on size-exclusion column packings is especially important when ionic sample components are to be chromatographically separated.

II.2 EXPERIMENTAL SECTION

II.2.1 REAGENTS AND CHEMICALS

CPG-Oxine (Pierce Chemical Co.), batch B (lot # 850605085), with particle diameter 125-177 μm and pore diameter of 50 μm, was used for all studies.

Controlled Pore Glass (Pierce Chemical Co., lot # 860313081). It has a particle diameter of 125-177 μm and pore diameter of 50 μm.

All solutions were prepared in nanopure (Barnstead/Thermolyne) water. The nanopure water was also used for column washing during all experiments.

Calcium stock solutions were prepared by dissolving analytical grade $CaCO_3$ (BDH Chemicals) in concentrated HNO_3.

4-(2-Hydroxyethyl)-1-piperazineethanesulfonic acid, HEPES (Sigma manufacturers), was used as a buffering agent.

Sodium perchlorate (hydrated), $NaClO_4 \cdot H_2O$ (Fisher Scientific Co.) was used as an ionic strength modifier.

Nitric acid, HNO_3 (BDH standard stock), analytical reagent grade, was used to prepare the eluent.

Sodium hydroxide, NaOH (BDH chemicals), and ammonium hydroxide, NH_4OH (Fisher standard stock) were used to adjust the pH.

Copper stock solution was prepared by dissolving fine copper metal powder (Baker and Adamson) in 5 M HNO_3.

Sodium Acetate, $NaC_2H_3O_2$-$3H_2O$ (Anachem) was used to prepare a buffer for use in the capacity study.

II.2.2 APPARATUS

The column equilibration apparatus is shown in Figure 2.1. It was similar to the one used in earlier studies of Ca^{2+} sorption (46), with some notable modifications. Sample solution, eluent and either water or preconditioning solution were all pumped by a variable speed Minipuls peristaltic pump (P) (Gilson, Minipuls 2, Model #46963) using 0.110 inch i.d. (Standard PVC mainfold pump tubing, Fisher Scientific) pump tubes. Sample solution, containing Ca^{2+}, was continuously pumped through one of the two channels on valve V1, to waste. This valve, which contained the "column" of CPG-Oxine, is shown in more detail in Figure 2.2, and the column itself is shown in even more detail in Figure 2.3. Eluent was continuously pumped through the 10 μL slider injection valve V2 (Model CSV10, Laboratory Data Control, Supelco) into a 4-port selector valve V3 (Model CAV-4031, LDC). Water, or alternatively preconditioning solution when the latter was required in an experiment, was also pumped continuously into valve V3. Valve V3 directed either the water/preconditioning solution or the eluent through the second channel in valve V1, while diverting the other to waste. When either water or eluent was flowing through V1 it exited *via* a Teflon capillary tube into the nebulizer of the spectrometer. When preconditioning solution was flowing through V1 the tube connecting V1 to the spectrometer was disconnected and the preconditioning solution was allowed to flow to waste. This was done to prevent the relatively high salt concentration in the preconditioning solution from entering the nebulizer. Valves V1, V2 and V3, along with the solution reservoirs, were immersed in a large water bath thermostated at 25 ± 1°C.

All glassware was cleaned with dilute nitric acid and rinsed with distilled water. Measurements of pH were made with a pair of glass and calomel electrodes using an Accumet Model 320 pH Meter (Fisher Scientific). Flame atomic absorption (AA) measurements of calcium were made at 422.7 nm using a Model 4000 spectrometer (Perkin Elmer) or a model SpectraAA-10 spectrometer (Varian). The inlet capillary to the nebulizer

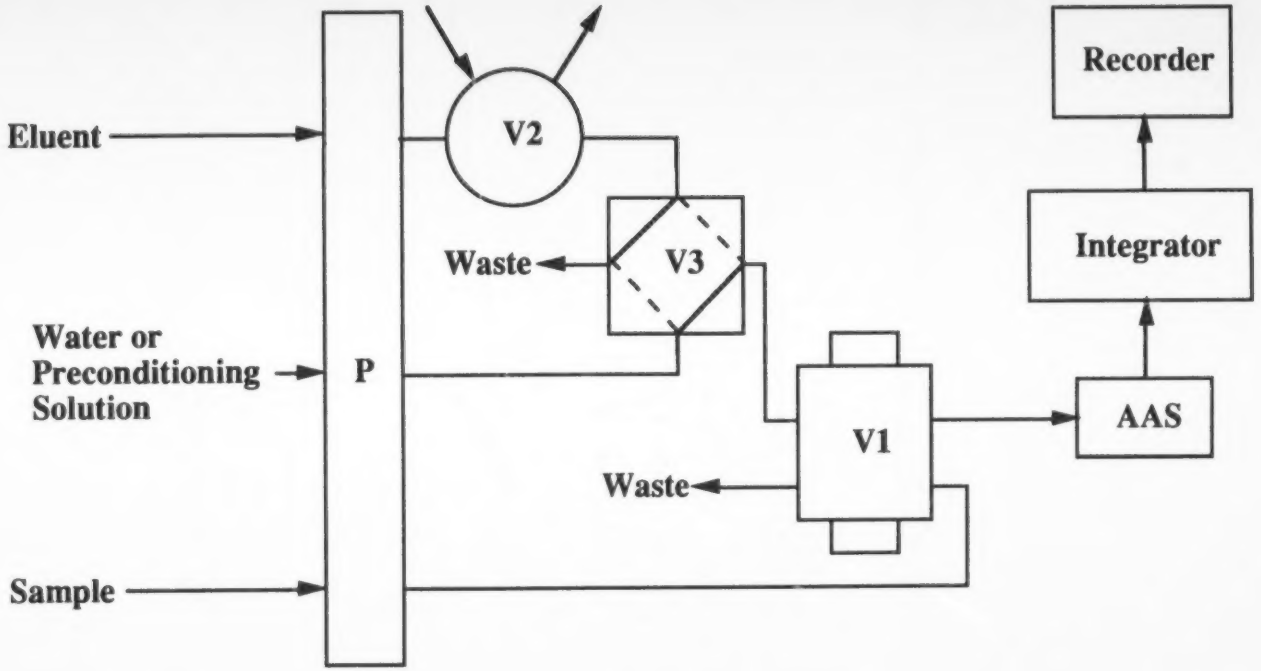

Figure 2.1 : Diagram of operating system

of the instruments was connected to the column equilibration apparatus as described below. The AA signals were in the form of peaks, the areas of which were measured with the digital integrator on-board the spectrometer. Flame atomic emission (AE) measurements of sodium were made at 589.0 nm on a model AA-10 spectrometer (Varian) by connecting the column equilibration apparatus directly to the nebulizer *via* a capillary, as described below. Flame atomic absorption measurements of copper, made as described below in connection with the determination of complexation capacity of CPG-OXINE, were made on a Model 290B spectrometer (Perkin Elmer). Peak areas in this case were measured with a Model CR601 digital integrator (Shimadzu Corp.). The peristaltic pump rates and AAS conditions are listed in tables 2.1- 2.3.

II.2.3 COLUMN PREPARATION

The CPG-Oxine particles are orange in colour. The commercially available CPG-Oxine originally contained some opaque white particles which the manufacturer believed were underivatized glass beads (55). Prior to packing the column the CPG-Oxine was spread out on a piece of paper and the large opaque particles were removed. The remaining CPG-Oxine was then washed several times with nanopure water. After each washing the fines were removed by decantation. The washed CPG-Oxine was then air dried overnight and was then ready to use.

In Figures 2.2 & 2.3 the column from valve V1 is shown in more detail . Shown are the two Teflon face-plates and the Kel-F slider. Valve V1 is a slider injection valve that has been modified by widening the three holes through the Kel-F slider so that they are each 2.13 mm wide × 6.10 mm long. The middle hole in Figure 2.2 is the "column" which is shown enlarged in Figure 2.3. Inserted in each end of this column is a bed-support which is composed of a 2.08 mm × 0.75 mm Kel-F disk, through which has been drilled 25 holes that are 0.0033 mm in diameter. Between the disk and the bed of CPG-Oxine is a pad of

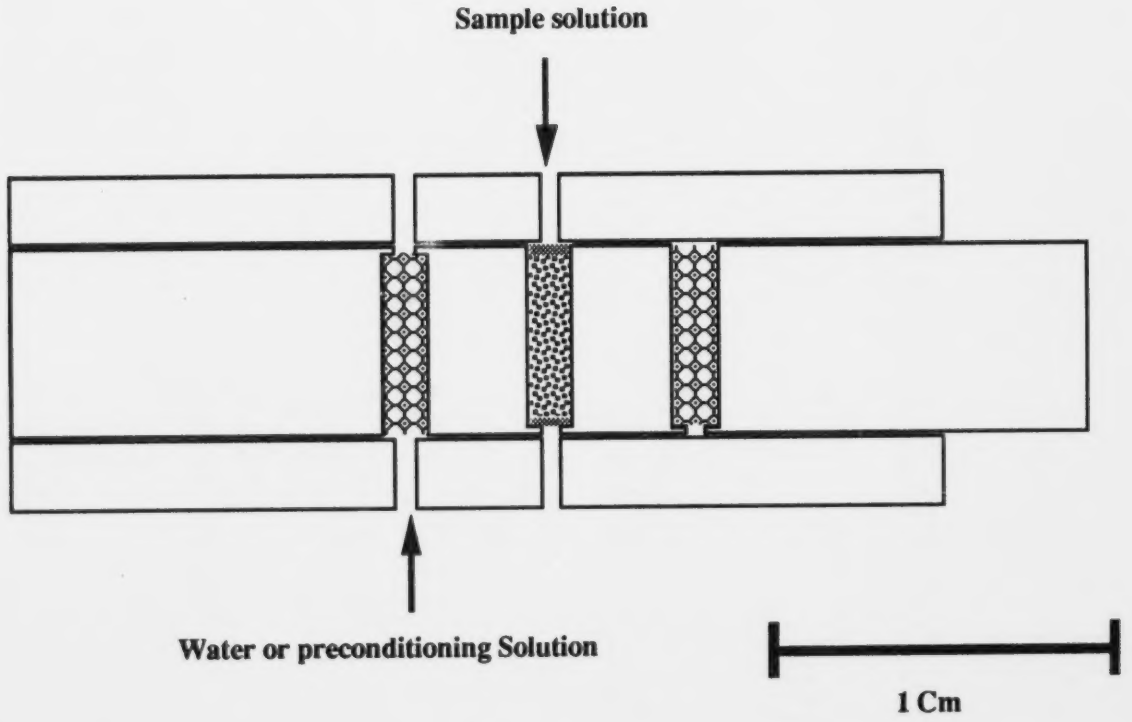

Figure 2.2: Slider from valve V1 in Figure 2.1. Centre hole contains the CPG-Oxine packing. Two side holes contain sintered glass frits (nominal pore size 50 μm)

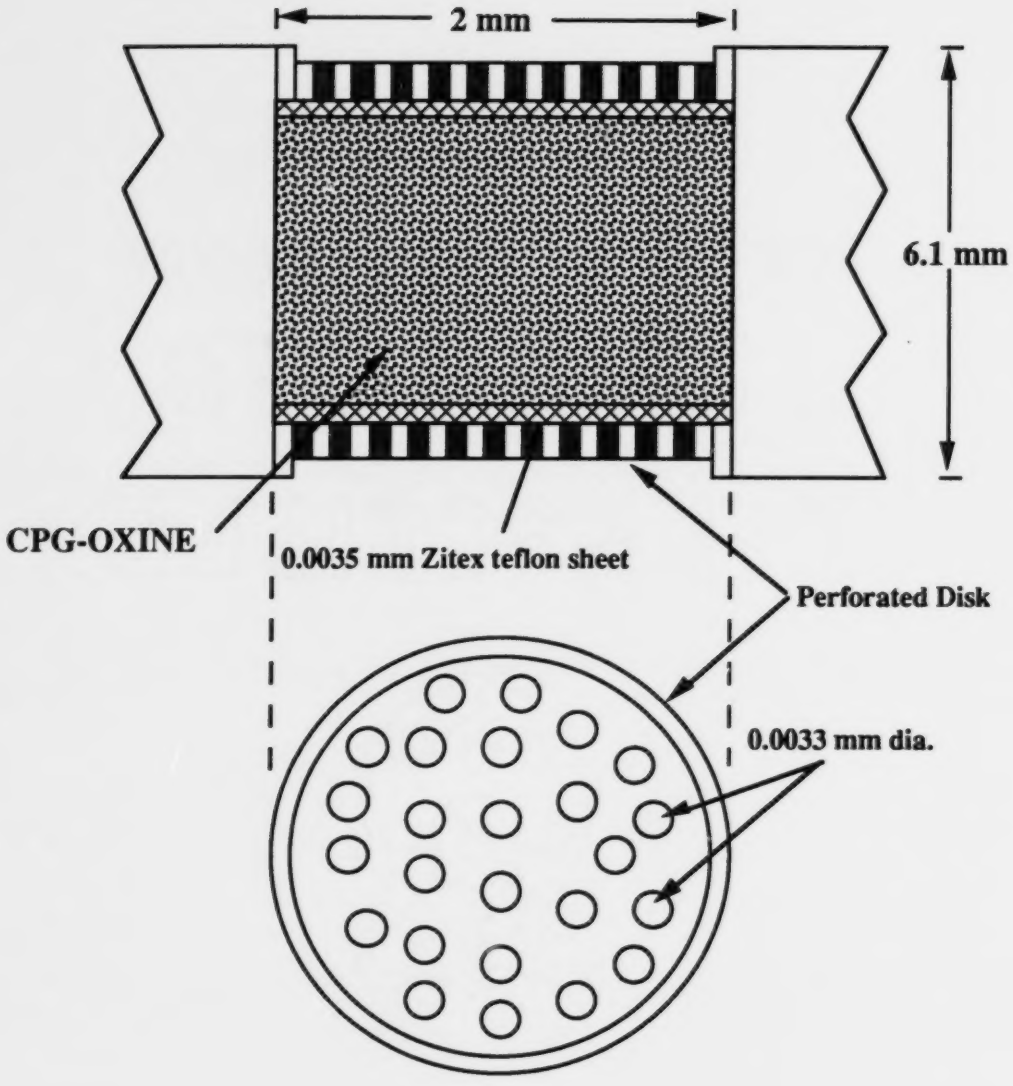

Figure 2.3 : Enlargement of center hole (column area) from Figure 2.2.

Table 2.1 : Instrument conditions for monitoring Calcium and Sodium with the PE Model 4000 AAS

Wavelength	422.7 nm (Ca); 589.0 nm (Na)*
Spectral Slit Width	0.7 nm (Ca); 0.2 nm (Na)*
Lamp Current	15 mA
Flame	Oxidizing (Lean, blue)
Acetylene Pressure	8 psig
Air Pressure	30 psig
Aspiration Rate	5.4 mL/min
Eluent Flow Rate	5.0 mL/min
Sample Flow Rate	4.5 mL/min
Recorder Type	Fisher Recordall 5000
Voltage Range	1 to 10 mV full scale
Chart Speed	1.25 cm/min

* : Sodium was determined by atomic emission (AE) spectrophometry

Table 2.2 : Instrument conditions for monitoring Calcium and Sodium with the Varian SpectraAA-10 Spectrometer

Wavelength	422.7 nm (Ca); 589.0 nm (Na)*
Spectral Slit Width	0.5 nm (Ca); 0.2 nm (Na)*
Lamp Current	10 mA
Flame	Oxidizing (Lean, blue)
Acetylene Pressure	1.5 psig
Air Pressure	3 psig
Aspiration Rate	5.0 mL/min
Eluent Flow Rate	5.0 mL/min
Sample Flow Rate	4.5 mL/min
Recorder Type	Computer Acquisition of data

* : Sodium was determined by atomic emission (AE) spectrophometry

Table 2.3 : Instrument conditions for monitoring Copper with the PE Model 290B AAS

Wavelength	281.5 nm
Spectral Slit Width	0.7 nm
Lamp Current	10 mA
Flame	Oxidizing (Lean, blue)
Acetylene Pressure	8 psig
Air Pressure	32 psig
Aspiration Rate	2.25 mL/min
Eluent Flow Rate	2.25 mL/min
Sample Flow Rate	2.05 mL/min
Recorder Type	Model CR601 Shimadzu digital integrator

porous Teflon (2.08 × 0.19 mm with 30–60 μm pores, Part #K1064-122D Zitex, Chemplast Inc.). The bed supports retain the 5.4 mg, 4.5 mm long bed of CPG-Oxine. Each of the two side holes through the Kel-F slider in valve V1 is fitted with an approximately 6 mm long plug of sintered glass (nominal pore size 50 μm) to provide the same resistance to flow as that of the "column" in the centre hole. By incorporating the CPG-Oxine in the slider, the hold-up volume (≈17 μL) associated with the column was reduced compared to what it was in the previous design (46) (≈76 μL).

In one study, underivatized Controlled Pore Glass (CPG) (Batch 860313081, Pierce Chemical Co.) was used. Particles were 125–177 μm diameter. The CPG was prepared and treated in the same way as the CPG-Oxine above. A weight of 4.7×10^{-3} g was dry packed into the central hole of the slider of valve V1.

A second column containing 32.7 mg of CPG-Oxine was designed for the sodium sorption studies. The CPG-Oxine was weighed and packed into a 7 cm length of 1.5 mm i.d. Teflon tubing flared at both ends and is shown in Figure 2.4. This length of tubing was required to accommodate the Cheminert fittings (LDC) and to give a larger column, thus giving larger sodium signals. The 32.7 mg of CPG-Oxine was prepared as previously discussed in II.2.2 and was dry packed into the tube as follows: Approximately 2 mm long glass frits were made by drilling cores from a sintered glass plate (nominal pore size 50 μm). One frit was pressed into one end of the tubing until flush with the flaring. With one end plugged the CPG-Oxine was slowly loaded into the tube with a small scoop. When all of the CPG-Oxine was loaded the 2mm space left at the top for the glass frit was filled with the glass frit. A tiny air space was left at the top to avoid excessively compacting the packing. The packed column was placed in a loop between two coupled 4-way valves (Model CAV-4031, LDC). This configuration, which has been described previously (28), allows simultaneous flow of two solutions, one through the column and one to waste. It was substituted for valve V1 in the apparatus shown in Figure 2.1

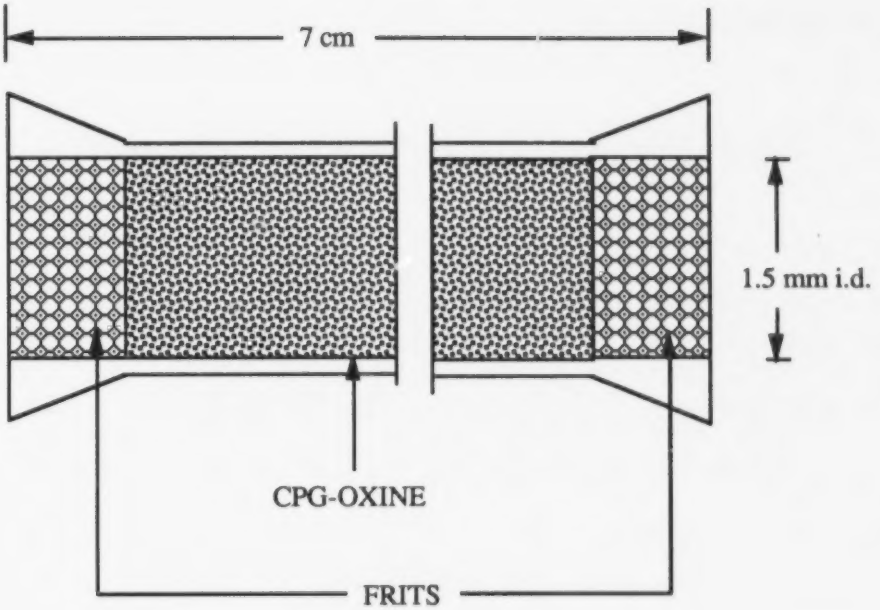

Figure 2.4: Diagram of 7 cm x 1.5 mm CPG-Oxine column

II.2.4 PREPARATION OF TEST SOLUTIONS

All solutions were prepared with nanopure water (Barnstead). All chemicals were reagent grade or purer. A calcium stock solution was prepared by dissolving analytical grade $CaCO_3$ (BDH Chemicals) in dilute nitric acid. A 0.50 M buffer stock solution was prepared by dissolving 4-(2-hydroxyethyl)-1-piperazinethane sulfonic acid (HEPES, Sigma Chemical Co.) in water and adjusting to pH = 7.00 with concentrated NH_4OH. A 1.00 M stock solution of $NaClO_4$ was prepared in water.

Calcium-containing sample solutions at various concentrations of Ca^{2+}, HEPES buffer and $NaClO_4$ were prepared volumetrically as in the following example of 2 x 10-5 M Ca^{2+} in 0.0200 M $NaClO_4$ at pH = 7.00: 40.0 mL of $NaClO_4$ stock solution (1.0 M) and 20 mL of HEPES buffer solution (1.0 M) were added to a clean (HNO_3 rinsed) 1000 mL beaker. About 1600 mL of nanopure water and 16 mL of Ca^{2+} stock solution (2.5 x 10^{-3} M) were added and the pH was adjusted to 7.00 with NH_4^+OH. The solution was then quantitatively transferred to a 2000 mL volumetric flask, diluted to almost 2000 mL and shaken well. The pH was then rechecked and readjusted with small amounts of dilute NaOH or HNO_3. The volume of the final solution was adjusted to the mark , shaken well, then vacuum filtered through a 40-60 μm mesh filter upon which it was ready to use. Calcium-free preconditioning solutions were prepared in an identical manner as the sample solutions except that the calcium solution was withheld.

II.2.5 EXPERIMENTAL PROCEDURE

All solutions were pumped at a flow rate of 5.0 mL/min, unless noted otherwise. Initially the column was in the *eluent/water line* of valve V1, Figure 2.1, and was washed with 0.15 M HNO_3 to clear the packing of any residual sample or preconditioning solution.

Dilute HNO_3 is a suitable eluent for calcium; its concentration is not critical because chelation between Ca^{2+} and $\overline{OX}^-$ is rather weak. Upon the start of an experiment the column was switched into the *sample line* of valve V1 and the Ca^{2+} sample solution was then pumped through the column by the peristaltic pump (P) and on into waste. As well, water and eluent were pumped respectively to valve V3. In this case, the eleunt would follow the dotted line thus flowing through channel 2 in valve V2 and on into the AAS. This eluent flow would thus form a stable baseline for the AAS integrator. Meanwhile, the water would flow to waste until needed. When the prescribed load time was reached, slider V1 was switched into the *eluent/water line* thus eluting the contents of the column into the AAS. A washing step was not needed to wash out the interstitial Ca^{2+} solution because the hold-up volume has been significantly reduced so as not to cause much error in the eluted Ca^{2+} results . In fact, the void volume usually contained an amount of Ca^{2+} equal to only about 1% of the sorbed Ca^{2+}.

The width of the resulting asymmetric calcium peak , measured from the point at which the resulting tracing left the baseline to the point when it rejoins the baseline was about 15 seconds. Therefore the integration time for the on board integrator was set at 20 seconds with the integrator of the Perkin-Elmer Model 4000 AAS measuring the resultant peak areas. Peak heights read from the chart paper, were found to be less precise and accurate.

Following the elution of the sample peak, a series of standard injections were made to quantify the eluted Ca^{2+} peak. While the column was still in the *eluent/water line* of V1, a 10 μL injection of a 2×10^{-3} M Ca^{2+} solution was injected using valve V2. Valve V2 is simply an injection valve with a load position and an inject position. While in the load position a syringe was used to fill the 10 μL injection loop. Then upon switching to the inject position a concentrated Ca^{2+} plug was sent to the AAS. After repeated standard injections the next loading experiment was undertaken.

II.2.6 CAPACITY MEASUREMENT (Performed by Oreola Donini)

The complexation capacity of batch B (Lot # 850605085) was determined in 3 steps using the column equilibration apparatus shown in Figures 2.1 and 2.2. The experimental procedure detailed above in section II.2.5 was modified slightly to include a wash step following the loading step. The washing step is needed in this case because the Cu^{2+} concentration in the void volume was too large to ignore when quantifying the amount of eluted Cu^{2+}. The Cu^{2+} quantification was done using a standard calibration curve created by injecting Cu^{2+} solutions under similar conditions through the column directly into the AAS and measuring the peak areas.

As a wash step was required, a wash time that would properly rinse out the interstital Cu^{2+} solution from the column was needed. A suitable wash time was determined by loading the column for 10 minutes with a solution containing 1.26×10^{-3} M Cu^{2+} and 0.0900 M HOAc/NaOAc (pH = 5.00) and then washing with N_2 sparged deionized water for increasing lengths of time. The Cu^{2+} in the column was then eluted directly into the flame of the AAS. As seen in Figure 2.5, a plot of moles Cu^{2+} eluted versus wash time reaches a plateau at around 10 minutes. From the plot it was concluded that a 10 minute wash time is suitable to wash the Cu^{2+} containing solution from the void volume.

To correctly determine the capacity of the CPG-Oxine, the sample solution must be in equilibrium with the CPG-Oxine. To determine the point at which equililibrium is achieved a loading experiment must be done. A solution containing 3.15×10^{-4} M Cu^{2+} and 0.0900 M HOAc/NaOAc (pH = 5.00) solution was pumped through the column for increasing lengths of time, washed for 10 minutes with N_2 sparged deionized water, and then eluted with 0.15 M HNO_3 directly into the AAS. By plotting the moles of Cu^{2+} sorbed versus load time, a loading curve is generated, shown in Figure 2.6, in which there is a gradual rise to an equilibrium value. Taking the point where the graph reaches a

plateau as the point of equilibrium between the sample and the sorbent, a load time of 2 minutes is sufficient.

To determine the CPG-Oxine capacity, a range of Cu^{2+} solutions (3.15×10^{-4} M to 4.72×10^{-3} M in 0.0900 M HOAc/NaOAc, pH = 5.00) were loaded for 2 minutes, washed for 10 minutes and finally eluted with 0.15 m HNO_3. Figure 2.7 shows a plot of moles Cu^{2+} sorbed versus Cu^{2+} concentration.

II.2.7 Ca^{2+} LOADING STUDIES

These were performed in the apparatus shown in Figures 2.1 and 2.2 using the Model 4000 AA spectrometer. Two different versions of the Ca^{2+} loading experiment were employed with the CPG-Oxine column: (i) the normal procedure, without preconditioning; and (ii) the procedure with column preconditioning. In the normal procedure the column was washed with water for 2.0 min after having been eluted with 0.15 M HNO_3 at the end of the preceding cycle. Next, in the loading step, the sample solution, containing 2.00×10^{-5} M Ca^{2+}, 0.0100 M HEPES buffer (pH = 7.00) and 0.0200 M $NaClO_4$, was pumped through the column for a specified period of time varying from 2 min to 4 hours. Immediately following the loading step the column was eluted for 4.0 min with 0.15 M HNO_3 directly into the AA spectrometer.

In the alternate procedure the elution step from the previous cycle was followed by pumping preconditioning solution, not water, for a specific period of time varying from 2 min to 4 hours. After this preconditioning step the same Ca^{2+}-containing solution described in the preceding paragraph was loaded onto the column for 2.0 min only. Finally, after the 2.0 min loading step, the column was eluted for 4.0 min with 0.15 M HNO_3 into the AA spectrometer.

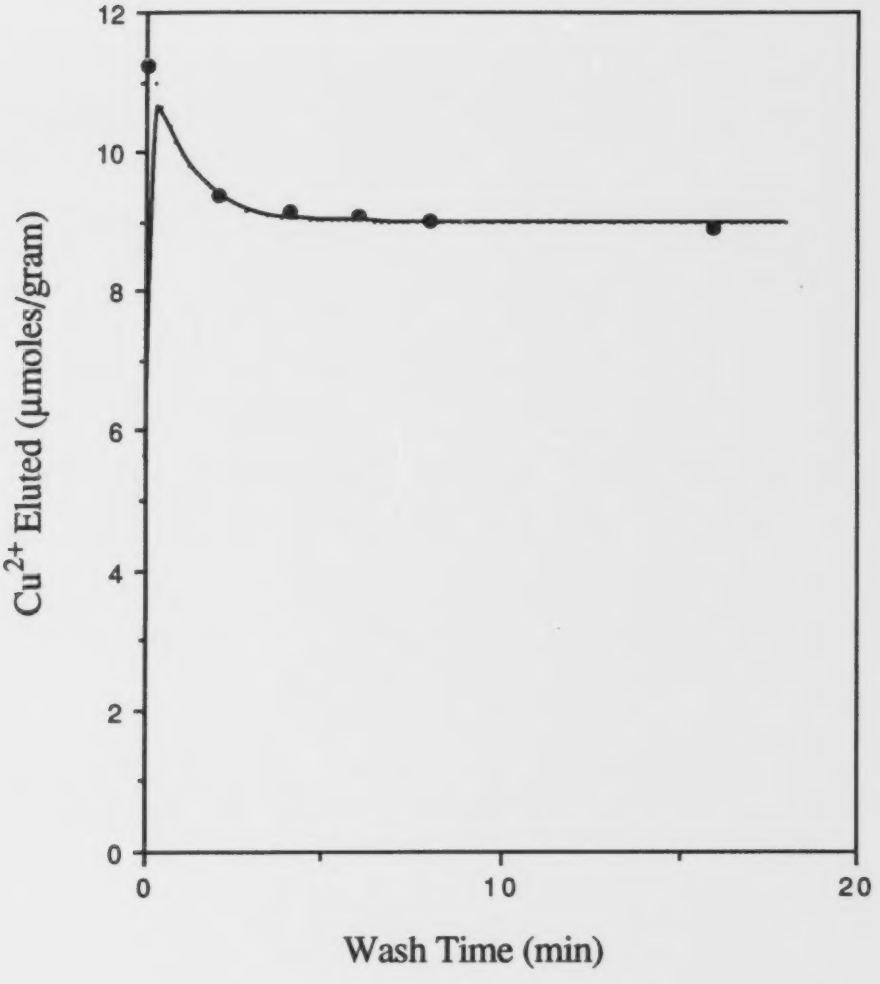

Figure 2.5 : Plot of capacity washing study data. A 1.26×10^{-3} M Cu^{2+} in 0.0900 M NaOAc (pH=5.00) loaded for 10-mins and washed for increasing lengths of time with N_2 sparged DI water.

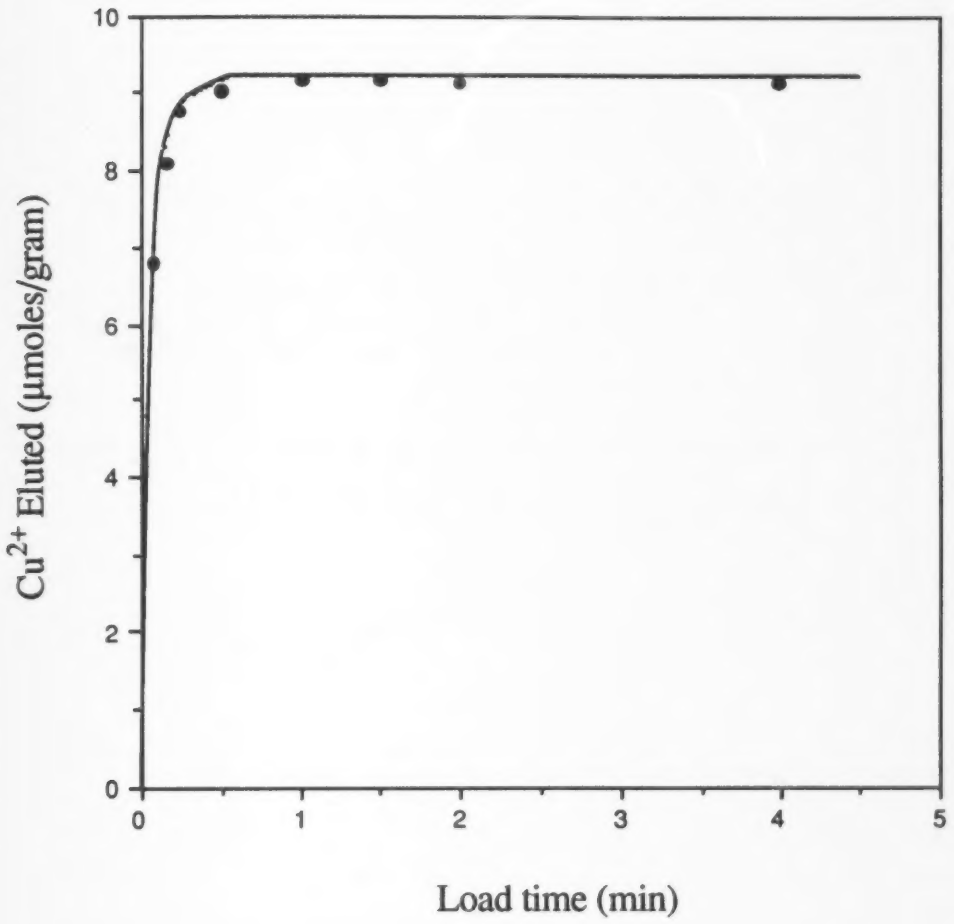

Figure 2.6 : Plot of loading study data for the capacity study. A 3.15 x 10^{-4} M Cu^{2+} solution in 0.0900 M NaOAc (pH=5.00) was loaded for increasing lengths of time and washed for 10-mins with N_2 sparged DI water.

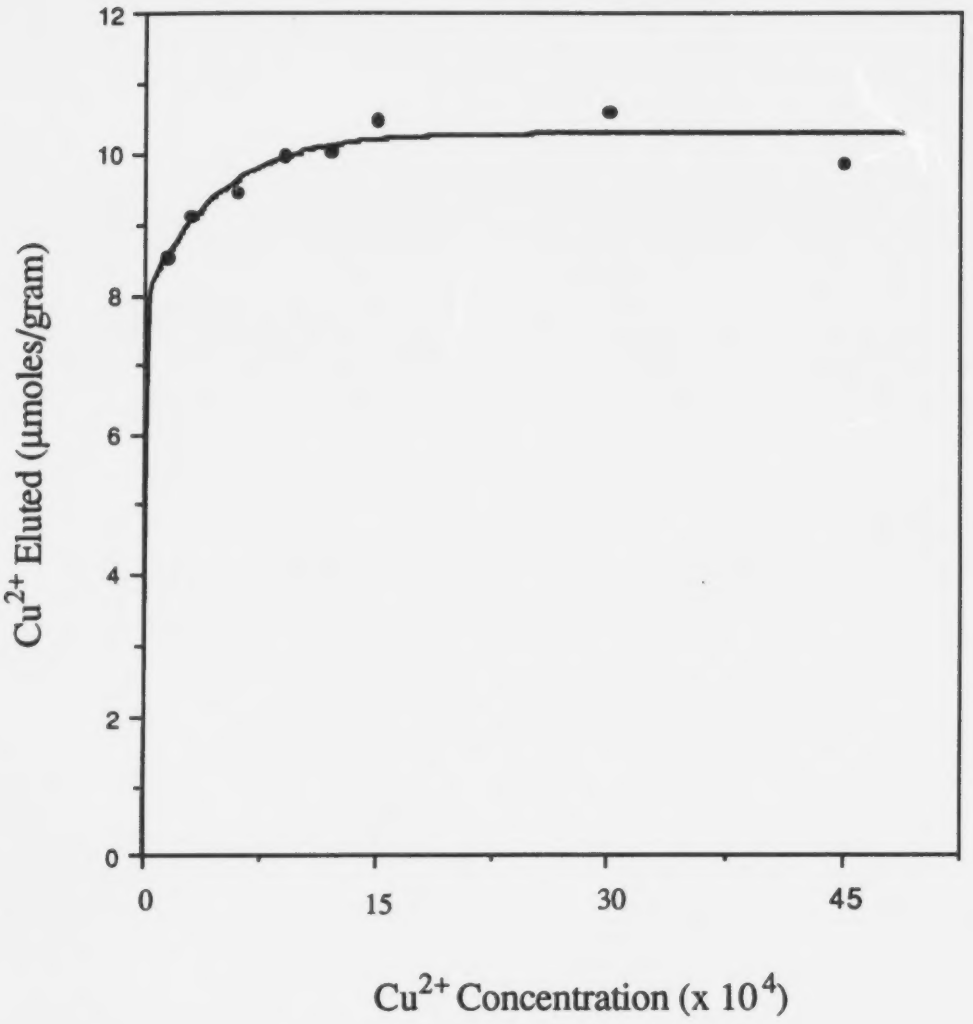

Figure 2.7 : Loading curve for Cu^{2+} in 0.0900 M NaOAc (pH = 5.00) on CPG-Oxine. CPG-Oxine capacity is 1.0×10^{-5} mol Cu^{2+} per gram of CPG-Oxine.

When the sample loading time in the normal procedure, or the preconditioning time in the alternate procedure, exceeded 30 min the pump speed was decreased to 1.2 mL/min during these steps in order to conserve sample or preconditioning solution, and was turned up to the original 5.0 mL/min a few minutes before switching to the next step. As discussed below, the rate of the slow Ca^{2+}-desorption occurring after the "overshoot" maximum is independent of flow rate.

In order to compensate for possible drift in instrument sensitivity and solution composition over the long periods of time involved in the loading studies, two types of calibrations were routinely performed. The first involved making five replicate injections of 10 μL of 2.5×10^{-3} M Ca^{2+} dissolved in 0.15 M HNO_3 immediately after completing every elution, while the nitric acid eluent was still being pumped through the column. Valve V2 was used for this purpose. The average of the areas of the five resulting peaks was divided into the area of the just-eluted sample calcium peak. The second routine calibration involved performing, in duplicate, a normal column loading experiment with a 2.0 min loading time after every loading experiment, whether normal or preconditioned. The average result from these duplicate 2.0 min calibration experiments was divided into the result of the preceding loading experiment. Thus, every point in Figures 2.8 – 2.15, below, represents a ratio of ratios and is effectively normalized by the value obtained in the 2.0 min normal loading experiment.

In the Na^+ sorption experiment the column was washed for 2.0 minutes with nanopure water after having been eluted with 0.15 M HNO_3. The sample solution, containing 2.00×10^{-5} M Ca^{2+}, 0.0100 M HEPES (pH = 7.00) and 0.0200 M $NaClO_4$, was then pumped through the column for various periods of time, after which it was washed with a 0.0200 M HEPES buffer (pH = 7.00) solution for 30 seconds and then eluted with 0.15 M HNO_3. The effluent was directly aspirated into the Varian SpectraAA-10 spectrometer to determine the Na^+ sorption.

II.2.8 PRECONDITIONING STUDIES

As above, the column was first washed with 0.15 M HNO_3 for 4 minutes. Next, a preconditioning solution was pumped through the column for a specific period of time varying from 2 min to 4 hours. The preconditioning solutions are as follows and were adjusted to pH = 7.00 with concentrated ammonia water or dilute NaOH depending on whether HEPES buffer was present or not. The preconditioning solutions are (1) 0.0100 M HEPES only, (2) 0.0200 M $NaClO_4$ only, (3) 0.100 M HEPES + 0.0200 M $NaClO_4$ and (4) 0.0100 M HEPES + 0.200 M $NaClO_4$. Following this preconditioning step a sample solution containing 2.0×10^{-5} M Ca^{2+}, 0.0100 HEPES and 0.0200 M $NaClO_4$ was loaded onto the column for 2.0 min only. Finally, after the 2.0 min loading step, the column was eluted for 4.0 min with 0.15 M HNO_3 into the Perkin Elmer 4000 spectrometer. As in the Ca^{2+} loading experiment the two routine calibrations were performed after every preconditioning step.

II.2.9 Na^+ SORPTION STUDIES WITH WATER WASH

Although this experiment was similar in principle to the Ca^{2+} loading study, it required significant modifications of the apparatus and procedure. First, an extensive water washing step was implemented between the loading and the elution steps in order to remove non-sorbed Na^+ both from between the particles of CPG-Oxine and from within the particle pores. This is due to the high Na^+ concentration (0.0200 M) within the void volume. Second, rather than being able to elute directly into the flame of the AE spectrometer, it was necessary to collect the effluent in a volumetric flask during the acid-elution step and subsequently to determine its Na^+ concentration by direct aspiration. There are two reasons for collecting the effluent and then using direct aspiration to determine the amount of sorbed sodium; Firstly, the maximum flow rate achievable through

the longer column (see Figure 2.4) was 2.2 mL/min and at such a low aspiration rate the AES is far from optimal, therefore making it hard to measure the sodium. Secondly, and most importantly, the sorbed sodium comes off very slowly, in this case with the larger column, in something over 2 minutes. This is a problem because the PE 4000 spectrometer has a maximum integration time for peak area of only 60 seconds, therefore the resultant peak area is unreadable.

II.2.10 Na^+ SORPTION STUDIES WITH BUFFER WASH

This experiment was performed to look for Na^+ sorbed in the hydrated gel layer. It was performed using the same apparatus as shown in Figures 2.1 and 2.2, except that flame atomic emission was employed to measure Na^+. The procedure, though similar to the Ca^{2+} loading study, was modified to include a wash step between the load and elute steps in order to remove the 0.0200 M $NaClO_4$ solution from between the CPG-Oxine particles and from within their pores.

The experiment was performed by loading CPG-Oxine for various periods of time with the usual sample solution containing 2×10^{-5} M Ca^{2+}, 0.0100 M HEPES buffer (pH = 7.00) and 0.0200 M $NaClO_4$. Next, a 30 second washing was performed with 0.0200 M NH_4^+-HEPES solution (pH = 7.00) to remove all Na^+ that has not been sorbed into the gel layer, followed by eluting with 0.15 M HNO_3 for 90 seconds directly into the flame. A 90 second elution has previously been shown to elute all of the Na^+ sorbed by CPG-Oxine (47).

II.3 RESULTS AND DISCUSSION

II.3.1 CAPACITY

The capacity of Batch B was determined by a variation of the established literature method involving the sorption of Cu^{2+} (13,20,56-59). In this experiment copper forms a 1:1 complex with bound 5-P-Oxine (13,58-59). The plateau on the sorption isotherm (Figure 2.7) corresponds to 1.0×10^{-5} mol Cu^{2+} per gram of CPG-Oxine, which is taken as the complexation capacity. This is agreement with the manufacturer's claim of 10 μmol/g (55). The manufacturer's method of determination is not stated explicitly. Other literature values range from 5.5 μmol/g (19), determined with a Zn^{2+} column method, to 12.8 μmol/g (56), determined with an Fe^{2+} method.

A microdetermination of the nitrogen or carbon content of the CPG-Oxine cannot be taken as a reliable check (47) because the synthetic structure for CPG-Oxine is known to leave a substantial amount of N- and C- containing byproducts as impurities covalently bound to the glass surface (56,57).

II.3.2 Ca^{2+} LOADING STUDIES

Loading experiments were performed by pumping the sample solution containing 2.00×10^{-5} M Ca^{2+}, 0.0100 M HEPES buffer and 0.0200 M $NaClO_4$ through the column for various periods of time, eluting with 0.15 M HNO_3 and determining the amount of Ca^{2+} that had been sorbed using AA spectroscopy. The loading curves for Ca^{2+} on CPG-Oxine and on CPG are presented in Figures 2.8 and 2.9. All experimental points, including those on CPG, are normalized by the value obtained from a 2 min loading on CPG-Oxine. (In Figures 2.8 thru 2.19 the amount of Ca2+ in the hold-up volume has been subtracted). As seen in Figure 2.8, the loading curve reaches what appears to be a plateau value after just a few minutes. Usually, such a plateau would be taken as evidence that

Ca^{2+} sorption had reached equilibrium. However, when loading is continued for a considerably longer time Ca^{2+} desorbs from the column over a period of about 2 hours as the system approaches the true equilibrium sorption value at about 60% of its 2 min value (Figure 2.9A).

The initial increase in moles of Ca^{2+} sorbed at times earlier than about 1 min (Figure 2.8) is consistent with the rapid sorption expected for particles of 125–177 μm diameter and was not studied in any detail. The anomalous decrease after the overshoot maximum, shown in Figure 2.9A, is the subject of this study. That is, data collected at times ≥ 2 min are of interest.

Shown in Figure 2.9B is the loading curve for Ca^{2+} on CPG, the controlled pore glass alone. Most noticeable is the fact that much less Ca^{2+} is sorbed per gram on CPG than on CPG-Oxine. This is, of course, because complexation by immobilized oxine is the principal sorption process on CPG-Oxine (46). Sorption onto the glass surface probably occurs to about the same extent on the glass surface of CPG-Oxine as it does on CPG. It is probably due to cation exchange in the diffuse layer, as discussed above. It can be seen in Figure 2.9B that sorption of Ca^{2+} by the glass surface also decreases with time.

II.3.3 PRECONDITIONING STUDIES

II.3.3.1 PRECONDITIONING WITH BUFFER/ELECTROLYTE

In order to determine whether Ca^{2+} itself is involved in causing the slow process which gives rise to the decrease in its sorption, the CPG-Oxine column was preconditioned with a solution containing the identical concentration of HEPES buffer and $NaClO_4$ as the sample solution, but containing no Ca^{2+}. After preconditioning it was loaded for 2 mins

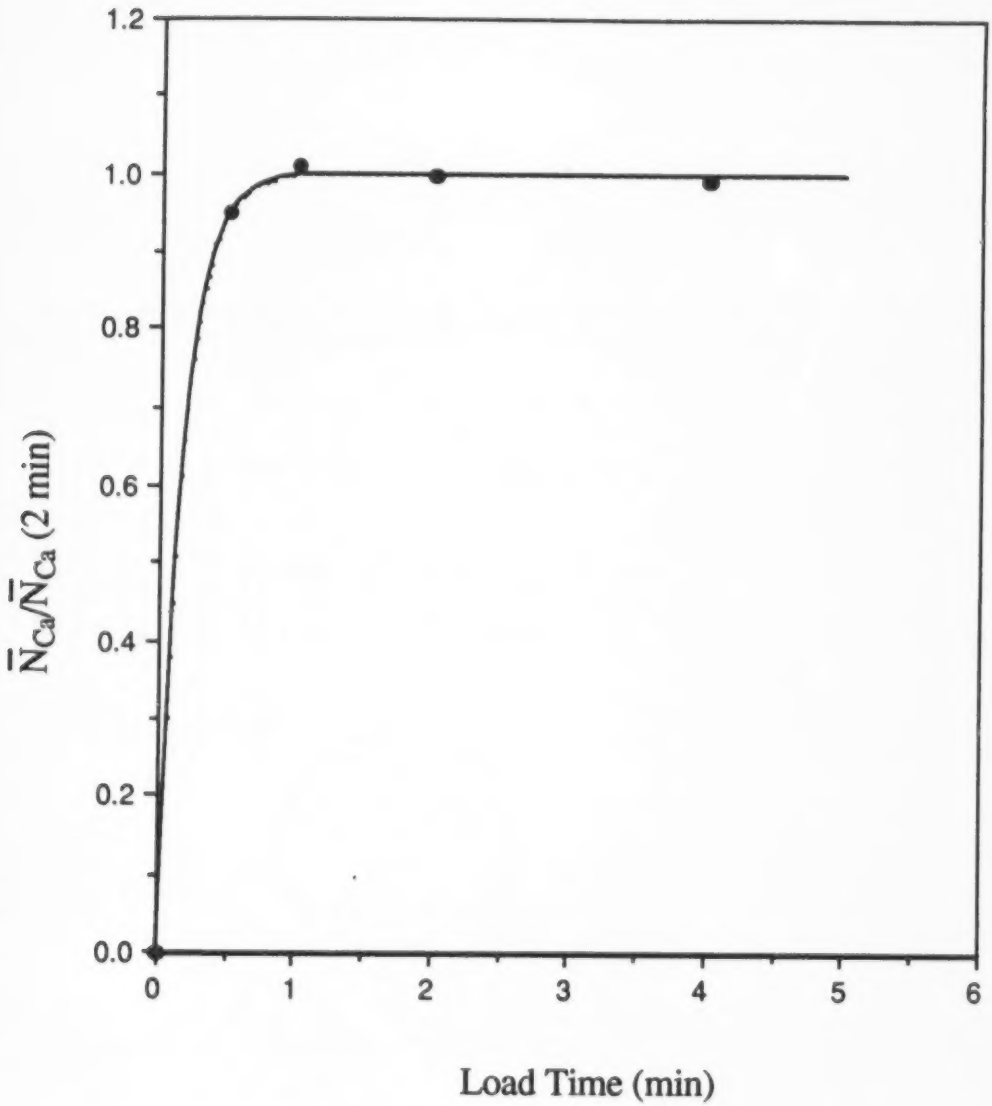

Figure 2.8 : Loading curve for Ca^{2+} on CPG-Oxine normalized by the 2 minute value for CPG-Oxine. Value for $\bar{N}_{Ca}$ for the 2-min load is 5.94×10^{-4} mmol/gram.

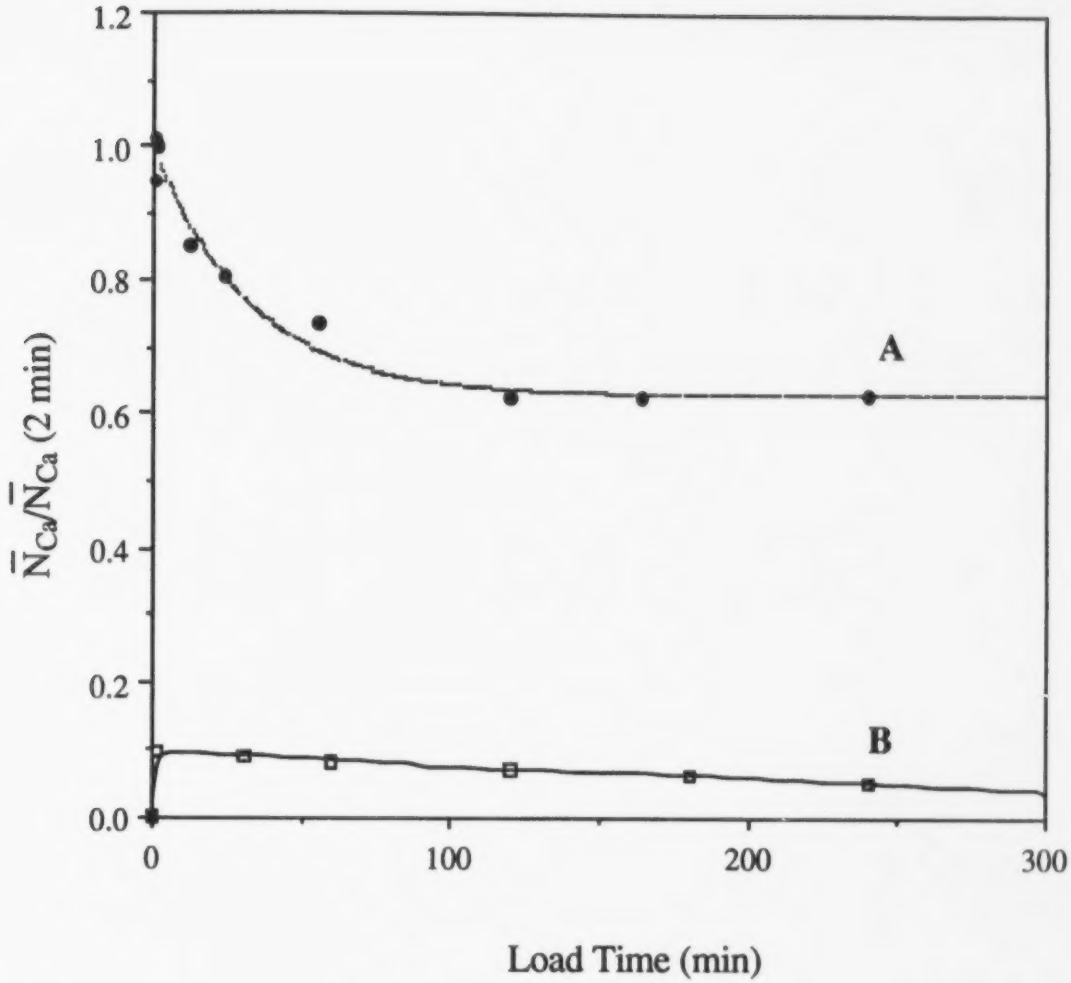

Figure 2.9 : Loading curves for Ca^{2+} on CPG-Oxine (curve A) and CPG (curve B), all normalized by the 2-min value for CPG-Oxine. Value of $\bar{N}_{Ca}$ for 2-min load is 6.00×10^{-4} mmol/g. Solid line in A is first-order fit using k_{Ca} obtained from Figure 2.19. Solid line in B is an empirical fit.

with the Ca^{2+}-containing sample solution. The results of this experiment are presented as open squares in Figure 2.10. The solid circles are a repeat of the loading curve data from Figure 2.9A. The two curves are identical. This indicates clearly that the changes occurring in CPG-Oxine, which cause the decrease in Ca^{2+} sorption during the Ca^{2+} loading experiment (Figure 2.9A), do not involve Ca^{2+}. It may be concluded that the rates of diffusional mass transfer of Ca^{2+} and the rates of complexation/decomplexation of Ca^{2+} with immobilized oxine are fast. Evidently, the slow process involves one or more of the other components of the sample solution than Ca^{2+}.

A prediction of what the slow process might be requires an understanding of both the equilibrium and kinetic aspects of Ca^{2+} sorption by CPG-Oxine. Fortunately, the equilibrium aspects previously have been elucidated (46). The kinetic aspects can be imagined from theoretical considerations and will be discussed in section II.3.3.3 below.

II.3.3.2 ADDITIONAL PRECONDITIONING STUDIES

As before, the CPG-Oxine column was first preconditioned for various periods of time and was then loaded for 2 minutes with Ca^{2+}-containing sample solution and eluted into the flame. In these studies, however, the relative and absolute concentrations of HEPES buffer and $NaClO_4$ inert electrolyte were varied. The results of five different studies are summarized in Figures 2.11 to 2.15. For comparison, in each panel the solid circles reproduce the results of the same study that was shown in Figure 2.9A.

In Figure 2.11 is the result of preconditioning the column with a solution containing only 0.0100 M HEPES buffer. Prolonged contact with buffer alone evidently accomplishes the slow alteration of the CPG-Oxine, but at a significantly slower rate than when buffer and inert electrolyte are used together. In Figure 2.12 is the result of preconditioning with 0.0200 M $NaClO_4$ alone. Here too, some alteration of CPG-Oxine is accomplished, but at a slower rate than for buffer and inert electrolyte together.

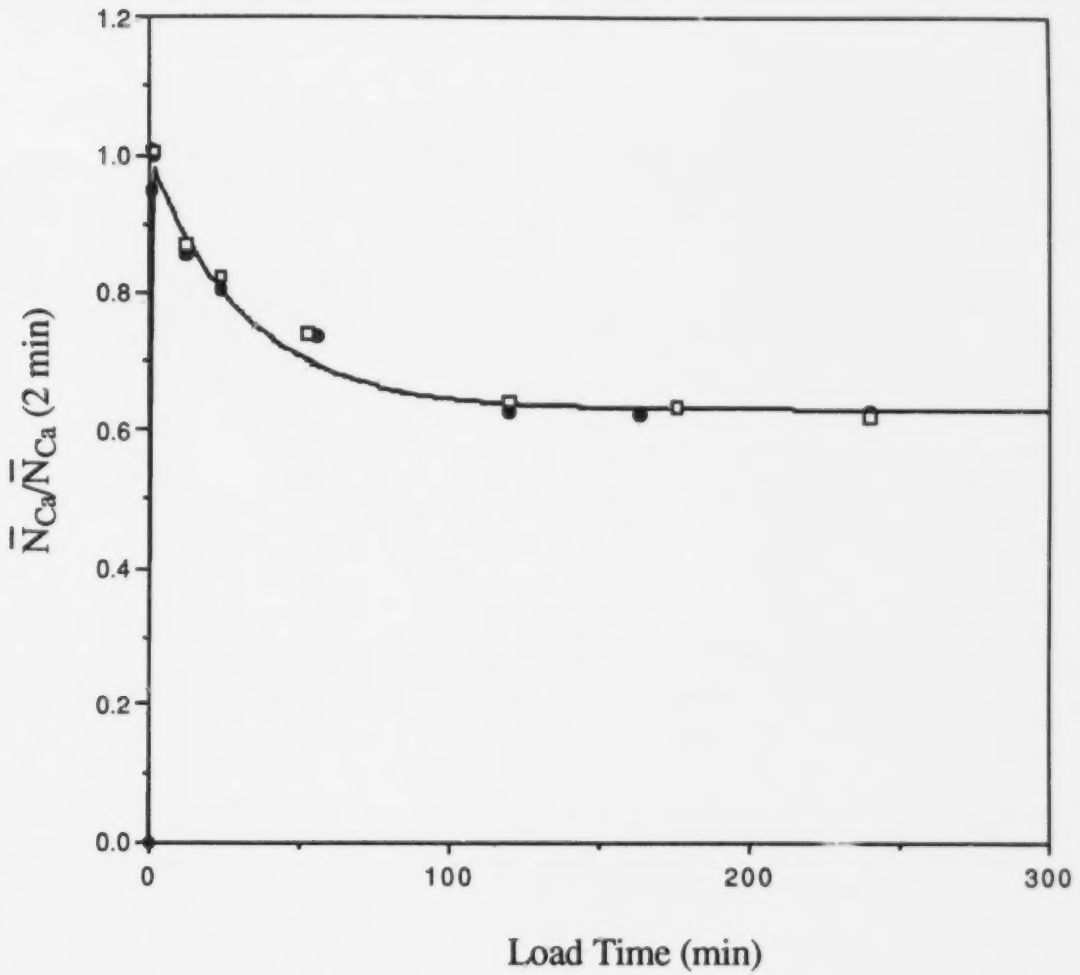

Figure 2.10 : Preconditioning curve (open squares) and loading curve (solid circles) for Ca^{2+} on CPG-Oxine, normalized by 2-min value from loading curve. Value of $\bar{N}_{Ca}$ for 2-min load is 5.94×10^{-4} mmol/gram. Solid line is first-order fit as in Figure 2.9A.

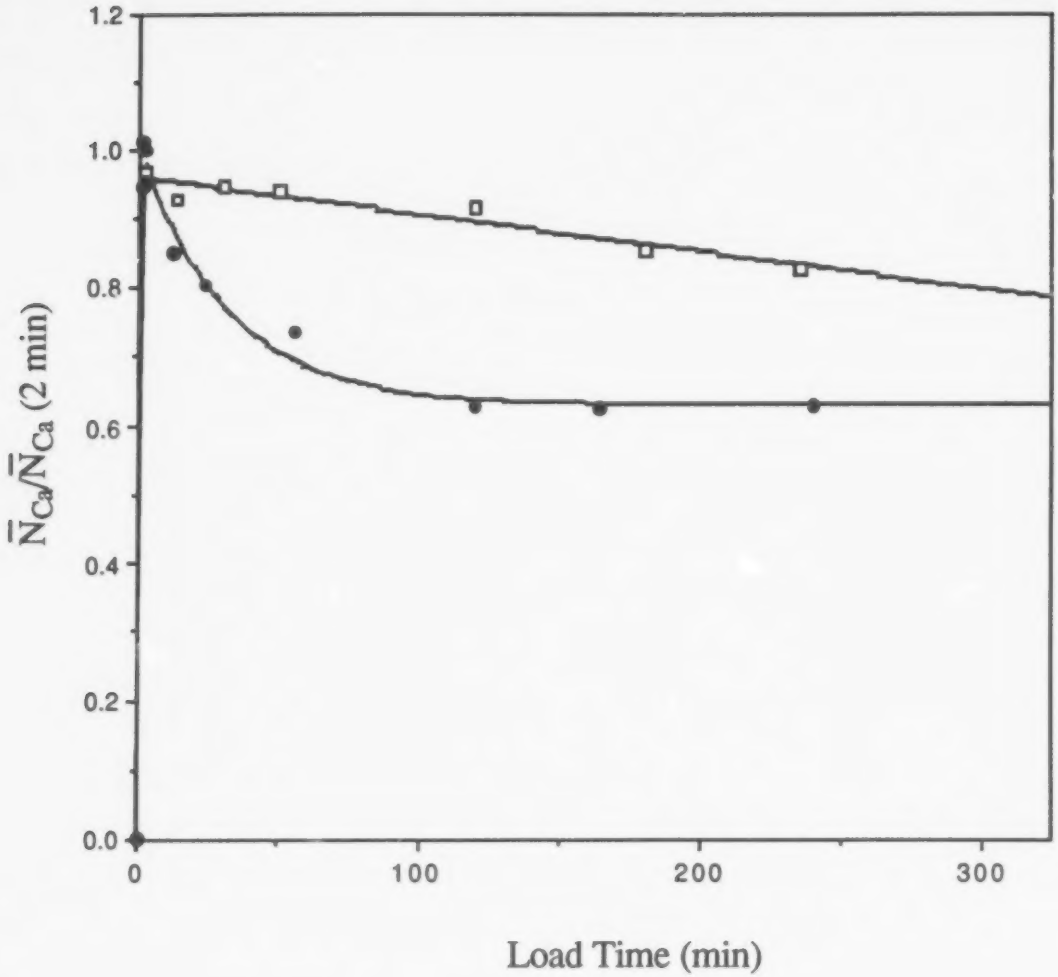

Figure 2.11 : Preconditioning curve (open squares) and loading curve (solid circles), both normalized by the 2-min value for CPG-Oxine. Value of $\bar{N}_{Ca}$ for 2-min load is 5.94×10^{-4} mmol/gram. Preconditioning is done with a solution containing only 0.0100 M HEPES buffer at pH = 7.00.

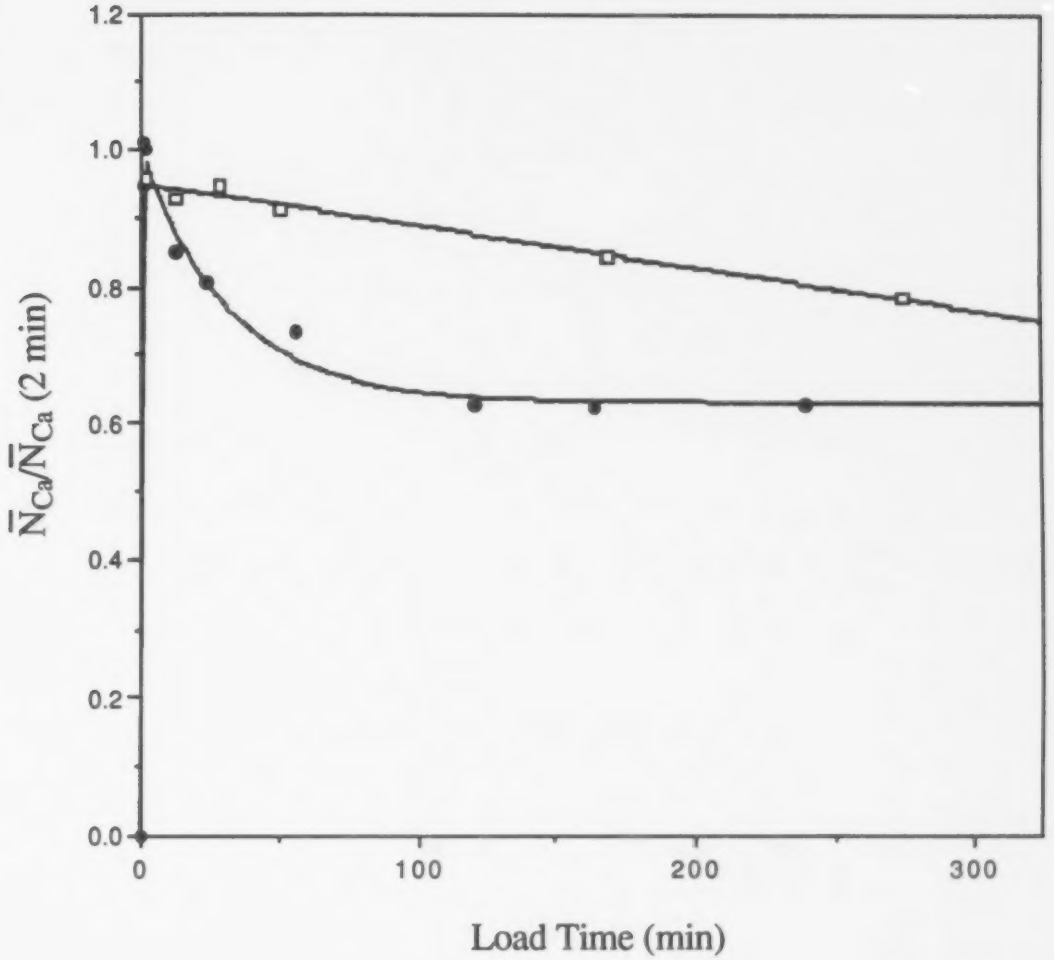

Figure 2.12 : Preconditioning curve (open squares) and loading curve (solid circles), both normalized by the 2-min value for CPG-Oxine. Value of $\bar{N}_{Ca}$ for 2-min load is 5.94×10^{-4} mmol/gram. Preconditioning is done with a solution containing only 0.0200 M $NaClO_4$ at pH=7.00.

Presumably, from their shapes, the HEPES-only and the $NaClO_4$-only curves in Figures 2.11 and 2.12 have not yet reached their equilibrium plateau values by 250 minutes.

At pH = 7.00 HEPES buffer is 76% in the neutral (zwitterion) form HA, and 24% in the anionic conjucate form A^- (60). Since buffer pH was adjusted with ammonia water, there is an NH_4^+ concentration equivalent to the concentration of the A^-. For 0.0100 M total HEPES concentration the concentration of NH_4A is 2.40×10^{-3} M. Thus, the HEPES-only solution is not a buffer-only solution but also contains some electrolyte. Likewise, the 0.0200 M $NaClO_4$-only solution is not an electrolyte only solution. It has a pH of about 6 to 7 (i.e. the same as water) and causes hydrolysis of the oxine and silanol groups, but at a slower rate than does HEPES buffer because it has a much lower buffer capacity than the HEPES solution. Thus, the slow alteration of CPG-Oxine seems to require both an ionizing action and also some effect of electrolyte on desorption rate. The fact that HEPES alone does not accomplish an equivalent alteration of CPG-Oxine suggests that the alteration is not merely a slow hydration of the freshly ionized surface.

In order to determine whether the neutralizing capacity of the solution could in some way be causing the rate of alteration of CPG-Oxine to be slow, a preconditioning was performed with a solution containing ten-times more buffer (i.e. 0.100 M HEPES, pH = 7.00) along with the original amount of $NaClO_4$ (i.e. 0.0200 M). As seen in Figure 2.13, the preconditioning rate is virtually identical to that achieved with the 0.0100 M HEPES and 0.0200 M $NaClO_4$ preconditioning solution. This demonstrates that not only is the quantity of buffer not the limiting factor, but also that the increase in NH_4A concentration from 2.40×10^{-3} M in 0.0100 M HEPES and 0.0200 M $NaClO_4$ to 2.40×10^{-2} M in 0.100 M HEPES and 0.0200 M $NaClO_4$ does not significantly change the rate of alteration. This latter observation has several possible explanations. Among them are the following: (a) 0.0100 M HEPES and 0.0200 M $NaClO_4$ is already at or above some concentration which produces a maximum electrolyte effect on the rate of alteration; (b) the electrolyte rate-effect is significantly greater for Na^+ than it is for NH_4^+.

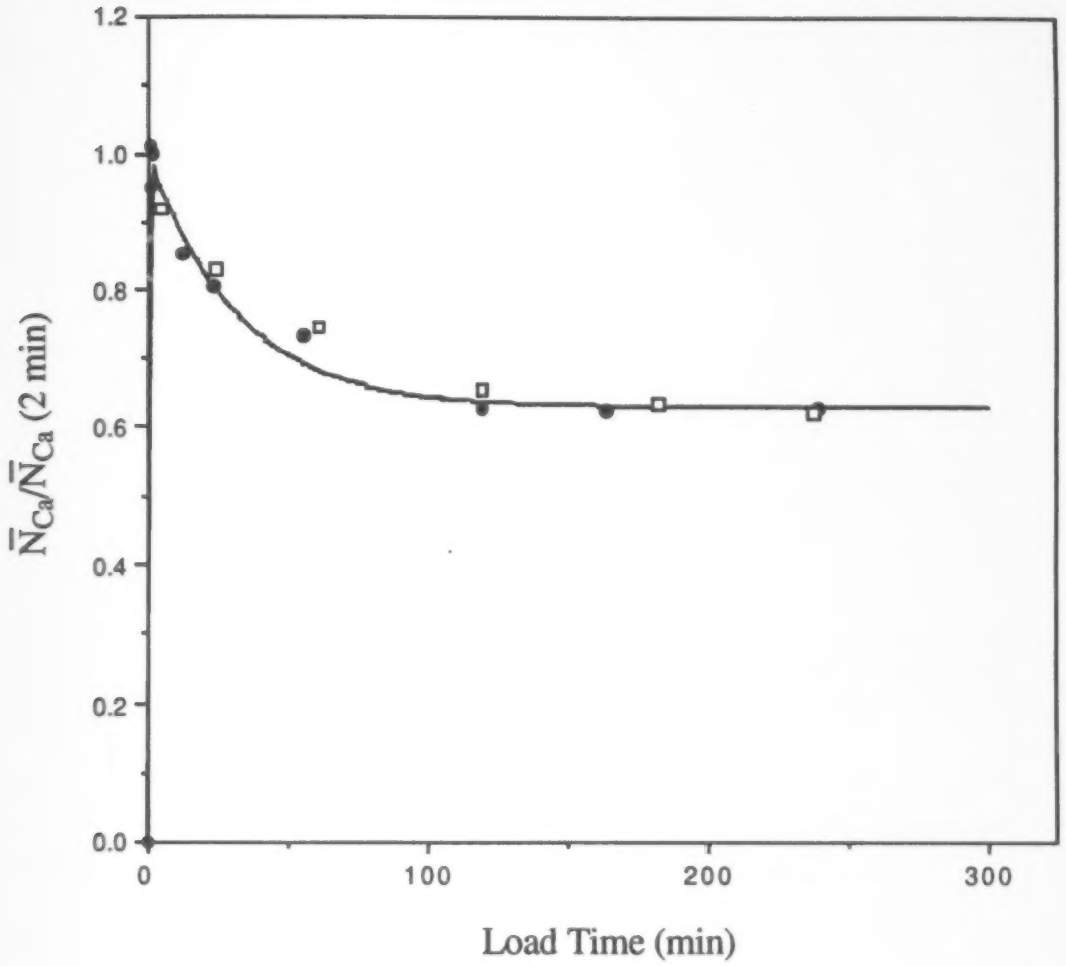

Figure 2.13 : Preconditioning curve (open squares) and loading curve (solid circles), both normalized by the 2-min value for CPG-Oxine. Value of $\bar{N}_{Ca}$ for 2-min load is 5.94×10^{-4} mmol/gram. Preconditioning is done with a solution containing 0.100 M HEPES and 0.0200 M $NaClO_4$ at pH=7.00.

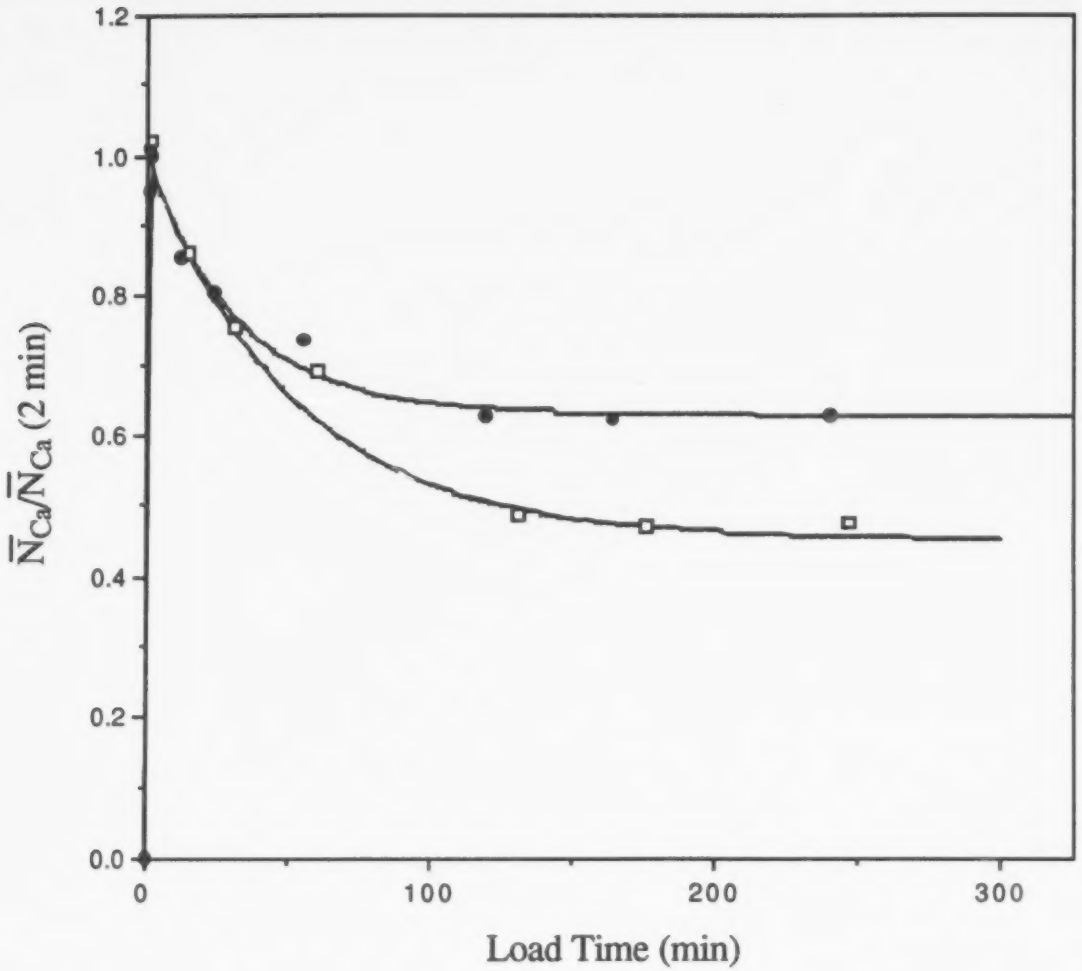

Figure 2.14 : Loading curves for Ca^{2+} on CPG-Oxine, all normalized by the 2-min value for CPG-Oxine. Solid circles represent normal sample conditions (2.00×10^{-5} M Ca^{2+} in 0.020 M $NaClO_4$). Open squares represent a 10 fold increase in the electrolyte concentration (2.00×10^{-5} M Ca^{2+} in 0.200 M $NaClO_4$). $\bar{N}_{Ca}$ for the 2-min load is 5.94×10^{-4} mmol/gram.

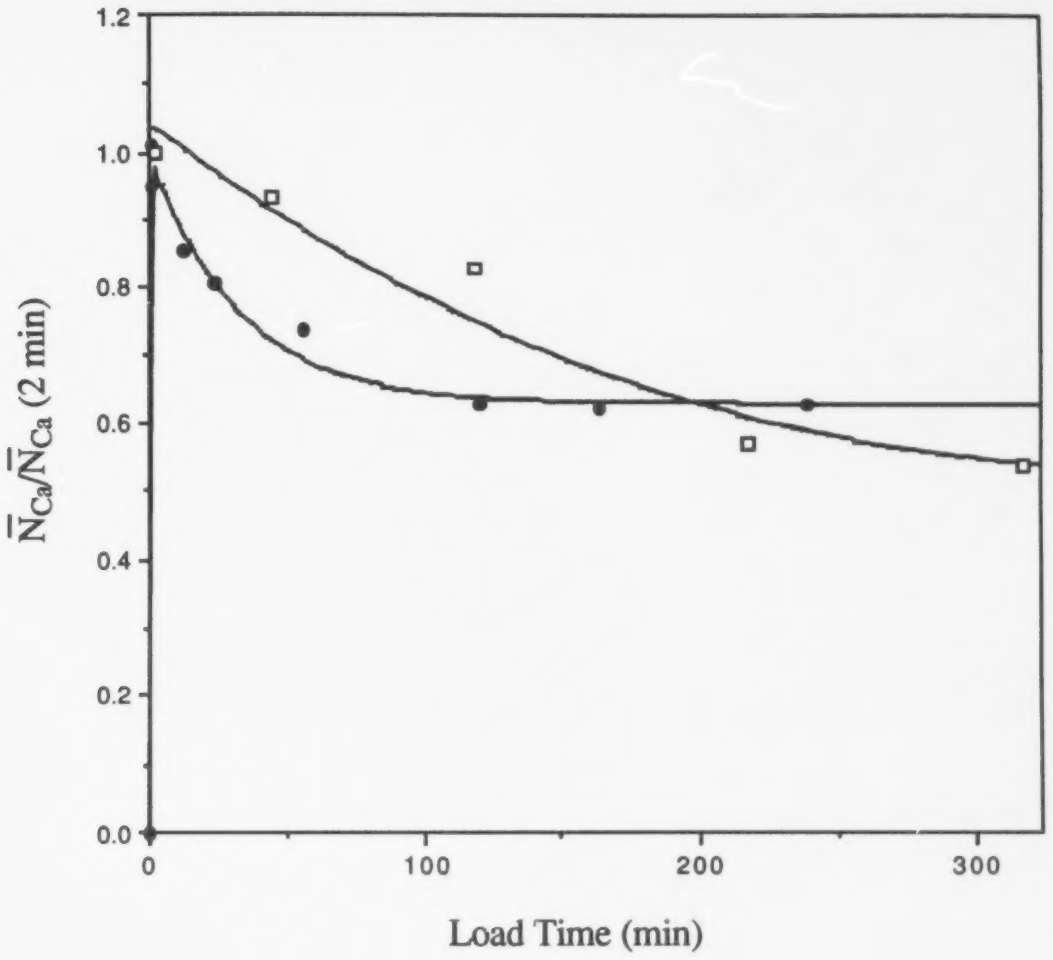

Figure 2.15 : Loading curves for Ca^{2+} on CPG-Oxine, both normalized by the 2 minute value for CPG-Oxine. Solid circles represent normal loading conditions (2.00×10^{-5} M Ca^{2+} in 0.0200 M $NaClO_4$ and 0.0100 M HEPES). Open squares represent a loading solution void of sodium; loading solution contains 2×10^{-5} M Ca^{2+} in 0.0200 M NH_4ClO_4 and 0.0100 M HEPES. $\bar{N}_{Ca}$ for the 2-min load is 5.94×10^{-4} mmol/gram.

In order to test the first of these possible explanations, a preconditioning experiment was performed with a solution containing ten-times more $NaClO_4$ (*i.e.* 0.200 M $NaClO_4$) along with the original amount of HEPES (*i.e.* 0.0100 M). From Figure 2.14, it is evident that a higher concentration of Na^+ does not greatly affect the relative *rate* of alteration of CPG-Oxine, but it does cause the final equilibrium plateau sorption value of Ca^{2+} to be significantly lower. The fact that the rate is relatively unaltered is consistent with explanation (a) from the paragraph above. The fact that the equilibrium plateau is lower reveals an equilibrium-effect of electrolyte concentration in addition to its rate effect.

A final preconditioning experiment was performed using a 0.0100 M HEPES and 0.0200 M NH_4ClO_4 solution. In this solution 0.0200 M NH_4ClO_4 has replaced 0.0200 M $NaClO_4$. The results are shown in Figure 2.15 (open squares) where it is seen that the *rate* of alteration of CPG-Oxine is slower than when Na^+ was used, but the magnitude of the effect on the final equilibrium loading of Ca^{2+}, if indeed equilibrium has been reached, is at least as great as that for Na^+. The former observation supports explanation (b) above, that the effect of Na^+ on the *rate* is greater than that of NH_4^+.

II.3.3.3 SORPTION PROCESSES

At flow rates of 5.0 mL/min and 1.2 mL/min, which were both used during the loading and preconditioning studies, the interstitial linear velocities of the solution through the column are 2.3 cm/s and 0.6 cm/s, respectively. Given the short length of the column and these relatively high linear velocities, "shallow-bed" kinetic conditions certainly prevail in the column after the first minute (48-50,61). That is, every particle of sorbent in the column is in contact with solution having, essentially, the unaltered composition of the influent solution being pumped. In addition the Ca^{2+} sorption equilibrium occurs in the linear region of the Ca^{2+} sorption isotherm because Ca^{2+} is a "trace" component in these experiments (46).

The following processes must take place in CPG-Oxine when the solution being pumped through the column is changed from 0.15 M HNO_3 to a solution containing HEPES buffer (pH = 7.00) and a relatively high concentration of the inert electrolyte $NaClO_4$:

(i) Buffer and electrolyte diffuse from the bulk solution through the Nernst diffusion film surrounding the particle and enter the pore liquid just inside the particle outer boundary. This process is fast. At these solution linear velocities the thickness, δ, of the Nernst film is approximately 1×10^{-3} cm (49). If the particles are approximated as spheres of 0.01 cm diameter the first order rate constant for steady-state film diffusion is approximately 0.3 s^{-1} (*i.e.* $t_{1/2} \approx 2$ s) (49,62).

(ii) Buffer and electrolyte diffuse in through the pores of the particle and HNO_3 diffuses out. During this process the conjugate base of HEPES becomes protonated by HNO_3 and the resulting excess conjugate acid of HEPES diffuses out through the pores.

(iii) The increase in pH of the pore liquid from 1 to 7 leads to deprotonation of all of the quinolinium groups and of a small fraction (*i.e.* <10%) of the phenolic groups on the immobilized oxine molecules (45,46).

(iv) The increase in pH of the pore liquid also leads to deprotonation of silanol groups at the glass surface lining the pores (63). Titration studies have shown that most of the surface-charge in CPG-Oxine at pH = 7.00 is due to the resulting anionic silanolate groups and that only a small fraction is due to the anionic oxinate groups (45).

(v) The negative charge of the glass surface causes it to have a negative electrical potential. A detailed description of the origin and influence of this potential requires the assumption of a physico-chemical model. Heretofore, a simple version of the "ionizable surface-group, site-binding model" (64,65) has provided an adequate description of the observed Ca^{2+} sorption behavior on CPG-Oxine (45,46). In this

version of the model the charge-surface on the glass is planar and only about one atom thick. When a proton is lost from a silanol group at this surface to produce the surface charge, the Na^+ or NH_4^+ ion which takes its place in a stoichiometric sense is considered not to be specifically adsorbed onto the surface but rather is considered to be located in the diffuse part of the electrical double layer (see below). The magnitude of the negative potential decays roughly exponentially from its highest value (ψ_0 volt) at the glass surface to a value of 0 volt in the bulk solution nearer the centre of the pore. The region adjacent to the surface, over which the potential is different from 0 volt is called the "diffuse part" of the electrical double layer. At any location, x, in this diffuse layer the activities of cations such as H_3O^+, Na^+ and Ca^{2+} are higher than they are in the bulk solution by an amount that is related to the local electrical potential (ψ_x) at x (equation 1.6, chapter 1). Thus, the pH at any location in the diffuse layer is lower than that in the bulk solution.

(vi) A third consequence of the negative charge on the glass surface is that a weak acid type cation exchanger has been created (34). In a macroporous glass the surface excess of cationic counterions (*e.g.* Na^+, NH_4^+) in the diffuse part of the electrical double layer constitute the exchangeable ions (64,66).

In the above model there are two processes responsible for the sorption of Ca^{2+} on CPG-Oxine: metal-ligand complexation by oxine, which depends on the electrical potential of the surface; and ion exchange, which does not depend on the surface potential but does depend on the surface charge density because surface charge creates the ion exchange capacity. As described previously, Equation 1.29 quantitatively expresses the moles of Ca^{2+} sorbed per gram of CPG-Oxine, $\overline{N}_{Ca}$, when Ca^{2+} is present at trace conditions:

$$\overline{N}_{Ca}(CPG\text{-}Ox) = [Ca^{2+}] \cdot \gamma_{Ca} \cdot \overline{\nu}_{Oxine} \cdot \overline{\beta}_1 \cdot \overline{K}_{a2} \cdot a_H^{-1} \cdot \exp\left(-\frac{F \cdot \psi_x}{R \cdot T}\right) +$$

$$[Ca^{2+}] \cdot 10^{-6} \cdot K_{IEX} \cdot \frac{\overline{\gamma}_{Na}^{2} \cdot \gamma_{Ca}}{\gamma_{Na}^{2} \cdot \overline{\gamma}_{Ca}} \cdot \frac{Q^2}{[Na^+]^2} \qquad (1.29)$$

The first term on the right hand side of Equation 1.29 accounts for complexation. It was derived in chapter 1 and experimentally verified (46). The second term accounts for ion exchange. This term is different from the second term in Equation 12 in reference 46 because a water-washing step is not performed in the present experiment. The potential at location x, described earlier, is given by equations 1.6 - 1.8, above.

At equilibrium, at a constant pH of bulk solution, Q is constant. Thus, from equations 1.29 and 1.6 - 1.8 it is evident that, at equilibrium in a solution of constant pH, constant $[Na^+]$ and constant $[Ca^{2+}]$, the value of $\overline{N}_{Ca}$ should be constant. What is of interest in the present study is the fact that Ca^{2+} sorption first proceeds to a value *above* the final equilibrium value and that it subsequently decreases (desorbs) to the final equilibrium value at a very slow rate. Hence, the effect of buffer and electrolyte which bring about the Ca^{2+} desorption must involve an alteration in the CPG-Oxine itself which occurs at a much slower rate than does the Ca^{2+} sorption process. This slow alteration must be reflected in a slow change of one or more of the parameters in Equation 1.29 and/or 1.6 - 1.8. Either a slow increase of $[Na^+]$ (and therefore c) in the pore liquid or a slow decrease in Q on the glass surface could cause a slow decrease in $\overline{N}_{Ca}$.

A model incorporating a slow increase of $[Na^+]$ can be envisioned. It could be that, since there is an excess of buffer present in the Ca^{2+}-containing sample solution, a 2-min loading achieves the final equilibrium value of Q and that the trace component species Ca^{2+} diffuses through all of the pores and achieves sorption equilibrium. If, at the same time, the electrolyte (*e.g.* $NaClO_4$) is slow to diffuse through the pore liquid, especially in the smallest (micro) pores then, in a 2-min loading time, Ca^{2+} would be sorbed on the

surfaces of these small pores in the presence of a lower than equilibrium value of $[Na^+]$ and, therefore, in excess of its final equilibrium value. The continued slow diffusion of $NaClO_4$ into the small pores toward the equilibrium value of $[Na^+]$ would then cause a slow desorption of Ca^{2+}. This model requires that the diffusion of $NaClO_4$ is much slower than that of Ca^{2+}. Hindered diffusion of an electrolyte through pores that have charged surfaces is well known (67–69). It is a consequence of the phenomenon of electrolyte exclusion (Donnan exclusion) which has been shown to occur in the smaller pores of controlled pore glass (69,70). However, the magnitude of this retarded diffusion, even in quite small pores, is nowhere near large enough to produce a desorption rate as slow as the observed one so that slow diffusion of $NaClO_4$ in the pores is not likely to be the cause of the slow alteration of CPG-Oxine.

Models which incorporate a slow decrease of Q are more promising. At the surface of glass which is in contact with water there is present a gel-like hydrated layer. In the simple version of the "surface-ionization, site-binding model" the finite thickness of this hydrated layer is not explicitly taken into account and the charge-surface, at which the ionizable silanol groups are located, is identified as the interface between the hydrated gel layer and the pore liquid. Another version of this model than the one used in deriving equations 1.29 and 1.6 - 1.8, has been proposed for electrical double layers on SiO_2. Since CPG is composed of a high (>95%) SiO_2-content Vycor glass (34,63,71), this model is relevant to CPG. In the model a direct binding or specific adsorption of cations such as Na^+ is also assumed to occur onto the ionized glass charge-surface (64,65). This process would lead to an effective neutralization of a more or less equivalent number of anionic silanolate surface sites and to a consequent decrease in Q. However, it is unlikely that this process would be slow since the surface is in direct contact with the pore liquid.

A more likely situation is described by the "porous gel model" of the surface-solution interface (64,72,73) in which ionization of silanols is assumed to occur not only at the gel-layer/pore-liquid interface, but also throughout the gel layer. The thickness of this

hydrated layer on SiO_2 is in the range 10 to 100Å and it is presumably about the same on Vycor. Deprotonation occurs rapidly within this layer because of the relatively high diffusivity of hydrogen and hydroxide ions. Instead of a planar charge-surface, there is, in this model, a three-dimensional charged gel. The slow process, leading to a decrease in Q, would be the diffusion of cations such as Na^+ into the hydrated gel layer. Radiotracer studies suggest that the diffusion coefficient of protons in hydrated gel layers on SiO_2 is 10^{-11} to 10^{-9} cm^2/s while that of Na^+ ions is 10^{-15} to 10^{-10} cm^2/s (74). This supports the view that the rate of ionization (*i.e.* deprotonation) of the gel, when buffer/electrolyte enters the pores, could be orders of magnitude greater than the rate of uptake of Na^+.

Several aspects of the "porous gel model" are of interest. First, to the extent that Na^+ takes the place of H^+ in the hydrated layer there has been a cation exchange of Na^+ for H^+. Second, whether or not Ca^{2+} will also enter to a significant extent into the hydrated layer of a high SiO_2 glass at pH = 7.00 is questionable (75–77). If it does, its effect on Q in equations 1.29 and 1.6 would be negligible in the present system because Ca^{2+} is a trace-ion. On the other hand, the entry of Ca^{2+} into the hydrated layer could significantly affect the apparent value of K_{IEX} in the second term of Equation 1.29. However, on CPG-Oxine the first term of Equation 1.29 is much larger than the second term so that diffusion of Ca^{2+} into the gel layer would not significantly alter the overall sorption of Ca^{2+} and it is therefore not relevant to explaining the "overshoot" phenomenon on CPG-Oxine. The third aspect of the "porous gel model" that is of interest is the fact that the "surface" charge due to the silanolate groups is not concentrated in a single plane and there is a gradient of electrical potential on both sides of the boundary between the hydrated layer and the pore liquid: one in the pore liquid and the other in the gel. It is clear that since the negative charge which gives rise to Q is spread into the gel layer, then the value of the potentials ψ_o and ψ_x, previously calculated by the simple version of the "surface-ionization, site-binding model" in references 45 and 46 , and in Equation 1.6, would be somewhat higher than the true values. Solution of the relevant Poisson-Boltzmann

equation for the porous gel (72,73) model would require more information about CPG-Oxine than is available and, in any event, the value of ψ_x given in Equation 1.6 would be approximately correct. Certainly ψ_x would decrease with time as more and more Na^+ was sorbed and this would cause a decrease in the amount of Ca^{2+} sorbed.

II.3.4 Na^+ SORPTION STUDIES WITH WATER WASH

The obvious test of the "porous gel model" for CPG-Oxine is to look for the presence of Na^+ in the hydrated gel layer. In the present work this was done by loading the CPG-Oxine for various periods of time with a solution containing 2.00×10^{-5} M Ca^{2+}, 0.0100 M HEPES buffer (pH = 7.00) and 0.0200 M $NaClO_4$, washing with N_2-sparged water for an extended period to remove interstitial and pore solution which contains Na^+ and then eluting with 0.15 M HNO_3 and measuring eluted Na^+ by flame emission spectroscopy.

There is an obvious problem with this simple experiment in that the wash water will slowly protonate the silanolate sites because of its low buffer capacity. Those sodium ions that are present as counterions for the silonate groups, even those Na^+ counterions that are not in the glass gel layer but are present in the diffuse layer in the pore liquid cannot be washed out of the CPG-Oxine until an equivalent number of silonates has been protonated and the cation exchange capacity diminishes. No sharp line will exist between the washing out of Na^+ counter-ions that have diffused into the gel layer and the washing out of Na^+ counterions that are in the diffuse layer. This is evident in Figure 2.16. The vertical axis is millimoles of Na^+ counterions per gram that remained sorbed after CPG-Oxine was first loaded for 2 minutes with the sample solution and then subjected to washing with water for various periods of time. The horizontal axis is the water-washing time. The millimoles of Na^+ that remained sorbed were determined by eluting for 4 min with 0.15 M HNO_3, which had previously been shown to elute *all* Na^+ sorbed by CPG-Oxine (47). After a 2 minute

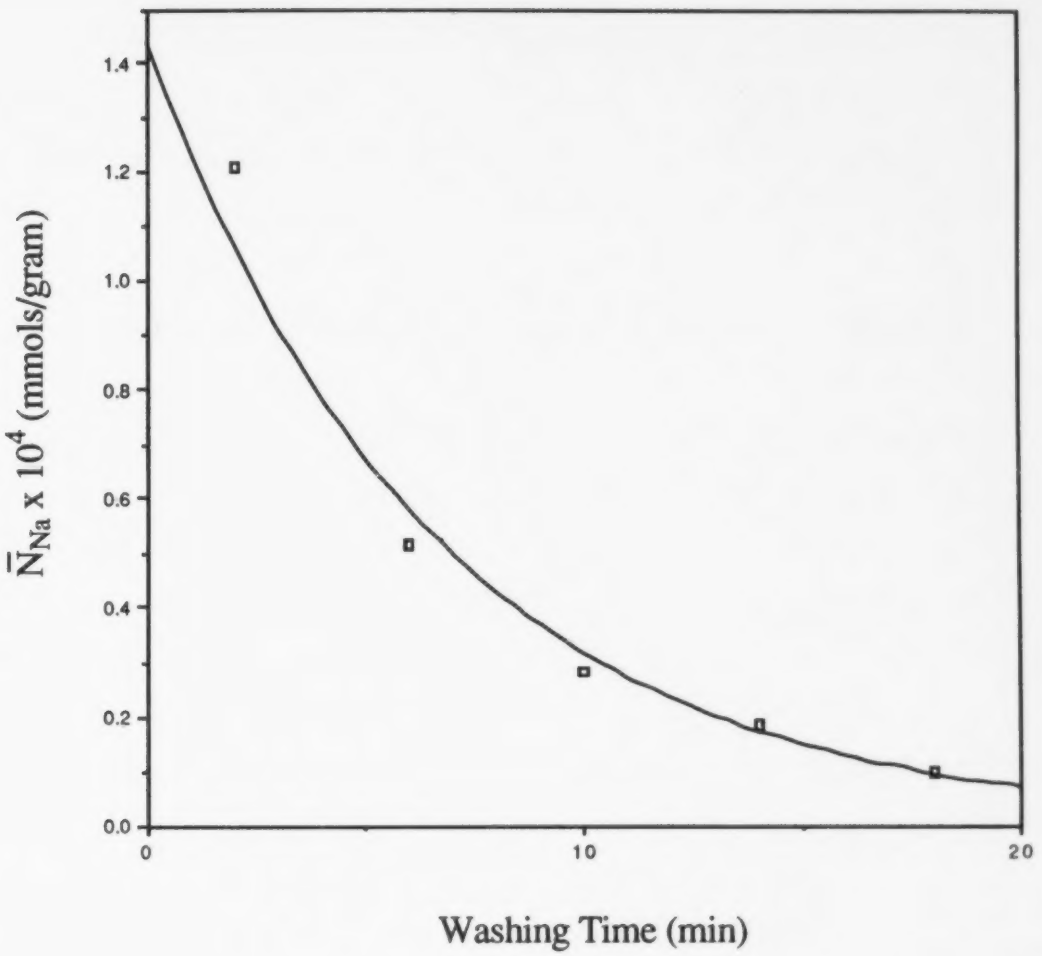

Figure 2.16 : Moles of Na^+ per gram that remains sorbed on CPG-Oxine after a 2-min loading followed by washing for increasing lengths of time with N_2 sparged, DI water

sample loading little Na^+ will have diffused into the gel layer and yet it is seen that there is a significant amount of Na^+ still in the CPG-Oxine after a 2 minute loading followed by 18 minutes of washing. This is presumably the result of ion exchange in the diffuse layer in the pore liquid. Because of this ambiguity with the water washing, different washing conditions were sought.

II.3.5 Na^+ SORPTION STUDIES WITH BUFFER WASH

As above, the presence of Na^+ in the hydrated gel layer is of interest. It is necessary first to remove the 0.0200 M Na^+ solution from the interparticle and intraparticle (pore) spaces. Rather than using water as a wash liquid, an aqueous solution at the same pH as the load solution, containing a non-sodium electrolyte is used. The conditions required to do this were investigated by loading CPG-Oxine with the usual sample solution for only 2 min, washing for various periods of time and then eluting with 0.15 M HNO_3 into the flame. During a 2 minute loading time Na^+ from the solution does not have time to be sorbed into the porous gel layer to a significant extent. The washing liquid in this case was 0.0200 M HEPES buffer (pH = 7.00). The pH in this case was adjusted to 7.00 with concentrated ammonia water in order to avoid putting sodium in the wash solution. The results are shown in Figure 2.17 as a plot of millimoles of Na^+ remaining in the CPG-Oxine after washing versus washing time.

It is evident from Figure 2.17 that the HEPES buffer solution very rapidly washes out the Na^+. After 30 seconds the amount of Na^+ remaining from a 2 minute sample load is 8×10^{-5} mmol/g. In the washing process $NaClO_4$ is rapidly flushed from between the particles and rapidly diffuses out of the pores in the particle. In addition, there is Na^+ present in the diffuse double layer near the glass surface as a counterion for the anionic silonate groups. This "counterion" Na^+ undergoes rapid cation exchange with NH_4^+ in the HEPES solution and diffuses rapidly out of the pores.

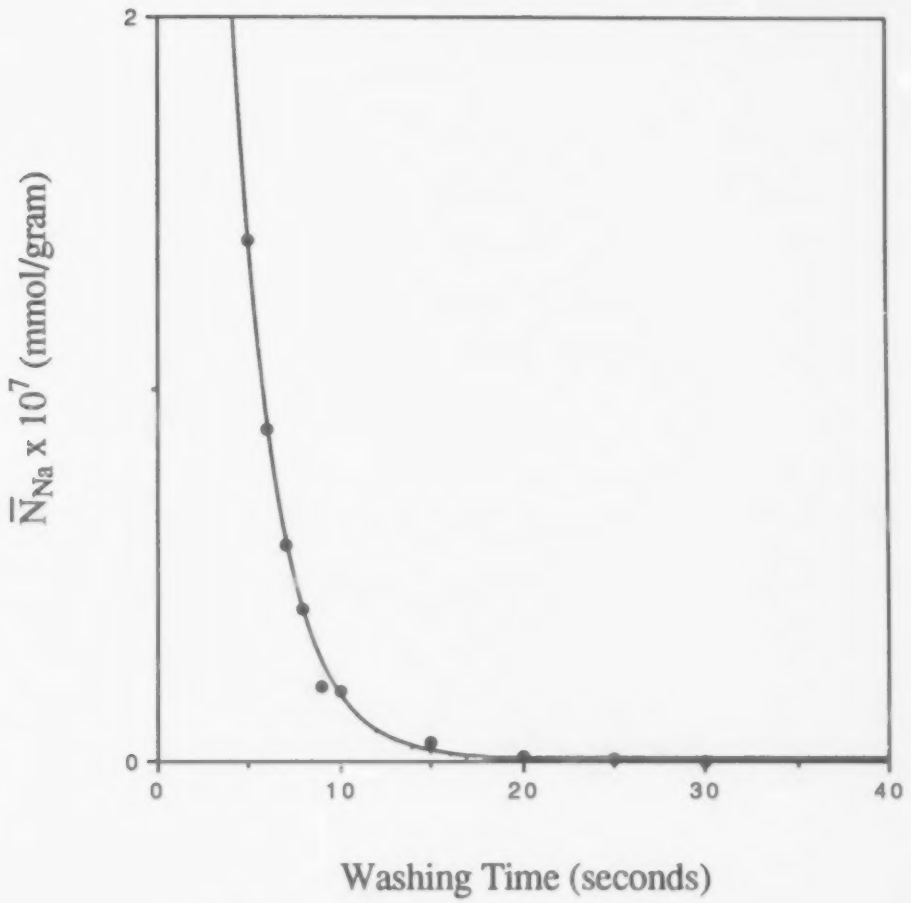

Figure 2.17 : Moles of Na^+ per gram that remains sorbed on CPG-Oxine after a 2-min loading followed by washing for increasing lengths of time with 0.0200 M HEPES solution (pH = 7.00).

Thus, the experiment to look for Na^+ sorbed in the hydrated gel layer was performed by loading CPG-Oxine for various periods of time with the usual sample solution containing 2.00×10^{-5} M Ca^{2+}, 0.0100 M HEPES buffer (pH = 7.00) and 0.0200 M $NaClO_4$; washing for 30 seconds with 0.0200 M HEPES solution (pH = 7.00) to remove all the Na^+ that has not been sorbed into the gel layer; and then eluting with 0.15 M HNO_3 for 4 minutes directly into the flame. A 4 minute elution has previously been shown to elute all of the Na^+ sorbed by the CPG-Oxine.

The amount of strongly sorbed sodium ($\overline{N}_{Na}$) measured in this way is plotted versus sample loading time in Figure 2.18. For comparison, the change (decrease) in Ca^{2+} sorbed ($\Delta\overline{N}_{Ca}$) is plotted in Figure 2.19 versus sample loading time, after 2 min. There is a remarkable similarity between these two curves. In fact they both can be approximated by the first-order rate law:

$$\overline{N}_i = \overline{N}_{i,\infty} \cdot (1 - \exp(-k_i \cdot t)) \qquad (2.1)$$

in which $\overline{N}_i$ is $\Delta\overline{N}_{Ca}$ for Ca^{2+} desorption and $\overline{N}_{Na}$ (strongly sorbed) for Na^+ sorption. Non-linear least squares curve fitting of the Ca^{2+} desorption data to Equation 2.1 yields $\Delta\overline{N}_{Ca,\infty} = (2.3 \pm 0.1) \times 10^{-4}$ mmol/g and $k_{Ca} = (2.73 \pm 0.11) \times 10^{-2}$ min^{-1}; and non-linear curve fitting of the Na^+ uptake data yields $\overline{N}_{Na,\infty} = (9.66 \pm 0.52) \times 10^{-3}$ mmol/g and $k_{Na} = (2.07 \pm 0.29) \times 10^{-2}$ min^{-1}. The uncertainties are standard deviations. The closeness of k_{Ca} to k_{Na} demonstrates the strong correlation between Ca^{2+} desorption and Na^+ uptake.

Assuming that the rate of Na^+ uptake is associated with the slow diffusion of Na^+ into the hydrated glass layer, the rate constant may be approximated as (78):

$$k_{Na} \approx \frac{\pi^2 \cdot \overline{D}_{Na}}{4 \cdot l^2} \qquad (2.2)$$

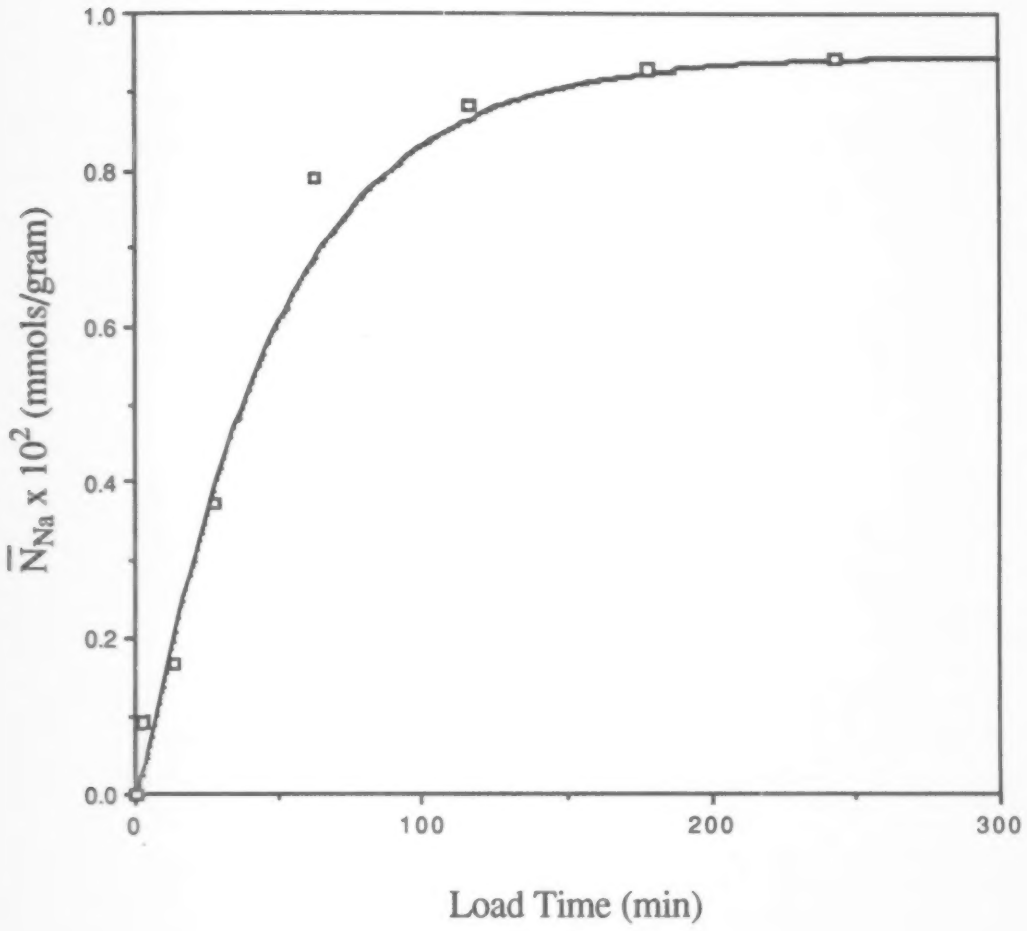

Figure 2.18 : Plot of strongly held Na^+ versus load time. Plot of actual data minus two minutes. Residual Na^+ washedwith 0.0200 M HEPES (pH = 7.00) for 30 seconds. Solid line is a first-order fit as per equation 2.1.

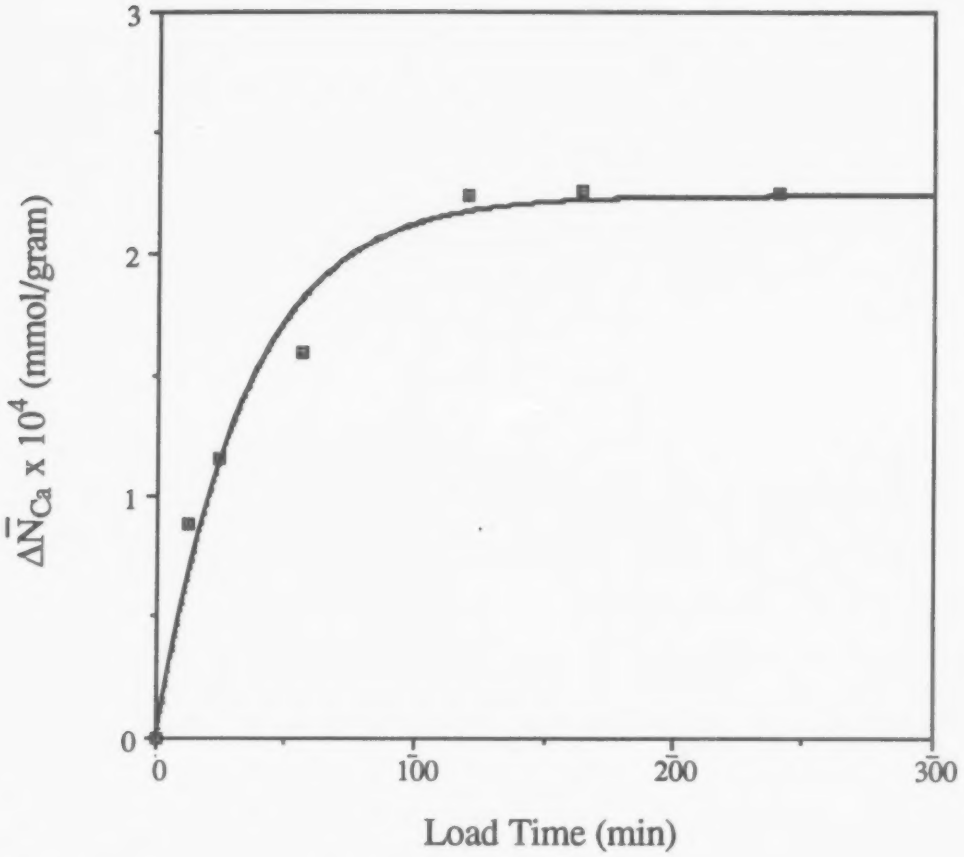

Figure 2.19 : Desorption curve for Ca^{2+}. Two minute loading point from Figure 2.9A is considered to be zero. All points are then determined as such: $\Delta\bar{N}_{Ca} = \bar{N}_{Ca,\ 2\ minutes} - \bar{N}_{Ca,\ load\ time\ (t)}$

where $\overline{D}_{Na}$ is the diffusion coefficient of Na^+ in a hydrated gel layer of thickness *l*. Equation 2.2 is obtained by employing a "linear driving force" approximation (79), in which only the first term is used in the series solution of the differential equation describing diffusion into a plane with one impermeable surface from a solution of constant composition (31). Substituting the value of k_{Na} from above (with units ofs) into Equation 2.2 and taking *l* to be about 5×10^{-7} cm (50 Å) (74) yields a valueof $\overline{D}_{Na} = 3 \times 10^{-17}$ cm^2/s which is in the expected range for diffusion through hydrated SiO_2 (74).

A quantitative comparison between the absolute rates of Na^+ sorption and Ca^{2+} desorption shows that the sorption rate for Na^+ is about forty times greater than the desorption rate for Ca^{2+}. That is, the desorption of one Ca^{2+} ion is brought about by the sorption of 40 Na^+ ions. This clearly demonstrates that the effect of Na^+ sorption on Ca^{2+} is not (mainly) due to a stoichiometric process such as cation exchange, but rather is due to a nonstoichiometric process such as a change in the local electrical potential; which is implied in equations 1.6 and 1.29.

II.4 CONCLUSIONS

The results of the preconditioning study combined with the fact that the rate of increase in the amount of difficult-to-elute Na^+ correlates strongly with the rate of desorption of Ca^{2+} constitutes strong evidence that the "overshoot" of the Ca^{2+} sorption equilibrium on CPG-Oxine results from the rapid ionization of silanols, probably in a hydrated gel layer, followed by a slow uptake of Na^+ (or NH_4^+) which "neutralizes" $-SiO^-$ groups and reduces Q. The decrease in Q causes a decrease in both the first term, *via* ψ_x, and the second (ion exchange) term in Equation 1.29 but the nonstoichiometric ratio of Ca^{2+} desorbed to Na^+ sorbed indicates that the influence of Na^+ is mediated primarily *via* the first term. Although Equation 1.6 would have to be modified to accurately express the

dependence of ψ_x on Q in terms of the "porous gel model", Equation 1.29 should still be reasonably accurate.

The reason for the "overshoot" of equilibrium in CPG-Oxine is different from the reason for overshoot in the ion exchange resin systems that were discussed in the Introduction to this chapter (48-50). In the ion exchange resin case, diffusion was occurring through a large distance (*e.g.* ≈ 1 mm), over which electroneutrality had to be maintained, and therefore, the ionic diffusion rates were "coupled" to one another (79). That is, for example, the silver-cyano complex ion had to diffuse in at the same rate that CN^- diffused out of the particle and the slower zinc-cyano ion had to diffuse in at a rate equal to the combined rate of outward diffusion of CN^- and silver-cyano species. In contrast, in the CPG-Oxine system the slow diffusion is occurring across the porous gel layer which has a thickness of only about ten or twenty hydrated ionic diameters. Over such short distances electroneutrality need not be maintained. (In fact, it is the violation of electroneutrality over such short distances that gives rise to interfacial potentials such as Donnan potentials and potentials of ion selective electrodes.) Thus, diffusion of Na^+ and H_3O^+ through the gel layer need not be coupled and it is the fact that H_3O^+ diffuses out of the gel faster than Na^+ diffuses in that creates the overshoot of equilibrium electrical potential.

The proposal that it is a slow uptake of Na^+ in the hydrated layer which reduces the (negative) potential on CPG-Oxine receives further support from studies performed on glass membrane ion selective electrodes (*e.g.* the glass electrode for pH). "Overshoot" of the equilibrium potential of these electrodes is often observed in solutions containing H_3O^+ and Na^+ when, for example, the concentration of H_3O^+ is changed (32,33). This overshoot usually occurs on a much shorter time scale than that observed with CPG-Oxine, due to the higher ionic diffusion coefficients in the hydrated gel layers of the much more hydrophilic electrode-glasses.

The results of the present study are relevant not only to the sorption of ions on CPG-bound ligands but also to affinity sorption and to size-exclusion chromatography of ionic species on CPG and, indirectly, to glass membrane electrodes. The rate of desorption of Ca^{2+} from surface-bound oxine serves as a probe of the rate of change in electrical potential near the glass surface.

In the next chapter the cause-effect relationship between Na^{+} sorption and Ca^{2+} sorption on CPG-Oxine will be examined quantitatively in terms of the electrical double layer theory.

CHAPTER THREE

Quantitative Explanation of the Relationship Between the Sorption of Ca^{2+} and Na^{+} on Controlled Pore Glass-Oxine in Terms of an Electrical Double Layer Model

III.1 INTRODUCTION

The development of a quantitative expression for the various electrical double layer effects described in chapters 1 and 2 that are produced by ionization of the CPG-Oxine surface and the slow sorption of Na^{+} requires the adoption of a detailed physiochemical model to describe the system. It has been found that most of the equilibrium properties related to the complexation of Ca^{2+} ions by the immobilized oxine ligand in CPG-Oxine could be explained by a simple version of the "ionizable surface group, site binding model" (45,46). This type of model is used widely in surface and colloid chemistry (64,65).

More recently, the studies in the previous chapter were undertaken to explain an anomalous aspect of the kinetics of Ca^{2+} sorption by CPG-Oxine. The anomalous behavior was an "overshoot" of equilibrium during the loading of Ca^{2+} on the small columns of CPG-Oxine, which had previously been rinsed thoroughly with water. The Ca^{2+}-loading curve, which is a plot of moles Ca^{2+} sorbed versus time, rose to a maximum in about 2 minutes and then decreased very slowly (hours), following a first-order rate curve, to a final equilibrium plateau value. Two aspects of this kinetic overshoot phenomenon were identified: First, the overshoot can be can be prevented by preconditioning the CPG-Oxine with a solution which contains the same buffer and $NaClO_4$ electrolyte concentrations as are in the sample solution, but which contains no Ca^{2+}. Second, when contacted either with the preconditioning solution (buffer and $NaClO_4$ electrolyte) or with the sample solution (buffer, $NaClO_4$ electrolyte and Ca^{2+}), the

CPG-Oxine sorbs Na^+, the amount of which increases according to a first order rate curve. This Na^+ sorption rate constant has the same value, within experimental variances, as does the first-order rate constant for the decrease in Ca^{2+} sorption; However, the absolute rate of moles of Na^+ sorbed is roughly 40 times faster than the absolute rate of moles of Ca^{2+} desorbed.

Based on these observations, the following conclusions were suggested. The slow desorption of Ca^{2+} from its overshoot sorption value to its equilibrium sorption value is caused by the sorption of sodium ions. The causal relationship is not a stoichiometric one, such as ion exchange would be, but rather results from the effect that Na^+-uptake into the hydrated glass layer has on the electrical double layer region in which the immobilized oxine ligand is located. Furthermore, it was suggested that the reason why the sorption of Na^+ is a slow process is because it involves diffusion of Na^+ into the "porous gel" hydrated glass layer, within which the diffusion coefficient of Na^+ is very small, as discussed in chapter two.

In the present chapter the kinetic aspects of the cause/effect relationship between sorbed Na^+ and sorbed Ca^{2+} are explained quantitatively in terms of the electrical double layer theory. In addition the equilibrium sorption isotherm of Na^+ in the hydrated glass layer is quantitatively characterized.

III.2 EXPERIMENTAL SECTION

III.2.1 REAGENTS AND CHEMICALS

All solutions were prepared with nanopure water (Barnstead/Thermolyne) and all chemicals used are reagent grade or purer (as in II.2.1). Preparations of the Ca^{2+} containing sample solutions was described previously in II.2.4. For use in the sorption rate studies of Ca^{2+} on CPG-Oxine and CPG and in the sorption rate study of Na^{+} on CPG-Oxine, the single solution contained 2.00×10^{-5} M Ca^{2+}, 0.0100 M HEPES buffer and 0.0200 M $NaClO_4$. It was prepared from stock solutions as described in II.2.4, adjusting its pH = 7.00 with NH_4OH. The solution had an ionic strength of 0.0224 M.

For use in the equilibrium Na^{+}-sorption study, a series of solutions were prepared which contained 2.00×10^{-5} M Ca^{2+} and various concentrations of $NaClO_4$ between 0.00100 M to 0.1400 M. The solutions contained no HEPES buffer but, rather, were adjusted to pH = 7.00 using NaOH and HNO_3. Since no buffer was used, the pH was checked frequently in both the solution reservoir and in the effluent from the CPG-Oxine column.

III.2.2 Ca^{2+}-SORPTION RATE

The manner in which the sorption rate measurements of Ca^{2+} on both CPG-Oxine and CPG were conducted has been described in detail in II.2.5. Briefly, the solution containing 2.00×10^{-5} M Ca^{2+}, 0.0100 M HEPES buffer (pH = 7.00) and 0.0200 M $NaClO_4$ was pumped through the bed of either CPG-Oxine or CPG only for various periods of time between 2 minutes and 250 minutes after which a 4 minute elution with 0.15 M HNO_3 was used to remove all Ca^{2+} from the column (Note: the Ca^{2+} eluted quickly, < 1 minute, but to standardize the experiments, a fixed elution of 4 minutes time

was used). The Ca^{2+} was eluted directly into the flame of the spectrometer. In this type of experiment the amount of Ca^{2+} in the column hold-up volume (17 μL) must be subtracted from the amount eluted in order to determine the amount sorbed (51,88). In the Ca^{2+} sorption rate study on CPG-Oxine the hold-up volume correction was less than 2% of the equilibrium amount of sorbed Ca^{2+}. After calibrating with standard Ca^{2+} solutions, the resulting peak area yielded the amount of Ca^{2+} sorbed on the column packing during the loading time. Following the acid elution the column was washed with nanopure water and thus was ready for the next loading operation.

III.2.3 Na^+-SORPTION RATE

As above, the manner in which the sorption rate of Na^+ on the Oxine was measured has been described in detail in II.2.10. It is very similar to the Ca^{2+}-sorption rate procedure except that a washing step is interposed between the loading and elution steps. Immediately following the loading step the column was washed for 30 seconds with sodium-free 0.0200 M NH_4^+-HEPES buffer solution (pH = 7.00). This washing step was necessary to wash out all of the Na^+-containing interstitial and pore solution, due to its high Na^+ concentration. Following the washing step a 4 minute elution of the column with 0.15 M HNO3 removed all of the strongly sorbed Na^+ into the Atomic Emission Spectrometer. (Note: the majority of the Na^+ eluted in less than 2 minutes, but the Na^+ was not fully eluted for 4 minutes).

III.2.4 Na^+-EQUILIBRIUM STUDY

The sodium equilibrium experiments were performed on the CPG-Oxine column. A series of solutions containing 2.00×10^{-5} M Ca^{2+} and various concentrations of $NaClO_4$ at pH = 7.00 were pumped through the column for a sufficiently long time that sorption

equilibrium was achieved. Both 2 and 4 hour loading times were employed in order to verify that equilibrium was reached. Immediately following this loading step the column was washed with sodium free 0.0200 M NH_4^+-HEPES (pH = 7.00) for 30 seconds. The column was then eluted for 4 minutes with 0.15 M HNO_3 into the atomic emission spectrometer and the resultant peak areas were measured. As before, in order to compensate for possible drift in instrument sensitivity and solution composition over the long periods of time involved in the loading studies, sodium calibrations were run before and after each experimental run. A series of standards, 2.00×10^{-3} M to 10×10^{-3} M, were injected using valve V2 (Figure 2.1) before and after each experimental point, and the average values were used to determine the empirical amount of Na^+ eluted.

III.3 RESULTS AND DISCUSSION

Three aspects of the behavior of CPG-Oxine arising from the ionization of silanol groups on the surface and in the hydrated glass layer is quantified. First, the process responsible for sorption of Na^+ by CPG-Oxine are characterized. Second, a quantitative electrical double-layer model is developed in which the complexation of Ca^{2+} by immobilized oxinate ligand is related to sorption of Na^+ in the hydrated layer via the electrical potential Ψ_x. Finally, the desorption rate of Ca^{2+} from CPG-Oxine is quantified as a function of the sorption rate of Na^+, in terms of the derived model.

III.3.1 EQUILIBRIUM SORPTION OF Na^+

It was previously suggested in chapter 2 that the uptake of Na^+ by the hydrated gel layer can be treated as a cation exchange of Na^+ for H^+. The legitimacy of this view is tested experimentally in the present study by comparing the amount of Na^+ sorbed at equilibrium with the ionic activity of Na^+ in bulk solution, at a constant pH of 7.00. In this

study the CPG-Oxine column was brought to equilibrium with solutions containing various concentrations of $NaClO_4$, ranging from 0.0010 M to 0.1400 M. The solutions also contained 2.00×10^{-5} M Ca^{2+}, but the small amounts of Ca^{2+} both in solution and sorbed on the CPG-Oxine can be ignored in this study of Na^+ sorption. The solutions were adjusted to pH = 7.00 with small amounts of 0.10 M NaOH. Since no buffer was used, a check of the sample pH in both the reservoir bottle and the effluent from the CPG-Oxine column was done at the end of the loading experiments, and the pH drift was considered to be negligible (drift of 0.05 pH units). Establishment of equilibrium was verified by finding the same results (that is, the same amount of Na^+ eluted) for both the 2 and 4 hour loading times. The concentration of Na^+ sorbed at equilibrium, $\overline{N}_{Na,\,equil}$ (mmol/g) is plotted versus $[Na^+]$ in Figure 3.1, where it is seen that the amount of sorbed Na^+ increases toward a limiting value. This plot is a sorption isotherm for Na^+. The data is presented in Table 3.1.

Titration studies have shown that at equilibrium at pH = 7.00 there are 0.027 mmol of protons lost per gram for this batch of CPG-Oxine (45). This quantity, which will be called Q_{max}, is independent of $[Na^+]$ in solution; at least within the range $[Na^+] = 0.01$ to 0.20 (46). Since the amount of Na^+ sorbed increases with $[Na^+]$, this means that the degree of dissociation of SiOH groups in the hydrated glass layer, at fixed solution pH, is independent of the amount of Na^+ sorbed by the hydrated glass layer. Sorption on Na^+ may be represented as:

$$\overline{SiO^-} + Na^+ \Leftrightarrow \overline{SiONa} \qquad (3.1)$$

The implication of the above observations is that:

$$(\overline{SiO^-})_0 \equiv (\overline{SiO^-}) + (\overline{SiONa}) = \text{CONSTANT} \qquad (3.2)$$

Table 3.1 Parameters relating to the sorption of Na^+ on CPG-Oxine at pH = 7.00 at various bulk solution concentrations of Na^+.

$[Na^+]$ (mol/L)	γ_{Na} (a)	$\overline{N}_{Na,\ equil}$ (mmol/g)
1.00×10^{-3}	0.965	0.87×10^{-3}
5.00×10^{-3}	0.924	2.67×10^{-3}
20.00×10^{-3}	0.855	5.50×10^{-3}
40.00×10^{-3}	0.803	6.00×10^{-3}
80.00×10^{-3}	0.734	8.20×10^{-3}
120.00×10^{-3}	0.684	8.10×10^{-3}
140.00×10^{-3}	0.664	8.60×10^{-3}

(a) Activity coefficient calculated by the Davies Equation (90).

In these expressions a superscript bar indicates the hydrated glass layer, the absence of a bar indicates the bulk aqueous solution and parentheses indicate concentrations in the hydrated glass layer in units of mmol/g of dry CPG-Oxine. The equilibrium constant for the reaction in equation 3.1 is:

$$K_{Na} = \frac{(\overline{SiONa})}{(\overline{SiO^-}) \cdot [Na^+] \cdot \gamma_{Na}} \qquad (3.3)$$

where $[Na^+]$ is the bulk solution concentration (mol/L) and γ_{Na} is the activity coefficient of Na^+ in the bulk solution. Combining equations 3.2 and 3.3, substituting $\overline{N}_{Na,equil}$ for $(\overline{SiONa})$ and rearranging gives the expression:

$$\overline{N}_{Na,equil} = \frac{[Na^+] \cdot \gamma_{Na} \cdot K_{Na} \cdot (\overline{SiO^-})_o}{1 + [Na^+] \cdot \gamma_{Na} \cdot K_{Na}} \qquad (3.4)$$

Equation 3.4 predicts the relationship between $\overline{N}_{Na,equil}$ and $[Na^+]$. The activity coefficient γ_{Na} was calculated from the Davies equation with an ionic size parameter of 4.5×10^{-8} cm (90). Values of γ_{Na} are included in table 3.1. At constant pH, both K_{Na} and $(\overline{SiO^-})_o$ are constants. Equation 3.4 was fit to the data points in table 3.1 by nonlinear least squares curve fitting. The correlation coefficient is 0.991 and the constants K_{Na} and $(\overline{SiO^-})_o$ have values of (73.8 ± 14.7) L/mol $(9.61 \pm 0.48) \times 10^{-3}$ mmol/g, respectively. The line in figure 3.1 is predicted from equation 3.4.

The parameter $(\overline{SiO^-})_o$ is the charge in the hydrated glass layer at pH = 7.00 in the absence of sorbed Na^+. The fact that $(\overline{SiO^-})_o < Q_{max}$ is important because it reveals information about the properties of the hydrated glass layer. These properties are represented diagrammatically in Figure 3.2, which is discussed below. The specific surface area of CPG-Oxine is $A_{sp} = 7.0 \times 10^5$ cm^2/g (19). Nearly all of this surface lines the walls of the pores. This is the outer surface of the hydrated glass layer. There are

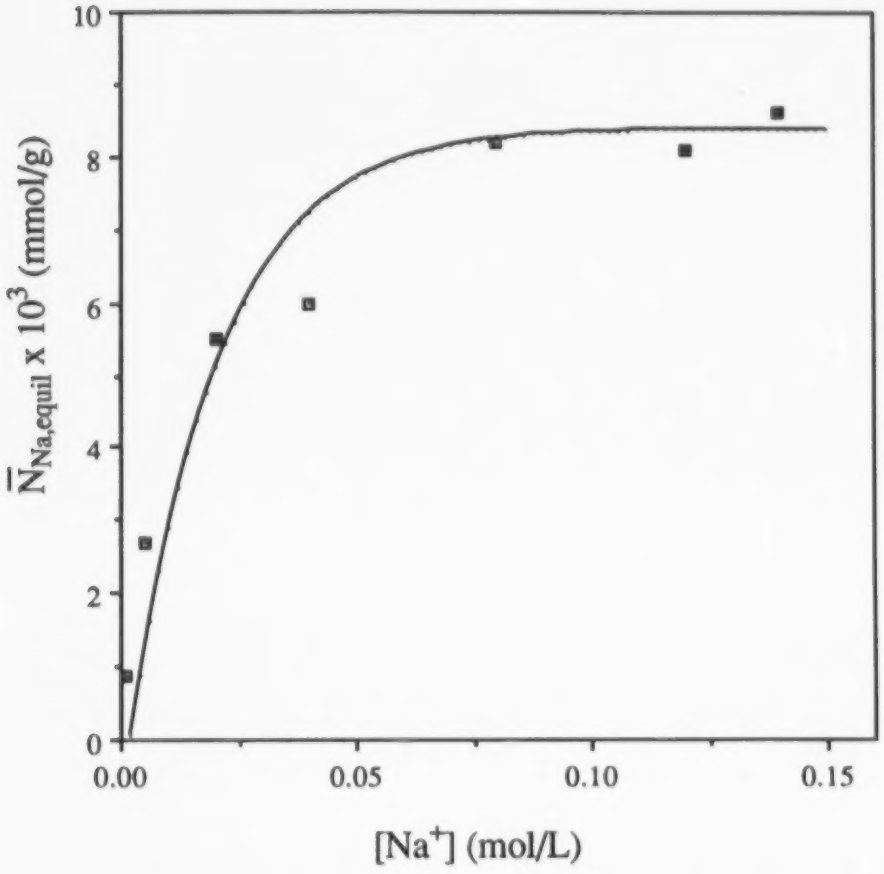

Figure 3.1 : Sorption isotherm of Na^+ on CPG-Oxine from pH = 7.00 bulk solution. The points are experimental data. The line is predicted from equation 3.4 using K_{Na} = 74 L/mol, $(\overline{SiO^-})_o$ = 9.61 x 10^{-3} mmol/g and γ_{Na} from table 3.1, as discussed in the text.

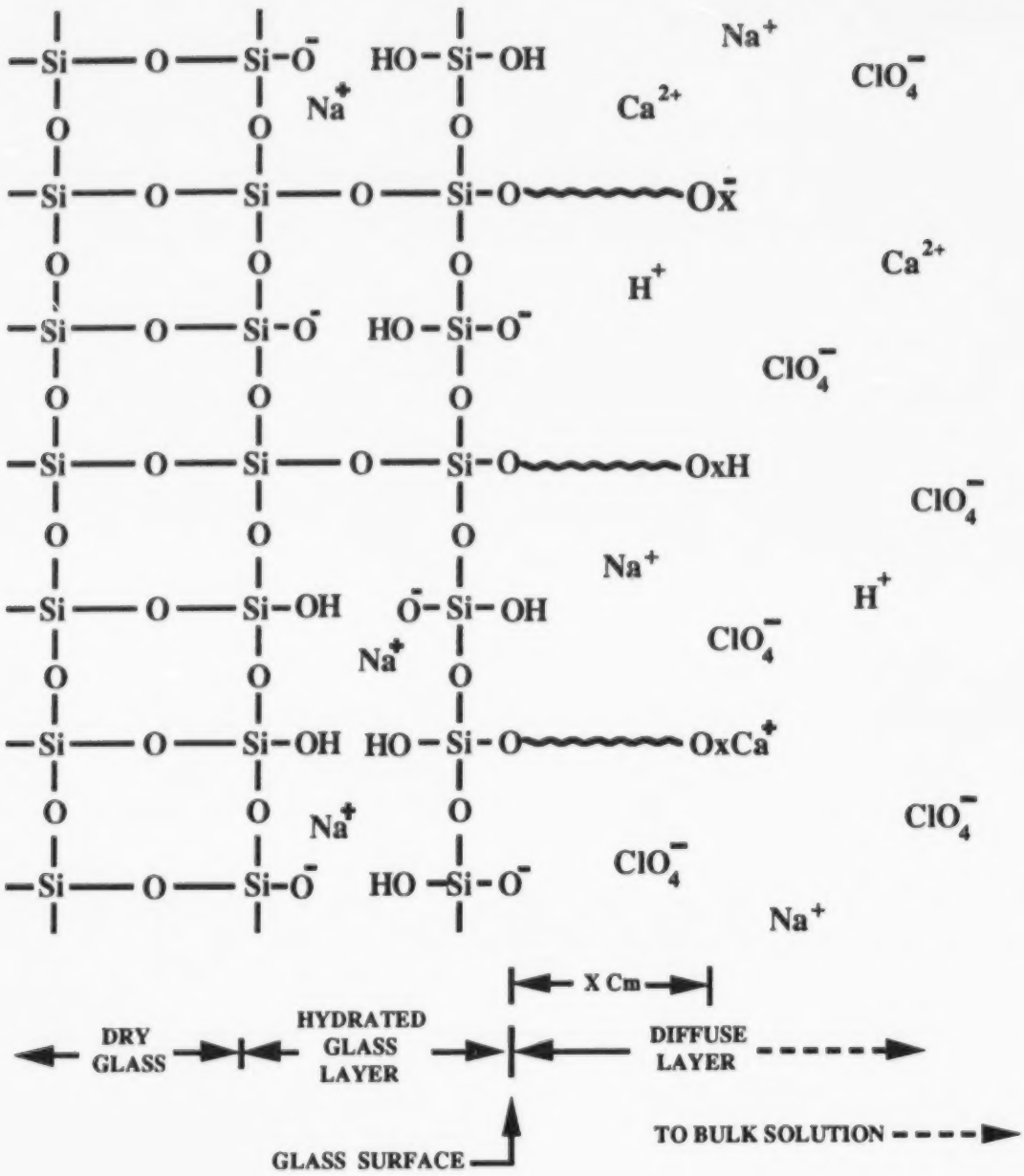

Figure 3.2 : Diagrammatic representation of the region near the glass-solution interface lining the pores in CPG-Oxine. Average pore diameter is 500 Å. Pore liquid contains both the diffuse layer and bulk solution. See text for details.

silanol groups on this surface, corresponding to between 0.4 and 0.9 mmol/g of CPG-Oxine (53,75,84,85). In addition, silanol groups are also present *within* the hydrated glass layer, which extends from the glass surface toward the underlying dry glass.

When the bulk solution pH is raised to 7.00 some of the silanols on the surface ionize to SiO^- and some of the silanols within the hydrated layer likewise ionize, the total amount of SiO^- being Q_{max} (*i.e.* 0.027 mmol/g). However, *Na^+ becomes sorbed only within the hydrated layer*, not at its surface. That is, Na^+ is sorbed and contributes to $\overline{(SiONa)}$ only when it has passed through the surface and entered *into* the hydrated layer, in which it "neutralizes" an equivalent number of SiO^- groups.

In contrast, SiO^- groups at the surface lie in a plane that is well separated from the plane of closest approach of Na^+ ions in the adjacent solution. The Na^+ ions in the solution adjacent to the surface are in the diffuse part of the electrical double layer in the pore liquid and would not be detected in this experiment because the pore liquid is washed out with NH_4^+ solution prior to the acid-elution step. Thus, the results of the previous titration experiments combined with the results of the present Na^+ sorption experiment shows that, at pH = 7.00, about one-third (*i.e.* 0.0096/0.027) of the ionized silanol groups lie within the hydrated glass layer and about two-thirds are to be found at the glass surface. These SiO^- groups at the glass surface represent about 3% of the number of SiOH groups at the glass surface (53,75,84,85). It will also be recalled that only a small fraction of the surface silanols have been derivatized with 5-phenylazo-8-hydroxyquinoline groups.

It should be noted that the sorption of Na^+ into the hydrated glass layer arises because H^+ ions have left that region, leaving behind excess negative charge. This phenomenon is therefore an "ion exchange" process. However, the hydrated glass layer is so thin (*i.e.* tens of Å , chapter 1) that electroneutrality is violated over the region spanning the hydrated glass layer and the diffuse part of the electrical double layer in the pore solution. As a consequence, there can be present at equilibrium a stoichiometric excess of SiO^- in the hydrated glass layer and stoichiometric excesses of cations in the diffuse layer

solution, so that a 1:1 stoichiometric exchange of Na^+ for H^+ in the hydrated glass layer is not required.

III.3.2 MODIFIED DOUBLE-LAYER SORPTION MODEL FOR Ca^{2+}

It has been shown that Ca^{2+} is sorbed on CPG-Oxine from a $NaClO_4$ solution by two different processes (46). One sorption process is complexation of Ca^{2+} by the immobilized oxinate ligand, the extent of which depends on the electrical potential as discussed above. The other sorption process probably is related to cation exchange of Ca^{2+} for Na^+ in the diffuse part of the electrical double layer. There is no evidence to suggest that Ca^{2+} enters the hydrated glass layer. The former of these two processes, complexation, is generally much more important than the latter.

The oxinate moiety of the immobilized 5-phenylazo-8-hydroxyquinoline, which is the anionic bidentate ligand that complexes Ca^{2+}, is located in the solution in the diffuse part of the electrical double layer at a distance x cm from the glass surface. It is the electrical potential Ψ_x (volt), at location x which influences the Ca^{2+} complexation of oxinate. According to the "ionizable surface group, site binding model" stated in chapter 1, the millimoles of Ca^{2+} complexed per gram of CPG-Oxine, $\overline{N}_{Ca}(CPG\text{-}Ox)$, is related to Ψ_x by combining equations 1.16, 1.19 and 1.21 to give the expression:

$$\overline{N}_{Ca}(CPG\text{-}Ox) = [Ca^{2+}] \cdot \gamma_{Ca} \cdot \overline{\nu}_{Oxine} \cdot \overline{\beta}_1 \cdot \overline{K}_{a2} \cdot a_H^{-1} \cdot \exp\left(-\frac{F \cdot \Psi_x}{R \cdot T}\right) + \overline{N}_{Ca,\,IEX} \qquad (3.5)$$

Ignoring $\overline{N}_{Ca,\,IEX}$ for now, rearranging equation 3.5 and taking the natural logarithm of both sides yields the expression:

$$\ln\left(\frac{\overline{N}_{Ca}}{\gamma_{Ca}}\right) = \ln\left([Ca^{2+}] \cdot \overline{\nu}_{Oxine} \cdot \overline{\beta}_1 \cdot \overline{K}_{a2} \cdot a_H^{-1}\right) - \frac{F \cdot \Psi_x}{RT} \qquad (3.6)$$

From equation 3.6 it is predicted that a plot of $\ln (\bar{N}_{Ca} / \gamma_{Ca})$ <u>versus</u> Ψ_x should be linear with a slope of - F/RT (*i.e.* -38.9).

The question then becomes how to calculate the surface potential, Ψ_o. Previously, in chapter 1 the relatively simple "surface ionization model" was used (45,46), in which it was assumed that the ionized silanolate groups are present only at the two-dimensioned glass surface located at the interface between the hydrated glass layer and the solution (45,46,63-65). This simple model is inconsistent with the "porous gel" assumption invoked in chapter 1 to explain the excessively slow sorption of Na^+ by the glass and which has been described above. In the porous gel model (64,72,73), ionization of silanol groups occurs throughout the hydrated glass layer which, as discussed in in chapter 1 has a thickness in the range of tens of Å units (40). The simple "surface ionization" model, which was previously used can be treated mathematically by the relatively simple Gouy-Chapman theory of the electrical double layer in order to obtain Ψ_o, while in contrast, the porous gel model involves a double-diffuse double layer, for which the theoretical calculation of Ψ_o is more complex (64,72,73). Although the evidence favours the view that a porous gel model should be used to calculate Ψ_o, it is not possible to do so with the information that is available on the properties of CPG-Oxine. Therefore, as an approximation, the system will be treated using the simpler "surface ionization model". That is, although some of the anionic silanolate groups are distributed throughout the hydrated glass, porous gel, layer across a distance in the range of tens of Angstroms, for purposes of calculating their contribution to Ψ_o, all of the silanolate groups will be treated as though they reside at the surface of the hydrated glass layer. The Gouy-Chapman theory will be employed. A result of this approximation is that the calculated values of the surface potential, Ψ_o, and of the potential at the location of oxine, Ψ_x, will be somewhat higher than their true values.

According to the Gouy-Chapman theory, the surface potential at the glass-solution interface is given by the expression:

$$\sinh\left(\frac{Z \cdot F \cdot \psi_o}{2 \cdot R \cdot T}\right) = (8.53 \times 10^4) \cdot c^{-1/2} \cdot \sigma_o \qquad (1.4)$$

where σ_o is the surface charge density (coul/cm^2) due to silanolate groups (39-41). The surface charge density is related to the excess concentration of negatively charged groups on the glass, Q_t (mmol/g), as follows:

$$\sigma_o = \frac{Z_- \cdot F \cdot Q_t}{1000 \cdot A_{sp}} \qquad (3.7)$$

Here Z_- has the value of minus one (-1). The quantity Q_t is equal, at time t, to the concentration of ionic silanolate groups (*i.e.* concentration of protons that have left both from within and from the surface of the hydrated glass layer) *minus* the concentration of Na^+ ions that have entered the hydrated layer.

III.3.3 DESORPTION RATE OF Ca^{2+}

Shown in Figure 3.2 is a diagrammatic representation of the interfacial region during the time that the slow sorption of Na^+ is taking place. Initially, the bed of CPG-Oxine was washed by pumping through it, first dilute acid and then water. Then the pH and the ionic strength were raised by pumping through it a sample solution containing buffer, electrolyte ($NaClO_4$) and Ca^{2+}. As discussed above, some fraction of the silanol groups in the porous gel layer and at the glass surface ionize to form silanolate and hydrogen ions. The dissociated hydrogen ions diffuse out of the gel layer at a relatively rapid rate. The resulting "surface excess" of negative SiO^- is the sum of SiO^- at the surface and within the hydrated glass layer. Gradients of negative electrical potential become established both in the hydrated glass layer and in the diffuse layer in the adjacent pore

liquid. Now, at a *rate much slower than that at which H^+ ions diffused out*, Na^+ ions diffuse into the gel layer until equilibrium is established. That is, the establishment of Na^+ sorption equilibrium within the hydrated glass layer is a slow process.

If $\overline{N}_{Na,t}$ (mmol/g) is the concentration of Na^+ sorbed at time t, then the concentration of ionic silanolate groups, Q_t, at time t is :

$$Q_t = Q_{max} - \overline{N}_{Na,t} \qquad (3.8)$$

where Q_{max} has the value 0.0270 mmol/g.

Values of $\overline{N}_{Na,t}$ are known from the previous Na^+ sorption rate study done in chapter 2. After only two minutes of loading, the H^+ produced by the ionization of SiOH groups has diffused out of the hydrated layer, but very little Na^+ has diffused in. That is, for t = 2 min, $\overline{N}_{Na,t} = 0$ and $Q_t \approx Q_{max}$. With time, Q_t continues to decrease as more Na^+ diffuses in, and this decrease in Q_t decreases σ_o, which in turn, makes Ψ_o and Ψ_x less negative and consequently decreases $\overline{N}_{Ca}$. After a sufficiently long time $\overline{N}_{Na,t}$ has increased to its constant equilibrium value $\overline{N}_{Na,equil}$ and as a consequence $\overline{N}_{Ca}$ has decreased to its equilibrium value. Kinetically, it is assumed that the rates of formation and dissociation of the Ca^{2+}-oxinate complex are much faster than the rate of Na^+ sorption into the hydrated glass layer.

Data for Na^+-sorption and Ca^{2+}- sorption are taken from earlier studies done in chapter 2. Based on the above discussion, the time 2.0 min from the start of the experiment is taken to be t = 0 min in both the Na^+-and Ca^{2+}-sorption rate experiments. The first column in Table 3.2 presents the times at which Na^+-sorption was measured experimentally on CPG-Oxine and the second column presents the experimentally measured amounts of Na^+ sorbed at these times.

In the third column are shown the amounts of Ca^{2+} sorbed on CPG-Oxine at the same times. These come from the data in Figure 2.9A, section II.3.2. Since Ca^{2+}-

Table 3.2 Parameters relating to the sorption of Ca^{2+} and Na^{+} from a solution containing 2.00 x 10-5 m Ca2+, 0.0200 M $NaClO_4$ and 0.0100 M HEPES buffer at pH = 7.00. Ionic strength is 0.0224 M. $\gamma_{Ca} = 0.549$ and $x = 5.7 \times 10^{-8}$ cm.

Load Time (min) (a)	$\overline{N}_{Na,t}$ (mmol/g) (b)	$\overline{N}_{Ca}$(CPG-Ox) (mmol/g) (c)	$\overline{N}_{Ca}$(CPG) (mmol/g) (d)	$\overline{N}_{Ca}$ (mmol/g)	Q_t (mmol/g)	σ_o (coul/cm^2)	ψ_o (Volt)	ψ_x (Volt)	$\ln\left(\frac{\overline{N}_{Ca}}{\gamma_{Ca}}\right)$
0	0	5.94×10^{-4}	5.71×10^{-5}	5.37×10^{-4}	0.0270	-3.72×10^{-6}	-0.0768	-0.0536	-6.93
3	0.93×10^{-3}	5.77×10^{-4}	5.68×10^{-5}	5.19×10^{-4}	0.0261	-3.59×10^{-6}	-0.0752	-0.0526	-6.97
14	1.67×10^{-3}	5.22×10^{-4}	5.55×10^{-5}	4.66×10^{-4}	0.0253	-3.49×10^{-6}	-0.0739	-0.0518	-7.07
28	3.74×10^{-3}	4.72×10^{-4}	5.39×10^{-5}	4.19×10^{-4}	0.0233	-3.20×10^{-6}	-0.0700	-0.0495	-7.18
62	7.89×10^{-3}	4.08×10^{-4}	5.00×10^{-5}	3.58×10^{-4}	0.0191	-2.63×10^{-6}	-0.0614	-0.0441	-7.34
116	8.81×10^{-3}	3.76×10^{-4}	4.38×10^{-5}	3.32×10^{-4}	0.0182	-2.51×10^{-6}	-0.0593	-0.0427	-7.41
179	9.30×10^{-3}	3.68×10^{-4}	3.65×10^{-5}	3.32×10^{-4}	0.0177	-2.44×10^{-6}	-0.0582	-0.0420	-7.41
244	9.44×10^{-3}	3.67×10^{-4}	2.90×10^{-5}	3.38×10^{-4}	0.0176	-2.42×10^{-6}	-0.0578	-0.0417	-7.39

(a) Real time for Na^{+} sorption minus 2 minutes
(b) Experimental data points for Na^{+} sorption on CPG-Oxine
(c) From equation 3.9, describing experimental Ca^{2+} sorption rate on CPG-Oxine
(d) From equation 3.10, describing experimental Ca^{2+} sorption rate on CPG.

sorption was measured experimentally at times not identical to these in the first column of Table 3.2 the amounts of Ca^{2+} sorbed that are shown in the third column were calculated from the least-squares curve fit to the data in Figure 2.9A, after subtracting the Ca^{2+} in the hold-up volume. The first order equation (starting t = 0 at 2 min) which describes the Ca^{2+}-sorption rate on CPG-Oxine is:

$$\overline{N}_{Ca}\,(\text{CPG-Oxine}) = (5.94 \pm 0.07) \times 10^{-4} - 2.275 \times 10^{-4} \cdot (1-\exp[\,(-0.0273 \pm 0.0011) \cdot t\,]) \qquad (3.9)$$

the correlation coefficient is 0.994 and the uncertainties are standard deviations.

In order to identify the amount of Ca^{2+} that is sorbed onto CPG-Oxine by processes other than complexation with immobilized oxinate, Ca^{2+} sorption on CPG (with no oxine) was also measured, at the same $[Ca^{2+}]$ in solution (Figure 2.9B, section II.3.2). The amount of Ca^{2+} sorbed on CPG is about 10% of the amount sorbed on CPG-Oxine and, taking 2 min to be zero time, its amount, $\overline{N}_{Ca}\,(\text{CPG})$, after subtracting the Ca^{2+} in the hold-up volume, is given as a function of time by the equation:

$$\overline{N}_{Ca}\,(\text{CPG}) = (5.71 \pm 0.05) \times 10^{-5} - (1.15 \pm 0.04) \times 10^{-7} \cdot t \qquad (3.10)$$

which has a correlation coefficient of 0.997. Values of $\overline{N}_{Ca}\,(\text{CPG})$ calculated for the times in the first column are presented in the fourth column of Table 3.2. Because such a small fraction of the silanol groups on the glass surface of CPG-Oxine is derivetized with oxine, it can be assumed that at any time t the amount of Ca^{2+} sorbed on CPG-Oxine by processes other than complexation with oxinate is equal to $\overline{N}_{Ca}\,(\text{CPG})$. Thus, the value of $\overline{N}_{Ca}$, corresponding to Ca^{2+} sorbed on CPG-Oxine and by complexation with oxinate, is given by the expression:

$$\overline{N}_{Ca} = \overline{N}_{Ca}\,(\text{CPG-Oxine}) - \overline{N}_{Ca}\,(\text{CPG}) \qquad (3.11)$$

Values of $\overline{N}_{Ca}$ are presented in the fifth column. In the sixth, seventh, and eighth columns of table 3.2 are presented the values of Q_t, σ_o and the surface potential Ψ_o which were calculated from equations 3.8, 3.7, and 1.4, respectively.

In the last column are shown values of the function $\ln (\overline{N}_{Ca} / \gamma_{Ca})$. The value of $\overline{N}_{Ca}$ to be used here is from column 5 and the value of γ_{Ca} is 0.549 (46), which is constant because the ionic strength of the bulk solution is constant.

Equation 3.6 describes the relationship between the amount of Ca^{2+} sorbed via complexation by oxinate on CPG-Oxine and the potential Ψ_x. The other parameters in equation 3.6, $[Ca^{2+}]$, γ_{Ca}, $\overline{\nu}_{Oxinate}$, $\overline{\beta}_1$ and $\overline{K}_{a2}$ are constants which would appear in the intercept of the plot on $\ln (\overline{N}_{Ca} / \gamma_{Ca})$ versus Ψ_x. The difficulty in making such a plot is the fact that the value of x, which is required in equation 1.6 to calculate Ψ_x, is not known. However, the value of x can be obtained by trial and error. A value is assumed for x and is used to calculate Ψ_x as a function of time. A plot is made of $\ln (\overline{N}_{Ca} / \gamma_{Ca})$ versus Ψ_x. The procedure is repeated for various assumed values of x. The correct value of x is the one which leads to a straight line plot with a slope of -38.9 (*i.e.* -F/RT). For the present system, x is found to be $(5.7 \pm 1.1) \times 10^{-8}$ cm (*i.e.* 5.7 Å). The corresponding values of Ψ_x from equation 1.6 are presented in column 9 of Table 3.2. and the plot of $\ln (\overline{N}_{Ca} / \gamma_{Ca})$ versus Ψ_x is shown in Figure 3.4. It is linear with a correlation coefficient of 0.980, a slope of -38.9 ± 2.9 and an intercept of -9.06 ± 0.14. the uncertainty in x is estimated from the uncertainty in the slope.

An experimental value of about 6 Å for x is quite reasonable since the spacer-arm which attaches the oxinate ligand to the glass surface, when fully extended, would place the oxinate about 18 Å away from the surface (20, 45). Thus, an observed value of $x \approx 6$ Å suggests that at pH = 7.00 and $c \approx 0.02$ the spacer-arm is folded back on itself, as had previously been suggested (45).

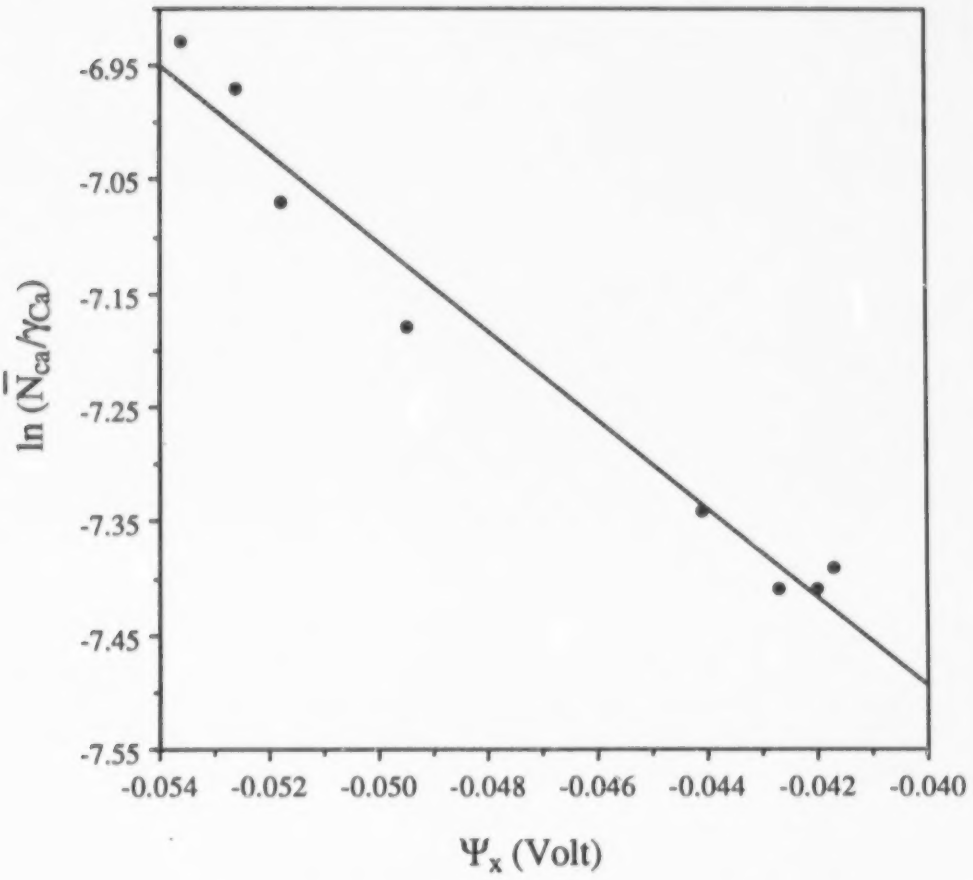

Figure 3.3 : Plot of ln ($\bar{N}_{C_a}/\gamma_{C_a}$) vs x to test the linear dependence predicted by equation 3.9. Points are data from columns 9 and 10 in table 3.2. Oxinate is located at x = 5.7 x 10^{-8} cm. The line is a least squares fit having a slope of -38.9.

III.4 CONCLUSIONS

By measuring the extent to which it complexes Ca^{2+}, the immobilized ligand oxine can be used as an indirect probe of electrical potential in the electrical double layer of the solution adjacent to the glass surface. In this study it has been demonstrated that, above the pH of zero charge of the glass, the surface potential Ψ_o and the potential at any location x in the diffuse layer undergo a slow decrease in magnitude of their negative value with time and eventually reach equilibrium values. This slow drift in Ψ_o and Ψ_x results from the slow sorption of Na^+, presumably as a result of a slow diffusion of Na^+ into the hydrated gel layer. This proposed explanation has been tested experimentally using the ionizable surface group, site-binding model to describe the complexation of Ca^{2+} by immobilized oxinate. The results quantitatively support both the use of the site-binding model for Ca^{2+} complexation and the cause-effect relationship between slow uptake of Na^+ and slow desorption of Ca^{2+}. Previously, in chapter 2, it was shown that the rate of Na^+ sorption by diffusion in the hydrated glass layer is consistent with the expected diffusion coefficient of Na^+ in hydrated glass.

The potential at some distance x from the glass surface correlates strongly with the electrokinetic ζ potential at the plane of shear. There is considerable interest in the ζ potential at the surface of fused silica as it relates to electroosmotic flow in the capillaries that are used for capillary zone electrophoresis. For example, in a recent study of electroosmosis, the results were interpreted in terms of the formation of a complex between alkali metal ions (e.g. Li^+ and Na^+) and SiO^- groups at the surface of the fused silica (86). The bound alkali metal was assumed to occupy the inner Helmholtz plane rather than to enter a hydrated layer.

However, it was mentioned that "to ensure equilibrium was reached between the silica and solution phases, the phosphate buffer...was loaded into the capillary at least 6

hours before the measurements were carried out" (86). In addition, it is often observed that long periods of "conditioning" are required for electroosmotic behavior to stabilize when electrolytes are first put into fused silica capillaries (89). Since CPG is a Vycor-type glass that is composed $\geq 95\%$ SiO_2, it might be expected that there would be some similarities between CPG and fused silica. In fact, a hydrated gel layer has been shown to form on fused silica (64, 87). Thus, it is likely that slow diffusion of ions such as Na^+ would occur into the hydrated layer on fused silica to produce a slow drift of ζ toward an equilibrium value after, for instance, an electrolyte of higher pH has been introduced to the capillary. In contrast, adsorption of such ions into an Inner Helmholtz plane located at the boundary between the silica capillary surface and the solution, should not be a particularly slow process (86).

Finally, it may be noted that when the surface potential, Ψ_o, is ≤ 0.025 volt the so-called Debye-Huckel approximation can be made. Then equation 1.4 simplifies to an expression in which (38):

$$\Psi_o \propto c^{1/2} \qquad (3.12)$$

and equation 1.6 simplifies to the form (38, 45, 46):

$$\Psi_x \approx \Psi_o \cdot \exp(-3.29 \times 10^7 \cdot c^{1/2} \cdot x) \qquad (3.13)$$

and Ψ_x can be expressed as:

$$\Psi_x \approx -\frac{4.38 \times 10^3 \cdot F \cdot c^{-1/2}}{1000 \cdot A_{sp}} \cdot Q_t \cdot \exp(-3.29 \times 10^7 \cdot c^{1/2} \cdot x) \qquad (3.14)$$

That is, Ψ_x becomes directly proportional to Q_t, the sum of the charge on the surface plus hydrated gel layer. Finally equation 3.6 can be replaced by an expression of the form:

$$\ln\left(\frac{\overline{N}_{Ca}}{\gamma_{Ca}}\right) = A + B \cdot Q_t \qquad (3.15)$$

where A and B are constants.

CHAPTER FOUR

FUTURE STUDIES

IV.1 DIRECTIONS FOR FUTURE WORK

IV.1.1 SODIUM SORPTION PHENOMENON ON OTHER GLASS SURFACES AND SILICA

In the present studies, CPG-Oxine was used as the packing in the column equilibration and shallow bed kinetic study of Ca^{2+} sorption. An interesting research project would be to study the effect of Na^{+} sorption on Fused Silica. Fused silica is similar to CPG-Oxine in that there is a high concentration of OH sites on the surface and therefore one would expect the same ion sorption properties. This experiment could be done with the same experimental apparatus with modified experimental parameters done to maximize the amount of Na^{+} sorbed and thus eluted.

IV.1.2 NEW AND IMPROVED PACKINGS AND SUPPORTS

In the present investigations the underlying reason for the anomalous overshoot of equilibrium was satisfactorily explained in terms of the porous gel model and the double-layer sorption model. In the course of these investigations a micro-column technique was developed that allowed shallow bed studies to be undertaken. With the CPG-Oxine packing, free Ca^{2+} can only be determined at the 10^{-5} M range. This range is not sensitive enough for use in detecting free Ca^{2+} in biological fluids. As stated previously (47), direct

measurement of Ca^{2+} in biological fluids should be possible if an immobilized ligand having a lower conditional stability constant than "oxine" is found. It is a logical continuation, therefore, to undertake similar studies using the shallow bed, column equilibration technique developed within this investigation with new and improved packings and/or supports to determine free Ca^{2+} and Mg^{2+} in biological fluids.

LITERATURE CITED

1. Smith, R.M.; Martell, A.E. (Eds.), *"Critical Stability Constants, Volume 2: Amines"*, Plenum Press, New York, 1975; Section IV.
2. Stary, J.; Zolotov, Y.A.; Pertrukhin, O.M. (Eds), *"Critical Evaluation of Equilibrium Constants involving 8-Hydroxyquinoline and its Metal Chelates"*, IUPAC Chemical Data Series No. 24, Pergamon Press, Oxford, 1979.
3. Malamas, F.; Bengtsson, M.; Johansson, G., *Anal. Chim. Acta* **1984**, 160, 1-5.
4. Guedes da Mota, M.M.; Romer, F.G.; Griepink, B, *Fresenius'Z. Anal.Chem.* **1977**, 287, 19-22.
5. Sturgeon, R.E.; Berman, S.S.; Willie, S.N.; Desaulniers, J.A.H., *Anal. Chem.* **1981**, 53, 2337-2340.
6. Allen, E.A.; Bartlett, P.K.N.; Ingram, G, *Analyst* **1984**, 109, 1075-1080.
7. Fang, Z.; Ruzicka, J.; Hansen, E.H., *Anal. Chim. Acta* **1984**, 164, 23-39.
8. McLaren, J.W.; Mykytiuk, A.P.; Willie, S.N.; Berman, S.S., *Anal. Chem.* **1985**, 57, 2907-2911.
9. Marshall, M.A.; Mottola, H.A., *Anal. Chem.* **1985**, 57, 729-733.
10. Ryan, D.K.; Weber, J.H., *Talanta* **1985**, 32, 859-863.
11. Allen, E.A.; Boardman, M.C.; Plunkett, B.A., *Anal. Chim. Acta* **1987**, 196, 323-327.
12. Moorhead, E.D.; Davis, P.H., *Anal. Chem.* **1974**, 46, 1879-1880.
13. Jezorek, J.R.; Freiser, H., *Anal. Chem.* **1979**, 51, 366-373.
14. Kuo, M.S.; Mottola, H.A., *Anal. Chim. Acta* **1980**, 120, 255-266.
15. Hill, J.M., *J. Chromatogr.* **1973**, 76, 455-458.
16. Shahwan, G.J.; Jezorek, J.R., *J. Chromatogr.* **1983**, 256, 39-48.
17. Risner, C.H.; Jezorek, J.R., *Anal. Chim. Acta* **1986**, 186, 233-245.

18. Sugawara, I.F.; Weetall, H.H.; Schucker, G.D., *Anal. Chem.* **1974**, 46, 489-492.

19. Product Bulletin, Pierce Chemical Co., Rockford, IL, 1986.

20. Marshall, M.A.; Mottola, H.A. *Anal. Chem.* **1983**, 55, 2089-2093.

21. Marshall, M.A.; Mottola, H.A. *Anal. Chem.* **1984**, 158, 369-373.

22. Bonner, O.D.; Rhett, V., *J. Phys Chem.* **1953**, 57, 254-256.

23. Bonner, O.D.; Livingston, L., *J. Phys. Chem.* **1956**, 60, 530-532.

24. Bonner, O.D.; Smith, L.L., *J. Phys. Chem.* **1957**, 61, 326-329.

25. Gregor, H.P.; Bregman, J.I., *J. Colloid Sci.* **1951**, 6, 323-347.

26. Bonner, O.D.; Overton, J.R., *J. Phys. Chem.* **1961**, 65, 1599-1602.

27. Walton, H.F.; Jordan, D.E.; Samedy, S.R.; McKay, W.N., *J. Phys. Chem.* **1961**, 65, 1477-1484.

28. Treit, J.; Nielsen, J.S.; Kratochvil, B.; Cantwell, F.F., *Anal. Chem.* **1983**, 55, 1650-1653.

29. Cantwell, F.F.; Nielsen, J.S.; Hrudey, S.E., *Anal. Chem.* **1982**, 54, 1498-1503.

30. Sweileh, J.A.; Lucyk, D.; Kratochvil, B.; Cantwell, F.F., *Anal. Chem.* **1987**, 59, 586-592.

31. Crank, J., *"The Mathematics of Diffusion"*, Oxford University Press, London, 2nd Edition, 1975, page 47-48 and 62.

32. Karlberg, B., *Electroanal. Chem. Interfacial Electrochem.* **1973**, 42, 115-126.

33. Lindner, E.; Toth, K.; Pungor, E., *"Dynamic Characteristics of Ion Selective Electrodes"*, CRC Press, Boca Ratan, Florida, 1988, Chapter 4.

34. Altug, I.; Hair, M. L. *J. Phys. Chem.* **1967**, 71, 4260-4263.

35. Helfferich, F (Ed.), *"Ion Exchange"*, McGraw-Hill, New York, 1962, Chapter 5.

36. Marinsky, J.A., J.A. Marinsky (Ed.), *"Ion Exchange: A Series of Advances, Vol. 1"*, Marcel Dekker, New York, 1966, Chapter 9.

37. Marinsky, J.A.; Wolf, A; Bunzl, K., *Talanta* **1980**, 27, 461-468.

38. Shaw, D. J. (Ed.), *" Introduction to Colloid and Surface Chemistry"*, Butterworths, Toronto, 3rd Edition, 1980, Chapter 7.

39. Grahame, D.C., *Chem. Rev.* **1947**, 41, 441-501.

40. Healy, T.W.; White, L.R., *Adv. Col. Interface Sci.* **1978**, 9, 303-345.

41 Cantwell, F.F.; Puon, S., *Anal. Chem.* **1979**, 51, 623-632.

42. Takamura, K.; Chow, R.S., *Coll. and Surfaces* **1985**, 15, 35-48.

43. Khater, M.M.; Issa, Y.M.; Shoukry, A.F., *J. f. prakt. Chemie* **1980**, 322, 470-474.

44. Chow, R.S.; Takamura, K., *J. Coll. Interface Sci.* **1988**, 125, 212-225.

45. Kolstad, A.K.; Chow, P.Y.T.; Cantwell, F.F., *Anal. Chem.* **1988**, 60, 1565-1569.

46. Chow, P.Y.T.; Cantwell, F.F., *Anal. Chem.* **1988**, 60, 1569-1573.

47. Chow, P.Y.T. Ph.D. Thesis, University of Alberta, Fall 1988.

48. Dranoff, J.S.; Lapidus, L., *Industrial and Eng. Chem.* **1961**, 53, 71-76.

49. Helfferich, F., *Ion Exchange*, McGraw-Hill: New York, 1963, Chapter 6.

50. Riveros, P.A.; Cooper, W.C., *Solvent Extraction and Ion Exchange* **1988**, 6, 479-503.

51. Persaud, G.; Cantwell, F.F., *Anal. Chem.* **1992**, 64, 89-94.

52. Persaud, G. Ph.D. Thesis, University of Alberta, Spring 1990.

53. Schnabel, R.; Langer, P., *J. Chromatogr.* **1991**, 544, 137-146.

54. Swaisgood, A. E.; Chaiken, I. M., *J. Chromatogr.* **1985**, 327, 193-204.

55. Pierce, Private Communication, 1984

56. Fulcher, C.; Crowell, M.A.; Bayliss, R.; Holland, K.B.; Jezorek, J.R. *Anal. Chim. Acta* **1981**, *129*, 29-47.

57. Jezorek, J.R.; Faltynski, K.H.; Blackburn, L.G.; Henderson, P.J.; Medina,H.D., *Talanta* **1985**, 32, 763-770.

58. Jezorek, J.R.; Fulcher, C.; Crowell, M.A.; Bayliss, R.; Greenwood, B.; Lyon, J. *Anal. Chim. Acta* **1981**, 131, 223-231.

59. Utkelov, B.A.; Yergozhin, Ye.Ye.; Mukhitdinova, B.A.; Rafikov, S.R., *Polymer Sci. USSR (Engl. Transl.)* **1978**, 20, 532-540.

60. Good, N.E.; Winget, G.D.; Winter, W.; Connolly, T.N.; Izowa, S.; Singh, R.M.M., *Biochemistry* **1966**, 5, 467-477.

61. Boyd, G.E.; Adamson, A.W.; Myers, L.S., *J. Am. Chem. Soc.* **1947**, 69, 2836-2848.

62. Danesi, P.R.; Chiarizia, R. *"The Kinetics of Metal Solvent Extraction, CRC Critical Reviews in Analytical Chemistry"*, 1980, pages 48-51.

63. Davidowicz, A.; Janusz, W.; Szeypa, J.; Waksmundzki, A., *J. Colloid Interface Sci.* **1987**, 115, 555-558.

64. Hunter, R.J. *"Zeta Potential in Colloid Science: Principles and Applications"*, Academic Press, New York, 1981, Chapter 7.

65. James, R.O.; Parks, G.A., "In *Surface and Colloid Science*", Vol. 12, Matijevic, E. (Ed.), Plenum Press, New York, 1982, Chapter 2.

66. Liu, H. J.; Cantwell, F. F., *Anal. Chem.* **1991**, 63, 2032-2037.

67. Helfferich, F.,*"Ion Exchange"*, McGraw-Hill, New York, 1963, Chapter 8.

68. Helfferich, F., *"Ion Exchange Kinetics in Ion Exchange"*, Marinsky, J.A. (Ed.), Marcel Dekker, New York, 1966, Vol. 1, Chapter 2.

69. Kraus, K.A.; Marcinkowsky, A.E.; Johnson, J.S.; Shor, A.J., *Science* **1966**, 151, 194-195.

70. Dresner, L., *J. Phys. Chem.* **1965**, 69, 2230-2238.

71. Bansal, N.; Doremus, R., *"Handbook of Glass Properties"*, Academic Press, New York, 1986, Chapter 2.

72. Perram, J.W.; Hunter, R.J.; Wright, H.J.L., *Chemical Physics Letters* **1973**, 23, 265-269.

73. Perram, J.W.; Hunter, R.J.; Wright, H.J.L., *Aust. J. Chem.* **1974**, 27, 461-475.

74. Smit, W.; Holten, C.L.M.; Stein, H.N.; De Goeij, J.J.M.; Theelen, H.M.J., *J. Colloid Interface Sci.* **1978**, 67, 397-406.

75. Ahmed, S. M.; Van Cleave, A. B., *Can. J. Chem. Eng.* **1965**, 43, 23-26.

76. Nardin, M.; Papirer, E.; Schultz, J., *J. Colloid Interface Sci.* **1982**, 88, 204-213.

77. Greenberg, S.A.; Chang, T.N.; Jarnutowski, R., *J. Polymer Sci.* **1962**, 58, 147-184.

78. Littlewood, A. B., *"Gas Chromatography"*, Academic Press, New York, 2nd Edition, 1970, Pages 170-175.

79. Helfferich, F., *"Ion Exchange"*, McGraw-Hill, New York, 1967, Chapters 6 and 9.

80. Marinsky, J.A., *J. Phys. Chem.* **1985**, 89, 5294-5302.

81. Verwey, E.J.; Overbeck, J.T. (Eds.), *"Theory of the Stability of Lyophobic Colloids"*, Elsevier, Amsterdam, 1948.

82. Honda, M., *J. Am. Chem. Soc.* **1951**, 73, 2943-2944.

83. Kielland, J., *J. Am. Chem. Soc.* **1937**, 59, 1675-1678.

84. Cukman, D; Jadnacak-Biscan, J; Vekski, Z; Haller, W, *J. Colloid Interface Sci.* **1987**, 115, 357-361

85. Janowski, F; Heyer, W *"Porose Glasser"*, VEB Deutscher Verlag Fur Grundstoffindustrie, Leipzig, 1981, chapter 4

86. Huang, T.-L.; Tsai, P.; Wu, C.-T.; Lee, C.S. *Anal. Chem* **1993**, 65, 2887-2893.

87. Smit, W.; Holten, C.L.M.; Stein, H.N.; DeGoeij, J.J.M.; Theelen, H.M.J. *J. Colloid Interface Sci.* **1978**, 67, 397-406

88. Persaud, G.; Cantwell. F.F. *Can. J. Chem.* **1992**, 70, 926-930

89 Dovichi, N. University of Alberta, Personal Communication

90 Davies, C.W. *Ion Association*, Butterworths, Toronto; 1962; Chapter 3

APPENDIX A

TABLES AND FIGURES FOR THESIS

In this appendix data which was presented in some of the figures in the thesis are tabulated. The corresponding figure in which the data were plotted is indicated in the tables. As well, some of the instrument calibration curves not shown in the thesis are shown.

Table A.1 Cu^{2+} washing study data. The composition of the solution pumped through the column for 10 minutes and then washed for varying lengths of time was 1.26×10^{-3} M Cu^{2+} in 0.0900 M HOAC/NaOAc (pH = 5.00). The flow rate was 5.0 mL/min. The data are plotted in Figure 2.5.

Wash Time (minutes)	Cu^{2+} Eluted (x 10^{-6}) mols/gram (a)
0	11.270 ± 0.220
2	9.375 ± 0.165
4	9.130 ± 0.120
6	9.115 ± 0.055
8	9.035 ± 0.035
16	8.928 ± 0.112

(a) Average and standard deviation of 2 runs.

Table A.2 Cu^{2+} loading study data. The composition of the solution pumped through the column for varying lengths of time and then washed for 10 minutes was 1.26×10^{-3} M Cu^{2+} in 0.0900 M HOAC/NaOAc (pH = 5.00). The flow rate was 5.0 mL/min. The data are plotted in Figure 2.6.

Load Time (minutes)	Cu^{2+} Eluted (x 10^{-6}) mols/gram (a)
0.083	6.795 ± 0.045
0.167	8.085 ± 0.065
0.250	8.455 ± 0.135
0.500	8.835 ± 0.205
1.000	9.180 ± 0.150
1.500	9.350 ± 0.030
2.000	9.015 ± 0.035
4.000	9.220 ± 0.079

(a) Average and standard deviation of 2 runs.

Table A.3 Cu^{2+} capacity study data. The composition of the solution pumped through the column for 2 minutes and then washed for 10 minutes with N_2 sparged DI water was 1.26×10^{-3} M Cu^{2+} in 0.0900 M HOAC/NaOAc (pH = 5.00). The flow rate was 5.0 mL/min. The data are plotted in Figure 2.7.

Cu^{2+} concentration (x 10^{-4} M)	Cu^{2+} Eluted (x 10^{-6}) mols/gram (a)
10	8.530 ± 0.011
20	9.135 ± 0.125
40	9.450 ± 0.150
60	9.980 ± 0.110
80	10.040 ± 0.000
100	10.485 ± 0.155
200	10.605 ± 0.005
300	9.850 ± 0.190

(a) Average and standard deviation of 2 runs.

Table A.4 Ca^{2+} loading curve data for a solution of 2.0×10^{-5} M Ca^{2+} in 0.0200 M $NaClO_4$ and 0.0100 M HEPES buffer solution at pH = 7.00. The data are plotted in Figure 2.8.
Note: $\overline{N}_{Ca}\,(CPG\text{-}Ox)_{(2\ minutes)} = 5.94 \times 10^{-4}$ mmol/g

Load Time (minutes)	$\frac{\overline{N}_{Ca}\,(CPG\text{-}Ox)}{\overline{N}_{Ca}\,(CPG\text{-}Ox)_{(2\ minutes)}}$ (a)
0.0	0
0.5	0.958 ± 0.008
1.0	0.981 ± 0.048
2.0	1.000
4.0	1.012 ± 0.048

(a) Average and standard deviation of 2 runs.

Table A.5 Ca^{2+} loading curve data for a solution of 2.0×10^{-5} M Ca^{2+} in 0.0200 M $NaClO_4$ and 0.0100 M HEPES buffer solution at pH = 7.00. The data are plotted in Figure 2.9A.
Note: $\overline{N}_{Ca}$ (CPG-Ox)$_{(2\ minutes)} = 5.94 \times 10^{-4}$ mmol/g.

Load Time (minutes)	$\frac{\overline{N}_{Ca}\ (CPG\text{-}Ox)}{\overline{N}_{Ca}\ (CPG\text{-}Ox)_{(2\ minutes)}}$
0.5	0.958 ± 0.008 (a)
1.0	0.981 ± 0.048 (a)
2.0	1.000
4.0	1.012 ± 0.048 (a)
12.0	0.852 ± 0.016 (b)
24.0	0.804 ± 0.022 (c)
56.0	0.732 ± 0.036 (a)
120.0	0.623 ± 0.007 (b)
164.0	0.620 ± 0.015 (a)
240.0	0.621 ± 0.006 (a)

(a) Average and standard deviation of 2 runs.

(b) Average and standard deviation of 3 runs.

(c) Average and standard deviation of 4 runs.

Table A.6 Ca^{2+} loading curve data for a solution of 2.0×10^{-5} M Ca^{2+} in 0.0200 M $NaClO_4$ and 0.0100 M HEPES buffer solution at pH = 7.00 on CPG (no bound oxine ligands). The data are plotted in Figure 2.9B. Note: $\overline{N}_{Ca}$ (CPG-Ox)$_{(2\ minutes)} = 5.94 \times 10^{-4}$ mmol/g

Load Time (minutes)	$\frac{\overline{N}_{Ca}\,(CPG)}{\overline{N}_{Ca}\,(CPG\text{-}Ox)_{(2\ minutes)}}$
0	0.000
2	0.096
31	0.090
60	0.083
120	0.071
180	0.063
240	0.049

Table A.7 Ca^{2+} loading curve data (solid circles) for a solution of 2.0×10^{-5} M Ca^{2+} in 0.0200 M $NaClO_4$ and 0.0100 M HEPES buffer solution at pH = 7.00 on CPG-Oxine. Preconditioning study data (open squares) where the column was preconditioned with a solution containing only the 0.0200 M $NaClO_4$ and 0.0100 M HEPES solution before the Ca^{2+} containing solution was loaded. The data are plotted in Figure 2.10.
Note: $\overline{N}_{Ca}$ (CPG-Ox)$_{(2\ minutes)} = 5.94 \times 10^{-4}$ mmol/g.

Load Time (minutes)	$\frac{\overline{N}_{Ca}\ (CPG\text{-}Ox)}{\overline{N}_{Ca}\ (CPG\text{-}Ox)_{(2\ minutes)}}$ (Solid circles)	$\frac{\overline{N}_{Ca}\ (CPG\text{-}Ox)}{\overline{N}_{Ca}\ (CPG\text{-}Ox)_{(2\ minutes)}}$ (Open squares)
0.5	0.958 ± 0.008 (a)	-
1.0	0.981 ± 0.048 (a)	-
2.0	1.000	1.005
4.0	1.012 ± 0.048 (a)	-
12.0	0.852 ± 0.016 (b)	0.870
24.0	0.804 ± 0.022 (c)	0.821
56.0 (53.0 Open squares)	0.732 ± 0.036 (a)	0.737
120.0	0.623 ± 0.007 (b)	0.636
164.0 (176.0 Open Squares)	0.620 ± 0.015 (a)	0.630
240.0	0.621 ± 0.006 (a)	0.615

(a) Average and standard deviation of 2 runs.

(b) Average and standard deviation of 3 runs.

(c) Average and standard deviation of 4 runs.

Table A.8 Ca^{2+} loading curve data (solid circles) for a solution of 2.0×10^{-5} M Ca^{2+} in 0.0200 M $NaClO_4$ and 0.0100 M HEPES buffer solution at pH = 7.00 on CPG-Oxine. Preconditioning study data (open squares) where the column was preconditioned with a solution containing only the 0.0100 M HEPES solution before the Ca^{2+} containing solution was loaded. The data are plotted in Figure 2.11. Note: $\overline{N}_{Ca}$ (CPG-Ox)$_{(2\ minutes)} = 5.94 \times 10^{-4}$ mmol/g.

Load Time (minutes)	$\frac{\overline{N}_{Ca}\ (CPG\text{-}Ox)}{\overline{N}_{Ca}\ (CPG\text{-}Ox)_{(2\ minutes)}}$ (Solid circles)	$\frac{\overline{N}_{Ca}\ (CPG\text{-}Ox)}{\overline{N}_{Ca}\ (CPG\text{-}Ox)_{(2\ minutes)}}$ (Open squares)
0.5	0.958 ± 0.008 (a)	-
1.0	0.981 ± 0.048 (a)	-
2.0	1.000	0.969
4.0	1.012 ± 0.048 (a)	-
12.0 (13.0 open squares)	0.852 ± 0.016 (b)	0.925
24.0 (30.0 Open squares)	0.804 ± 0.022 (c)	0.945
56.0 (50.0 Open squares)	0.732 ± 0.036 (a)	0.937
120.0	0.623 ± 0.007 (b)	0.915
164.0 (180.0 Open squares)	0.620 ± 0.015 (a)	0.855
240.0 (235.0 Open squares)	0.621 ± 0.006 (a)	0.826

(a) Average and standard deviation of 2 runs.

(b) Average and standard deviation of 3 runs.

(c) Average and standard deviation of 4 runs.

Table A.9 Ca^{2+} loading curve data (solid circles) for a solution of 2.0×10^{-5} M Ca^{2+} in 0.0200 M $NaClO_4$ and 0.0100 M HEPES buffer solution at pH = 7.00 on CPG-Oxine. Preconditioning study data (open squares) where the column was preconditioned with a solution containing only the 0.0200 M $NaClO_4$ solution before the Ca^{2+} containing solution was loaded. The data are plotted in Figure 2.12. Note: $\overline{N}_{Ca}$ (CPG-Ox)$_{(2\ minutes)} = 5.94 \times 10^{-4}$ mmol/g.

Load Time (minutes)	$\frac{\overline{N}_{Ca}\text{ (CPG-Ox)}}{\overline{N}_{Ca}\text{ (CPG-Ox)}_{(2\ minutes)}}$ (Solid circles)	$\frac{\overline{N}_{Ca}\text{ (CPG-Ox)}}{\overline{N}_{Ca}\text{ (CPG-Ox)}_{(2\ minutes)}}$ (Open squares)
0.5	0.958 ± 0.008 (a)	-
1.0	0.981 ± 0.048 (a)	-
2.0	1.000	0.958
4.0	1.012 ± 0.048 (a)	-
12.0	0.852 ± 0.016 (b)	0.930
24.0 (28.0 Open squares)	0.804 ± 0.022 (c)	0.946
56.0 (50.0 Open squares)	0.732 ± 0.036 (a)	0.911
120.0	0.623 ± 0.007 (b)	-
164.0 (169.0 Open squares)	0.620 ± 0.015 (a)	0.844
240.0 (275.0 Open squares)	0.621 ± 0.006 (a)	0.780

(a) Average and standard deviation of 2 runs.

(b) Average and standard deviation of 3 runs.

(c) Average and standard deviation of 4 runs.

Table A.10 Ca^{2+} loading curve data (solid circles) for a solution of 2.0×10^{-5} M Ca^{2+} in 0.0200 M $NaClO_4$ and 0.0100 M HEPES buffer solution at pH = 7.00 on CPG-Oxine. Preconditioning study data (open squares) where the column was preconditioned with a solution containing only the 0.0200 M $NaClO_4$ and 0.100 M HEPES solution before the Ca^{2+} containing solution was loaded. The data are plotted in Figure 2.13.Note:
$\overline{N}_{Ca}$ (CPG-Ox)$_{(2\ minutes)} = 5.94 \times 10^{-4}$ mmol/g.

Load Time (minutes)	$\frac{\overline{N}_{Ca}\ (CPG\text{-}Ox)}{\overline{N}_{Ca}\ (CPG\text{-}Ox)_{(2\ minutes)}}$ (Solid circles)	$\frac{\overline{N}_{Ca}\ (CPG\text{-}Ox)}{\overline{N}_{Ca}\ (CPG\text{-}Ox)_{(2\ minutes)}}$ (Open squares)
0.5	0.958 ± 0.008 (a)	-
1.0	0.981 ± 0.048 (a)	-
2.0	1.000	-
4.0	1.012 ± 0.048 (a)	-
5.0	-	0.916
12.0	0.852 ± 0.016 (b)	-
24.0 (25.0 Open squares)	0.804 ± 0.022 (c)	0.827
56.0 (6.0 Open squares)	0.732 ± 0.036 (a)	0.745
120.0	0.623 ± 0.007 (b)	0.654
164.0 (183.0 Open squares)	0.620 ± 0.015 (a)	0.634
240.0 (238.0 Open squares)	0.621 ± 0.006 (a)	0.616

(a) Average and standard deviation of 2 runs.

(b) Average and standard deviation of 3 runs.

(c) Average and standard deviation of 4 runs.

Table A.11 Ca^{2+} loading curve data (solid circles) for a solution of 2.0×10^{-5} M Ca^{2+} in 0.0200 M $NaClO_4$ and0.0100 M HEPES buffer solution at pH = 7.00 on CPG-Oxine. Preconditioning study data (open squares) where the column was preconditioned with a solution containing only the 0.200 M $NaClO_4$ and 0.100 M HEPES solution before the Ca^{2+} containing solution was loaded. The data are plotted in Figure 2.14.
Note: $\overline{N}_{Ca}$ (CPG-Ox)$_{(2\ minutes)} = 5.94 \times 10^{-4}$ mmol/g.

Load Time (minutes)	$\frac{\overline{N}_{Ca}\ (CPG\text{-}Ox)}{\overline{N}_{Ca}\ (CPG\text{-}Ox)_{(2\ minutes)}}$ (Solid circles)	$\frac{\overline{N}_{Ca}\ (CPG\text{-}Ox)}{\overline{N}_{Ca}\ (CPG\text{-}Ox)_{(2\ minutes)}}$ (Open squares)
0.5	0.958 ± 0.008 (a)	-
1.0	0.981 ± 0.048 (a)	-
2.0	1.000	1.020
4.0	1.012 ± 0.048 (a)	-
12.0 (15.0 Open squares)	0.852 ± 0.016 (b)	0.861
24.0 (31.0 Open squares)	0.804 ± 0.022 (c)	0.755
56.0 (60.0 Open squares)	0.732 ± 0.036 (a)	0.688
120.0 (131.0 Open squares)	0.623 ± 0.007 (b)	0.480
164.0 (176.0 Open squares)	0.620 ± 0.015 (a)	0.465
240.0 (247.0 Open squares)	0.621 ± 0.006 (a)	0.470

(a) Average and standard deviation of 2 runs.

(b) Average and standard deviation of 3 runs.

(c) Average and standard deviation of 4 runs.

Table A.12 Ca^{2+} loading curve data (solid circles) for a solution of 2.0×10^{-5} M Ca^{2+} in 0.0200 M $NaClO_4$ and 0.0100 M HEPES buffer solution at pH = 7.00 on CPG-Oxine. Preconditioning study data (open squares) where the column was preconditioned with a solution containing no sodium. This study was done with ammonium-perchlorate as the electrolyte buffer medium. The preconditioning solution composition was 0.200 M NH_4ClO_4 and 0.0100 M HEPES solution before the Ca^{2+} containing solution was loaded. The data are plotted in Figure 2.15.Note: $\overline{N}_{Ca}$ (CPG-Ox)$_{(2\ minutes)}$ = 5.94×10^{-4} mmol/g.

Load Time (minutes)	$\frac{\overline{N}_{Ca}\ (CPG\text{-}Ox)}{\overline{N}_{Ca}\ (CPG\text{-}Ox)_{(2\ minutes)}}$ (Solid circles)	$\frac{\overline{N}_{Ca}\ (CPG\text{-}Ox)}{\overline{N}_{Ca}\ (CPG\text{-}Ox)_{(2\ minutes)}}$ (Open squares)
0.5	0.958 ± 0.008 (a)	-
1.0	0.981 ± 0.048 (a)	-
2.0	1.000	1.000
4.0	1.012 ± 0.048 (a)	-
12.0	0.852 ± 0.016 (b)	-
24.0	0.804 ± 0.022 (c)	-
56.0 (45.0 Open squares)	0.732 ± 0.036 (a)	0.934
120.0 (118.0 Open squares)	0.623 ± 0.007 (b)	0.827
164.0	0.620 ± 0.015 (a)	-
240.0 (218.0 Open squares)	0.621 ± 0.006 (a)	0.564
318.0	-	0.535

(a) Average and standard deviation of 2 runs.

(b) Average and standard deviation of 3 runs.

(c) Average and standard deviation of 4 runs.

Table A.13 N_2 sparged DI water wash study data for CPG-Oxine. The column was loaded with a 0.0200 M sodium-perchlorate solution for two minutes and then subsequently washed for varying lengths of time. The data are plotted in Figure 2.16.

Wash Time (minutes)	$\overline{N}_{Na} \times 10^{10}$ (mmols/gram)
2.0	1.21
6.0	0.51
10.0	0.28
14.0	0.19
18.0	0.09

Table A.14 HEPES Wash study data for CPG-Oxine. CPG-Oxine column loaded for 2 minutes with 0.0200 M $NaClO_4$ followed by a varying length wash with 0.0200 HEPES only solution at pH = 7.00. The data are plotted in Figure 2.17.

Wash Time (seconds)	$\overline{N}_{Na} \times 10^7$ (mmol/gram)
5	1.4
6	0.89
7	0.58
8	0.41
9	0.20
10	0.19
15	0.048
20	0.015
25	0.0044
30	0.000805

Table A.15 Strongly held Na^+ desorption data. With increasing load times, a 0.0200 M $NaClO_4$ solution was loaded on the CPG-Oxine column and washed with a 0.0200 M HEPES solution for 30 seconds. The column was then eluted directly into the spectrometer with a 0.15 M HNO_3 solution. The data are plotted in Figure 2.18

Load Time (minutes) (a)	$\overline{N}_{Na} \times 10^2$ (mmol/gram)
0	0.000
3	0.926
14	1.670
28	3.740
62	7.892
116	8.815
179	9.302
244	9.443

(a) Note: This is the original experimental data minus two (2) minutes.

Table A.16 Desorption curve data for Ca^{2+}. The two minute loading curve point from Figure 2.9A is considered to be zero. The rest of the data is then generated as :

$\Delta\overline{N}_{Ca} = \overline{N}_{Ca,\ 2\ minutes} - \overline{N}_{Ca,\ load\ time\ (t \geq 2\ mins)}$.

The data are plotted in Figure 2.19.

Load Time (minutes) (a)	$\Delta\ \overline{N}_{Ca}$ x 10^4 (mmol/gram)
0.0	0.000
12.0	0.882
24.0	1.164
56.0	1.590
120.0	2.238
164.0	2.256
240.0	2.250

(a) Load time (minutes) = Experimental load time (minutes) - 2 minutes

Table A.17 Sodium sorption data. Data collected by loading the CPG-Oxine column, until equilibrium has been reached (2 hour load time verified by 4 hour load time) with 0.0200 M NaClO4 (pH = 7.00) and washing for 30 seconds with 0.0100 M HEPES solution (pH = 7.00).

$\bar{N}_{Na,\ equil}$ (mmol/g)	$[Na^+]$ = c (mol/L)
8.7×10^{-4}	0.001
2.7×10^{-3}	0.005
5.5×10^{-3}	0.020
6.0×10^{-3}	0.040
8.2×10^{-3}	0.080
8.1×10^{-3}	0.120
8.6×10^{-3}	0.140

Table A.18 Data for Na^+ sorption isotherm within the hydrated glass layer. Data from Figure 3.1 plotted according to equation 3.4.

$[Na^+]$	γ_{Na}	$[Na^+] \cdot \gamma_{Na}$	$\frac{1}{[Na^+] \cdot \gamma_{Na}}$	$\overline{N}_{Na,\ equil}$ $(\frac{mmol}{g})$	$\frac{1}{\overline{N}_{Na,\ equil}}$
0.001	0.964	0.000964	1037	0.87×10^{-3}	1.149×10^{3}
0.005	0.928	0.00464	216	2.67×10^{-3}	0.374×10^{3}
0.020	0.872	0.01744	57.34	5.5×10^{-3}	0.182×10^{3}
0.040	0.836	0.03336	29.98	6.0×10^{-3}	0.167×10^{3}
0.080	0.791	0.06328	15.80	8.2×10^{-3}	0.122×10^{3}
0.120	0.762	0.09144	10.94	8.1×10^{-3}	0.123×10^{3}
0.140	0.751	0.10514	9.51	8.6×10^{-3}	0.116×10^{3}